British Geological Survey

NATURAL ENVIRONMENT RESEARCH COUNCIL

Studies of possible controls on the variability of radon potential of two East Midlands ironstones

Chemical and Biological Hazards Programme

Internal Report IR/06/128

BRITISH GEOLOGICAL SURVEY

CHEMICAL AND BIOLOGICAL HAZARDS PROGRAMME

INTERNAL REPORT IR/06/128

Studies of possible controls on the variability of radon potential of two East Midlands ironstones

E S Hodgkinson, C Scheib, D G Jones, and J Davis

Keywords

Radon; ironstone; gamma spectrometry; autoradiography; radon emanation.

Bibliographical reference

HODGKINSON, E S, SCHEIB, C, JONES, D G AND DAVIS, J. 2012. Studies of possible controls on the variability of radon potential of two East Midlands ironstones. *British Geological Survey Internal Report*, IR/06/128. 104pp.

Keyworth, Nottingham British Geological Survey 2012

BRITISH GEOLOGICAL SURVEY

The full range of Survey publications is available from the BGS Sales Desks at Nottingham, Edinburgh and London; see contact details below or shop online at www.geologyshop.com

The London Information Office also maintains a reference collection of BGS publications including maps for consultation.

The Survey publishes an annual catalogue of its maps and other publications; this catalogue is available from any of the BGS Sales Desks.

The British Geological Survey carries out the geological survey of Great Britain and Northern Ireland (the latter as an agency service for the government of Northern Ireland), and of the surrounding continental shelf, as well as its basic research projects. It also undertakes programmes of British technical aid in geology in developing countries as arranged by the Department for International Development and other agencies.

The British Geological Survey is a component body of the Natural Environment Research Council.

British Geological Survey offices

Keyworth, Nottingham NG12 5GG

☎ 0115-936 3241 Fax 0115-936 3488
e-mail: sales@bgs.ac.uk
www.bgs.ac.uk
Shop online at: www.geologyshop.com

Murchison House, West Mains Road, Edinburgh EH9 3LA

☎ 0131-667 1000 Fax 0131-668 2683
e-mail: scotsales@bgs.ac.uk

London Information Office at the Natural History Museum (Earth Galleries), Exhibition Road, South Kensington, London SW7 2DE

☎ 020-7589 4090 Fax 020-7584 8270
☎ 020-7942 5344/45 email: bgslondon@bgs.ac.uk

Forde House, Park Five Business Centre, Harrier Way, Sowton, Exeter, Devon EX2 7HU

☎ 01392-445271 Fax 01392-445371

Geological Survey of Northern Ireland, Colby House, Stranmillis Court, Belfast, BT9 5BF

☎ 028-9038 8462 Fax 028-9038 8461

Maclean Building, Crowmarsh Gifford, Wallingford, Oxfordshire OX10 8BB

☎ 01491-838800 Fax 01491-692345

Sophia House, 28 Cathedral Road, Cardiff, CF11 9LJ

☎ 029–2066 0147 Fax 029–2066 0159

Parent Body

Natural Environment Research Council, Polaris House, North Star Avenue, Swindon, Wiltshire SN2 1EU

☎ 01793-411500 Fax 01793-411501
www.nerc.ac.uk

Foreword

The work detailed in this report was largely carried out under the Environmental Radioactivity project in the Chemical and Biological Hazards Programme between 2000 and 2005. The lead author left BGS in 2006 whilst this report was still unfinished. Emily had done a lot of good work on this and it deserved to be finished. Therefore Dave Jones continued this work in 2009 and Cathy Scheib then completed the report in 2012.

Acknowledgements

The authors would like to thank the following people and organisations for giving access to sites for sampling and testing: Leicestershire and Rutland Wildlife Trust (for access to Brown's Quarry, Holwell and Tilton cutting); Rockingham Forest Trust (for access to Twywell Country Park) and Peter Bennie Ltd (for access to Pitsford and Harlestone Quarries); Belvoir Estates, Scalford Lodge Farm and Ironstone Lodge and other farmers and landowners for access to other sites.

Thanks also to: Barbara Vickers for carrying out iron speciation tests; Gren Turner for assistance in carrying out radon emanation studies; Simon Chenery for providing the ICP-MS data and for advice on statistical analysis; Simon Carter for XRFS analysis; Mark Barron for an introduction to some of the field sites; and Don Appleton for advice and for provision of radon potential data.

Contents

FIGURES

PLATES

TABLES

1 Introduction

Jurassic ironstones consist of several formations, which, in the East Midlands, crop out in a thin band across the region. They stretch from north east of Gainsborough in Lincolnshire, through east Leicestershire, Northamptonshire and then curve gently towards the south-east, through Oxfordshire. Ironstones have been worked over a long period for their iron content, mainly opencast but with a limited number of underground workings (e.g. Hollingworth and Taylor, 1951; Tonks, 1989, 1991, 1992; Whitehead et al, 1952). Although no longer used as an iron ore, they are still quarried in a few places for buildings stone and as a source of aggregates.

The Jurassic ironstones are known to be associated with a higher than average radon risk, as determined by house and soil gas data (e.g. Appleton and Ball, 1995, Sutherland and Sharman, 1996), and this is not uniform across the ironstones. High resolution airborne survey data (HiRES-1, Peart et al, 2003) showed elevated levels of eU (equivalent uranium, derived from the ^{214}Bi gamma peak) and eTh (equivalent thorium, derived from the ^{208}Tl gamma peak) for the ironstones, but also showed variability in these elements. It has been suggested that the primary source of radon in the ironstones is in phosphates (Sutherland, 1992) but the regional variations have not been investigated in detail. The study presented here was carried out in order to examine possible geological factors that might give rise to geographical variations in radon both within each ironstone formation and between formations. The objectives were as follows:

(i) To characterise the large to medium (i.e. regional to outcrop) scale variation in the radioactivity of the ironstones, using airborne data acquired by the HiRES-1 project, and field-based gamma spectrometry.

(ii) To sample ironstones from a number of locations and undertake laboratory-based petrographic, geochemical and radiographic studies in order to determine the mineralogy/petrology of radiogenic minerals and their efficiency in radon generation.

(ii) To compare these two datasets and determine to what extent mineralogical and petrographical controls on radon levels affect surface radioactivity on a field scale.

(iii) Finally, to try to relate smaller scale variability (hand specimen to outcrop scale) to larger scale regional variations in radon risk based largely on indoor radon measurements.

2 Previous work

2.1 REGIONAL STUDIES

The ironstones have been known for some time to be associated with higher indoor and soil gas radon concentrations (e.g. Appleton and Ball, 1995; Sharman, 1991, 1992; Sutherland, 1991; Sutherland and Sharman, 1996; Wrixon et al, 1998). Sharman carried out extensive soil gas studies in Northamptonshire (Sharman, 1995) and Miles and Appleton (2005) have investigated the regional variation in radon potential within geological units by statistical interpolation of indoor radon data grouped by bedrock and superficial geology, and 1 km squares.

Examination of airborne radiometric data showed anomalies in eTh and eU associated with the Marlstone Rock Formation (Peart et al, 2003; Lahti and Jones, 2003). These appeared to be especially marked over areas where the ironstone had been worked.

2.2 MINERALOGICAL, GEOCHEMICAL AND PETROGRAPHIC APPROACHES

Detailed descriptions of the ironstones are contained in a series of memoirs from the late 1940s and 1950s when their extraction for iron was in its heyday (Taylor, 1949; Hollingworth and Taylor, 1951; Whitehead et al, 1952). These describe the mineralogy of the original iron-bearing phases and their alteration (weathering) products. They present summaries of the many chemical analyses, including in some cases the phosphate content, but not results for U and Th, which were not, at the time, of concern.

Sutherland and Sharman (1996) linked radon to phosphate nodules in a 'basal bed' in the Northampton Sand Formation, which they showed to have higher U content than the formation as a whole.

Hodgkinson (2002) examined three cores through the Northampton Sand Formation in Northamptonshire to assess the mineralogy and petrology of the radiogenic phases recognised through autoradiography (Hyslop, 2000). These subsurface samples showed that radiogenic phases included phosphatic grains but also that Fe, Ti and Mn oxides could be important in addition to detrital zircon and monazite.

3 Outline of present study

Two ironstone formations were chosen for the study: the Northampton Sand Formation (NSF) and the Marlstone Rock Formation (MRF). These are both associated with higher radon hazard (Appleton and Ball, 1995, Miles and Appleton, 2005) but there is a significant geographical variation in radon potential. For example, within Northampton and to the north west of the town < 4 % of houses are estimated to have indoor radon levels above the UK radon Action Level (AL) of 200 Bq m^{-3} whereas to the north of Northampton, and in Kettering and Wellingborough, >12% are above that level, with locally > 20 % above the AL (Miles and Appleton, 2005; Appleton et al, 2000; Miles and Appleton, 2000).

Ten field sites were studied; three on the Northampton Sand in areas with differing numbers of houses estimated to be above the AL (Appleton, pers. comm.) and seven on the Marlstone Rock. A combination of field and laboratory-based tests were carried out on rocks from these sites. The data thus obtained could then be evaluated in terms of the level of radon hazard for the area near each site.

The field-based studies consisted of lithological logging, gamma spectrometry, soil gas radon measurements and attempts to measure *in situ* rock permeability. The laboratory-based studies on samples from these sites comprised: i) alpha radiography linked with SEM petrography to investigate radioactive mineral phases; ii) XRD to identify mineral phases; iii) XRF/ ICP-MS to determine bulk chemical composition; iv) bulk determination of Fe speciation; v) gamma spectrometry of homogenised hand specimens; and, vi) measurement of radon emanation from hand specimens. Correlations amongst chemical and radiological properties were examined and discussed in relation to variations in radon potential.

4 Geological Setting

The two formations studied, the Lower Jurassic Marlstone Rock Formation (MRF) and the Northampton Sand Formation (NSF), from the basal part of the Middle Jurassic. These two formations, of generally similar nature, have an extensive outcrop in the English Midlands. The MRF occurs in the Worcester Basin and the East Midlands Shelf extending from Mendip to Market Weighton (BGS, 2006). The NSF outcrops from North Lincolnshire, just south of the Humber, to the Chipping Norton area of Oxfordshire.

The MRF comprises sandy, shell-fragmental and ooidal ferruginous limestone interbedded with ferruginous calcareous sandstone, and generally subordinate ferruginous mudstone beds (BGS, 2006). Locally, any of these lithologies may pass by increase in iron content into generally ooidal ironstone, and in places any of these may dominate. The iron content (as ooids, altered shell material or in the groundmass) is berthierine, a dark green iron-rich layered silicate formed in low-oxygen marine conditions. This alters to siderite. Fossil content is variable throughout but locally abundant, especially in limestone beds. The MRF overlies mudstone/siltstone of the Dyrham Formation, or (in the north of the East Midlands Shelf) mudstone of the Charmouth Mudstone Formation. The base is typically erosive and conglomeratic. Locally the MRF may rest on a sandstone bed at the top of the Dyrham Formation, which it may be impractical to map separately from the Marlstone Rock. The upper boundary is defined by the upward change to mudstone/nodular limestones of the Whitby Mudstone Formation (BGS, 2006).

The BGS Lexicon (BGS, 2006) describes the NSF as sandy, berthierine-ooidal and sideritic ironstone. This is greenish grey where fresh, weathering to brown limonitic sandstone, typically displaying a box-stone structure. The basal part is commonly muddy and less ferruginous. The uppermost beds are generally more or less ferruginous sandstone. The unit includes lenses of mudstone and limestone in places, and contains a fairly abundant marine fauna of bivalves, brachiopods and ammonites, which are not generally evident in weathered sections. The lower boundary of the NSF is a sharp, unconformable contact with mudstones of the Whitby Mudstone Formation (Lias Group), commonly marked by a pebble bed containing phosphatic nodules and derived fossils from the underlying Whitby Mudstone (BGS, 2006). The upper boundary is generally also a sharp erosional contact, but in some places appears to be transitional. To the north of the Kettering-Peterborough area, the NSF is overlain by a generally less ferruginous sandstone, siltstone or mudstone of the Grantham Formation, which in some places contains pebbles of reworked Northampton Sand. However, to the south of Kettering-Peterborough, there is a sharp erosional contact with essentially non-ferruginous sandstone, siltstone or mudstone, of probable non-marine origin, belonging to the Stamford Member of the Rutland Formation.

5 Field investigations

5.1 EARLY FIELD STUDIES, SUMMER 2000

In 2000, four sites in the Marlstone Rock Formation of north-east and east Leicestershire (Tilton Cutting, Holwell, Branston and Eaton, Figure 1) were selected for initial fieldwork. This was a small study linked to BGS field mapping and involved field assessments by mapping geologists, petrography, palaeontology and radiometrics. The aim was to assess the variability of the MRF and its correlation in the area using the best available outcrops. The known radon risk associated with the formation and its distinctive signature on the HiRES-1 airborne data also made it a formation of interest. Gamma spectrometry was carried out in the field to assess the radioelement content of the formation and the over and underlying beds, and samples were collected for petrographic and palaeontological study.

5.1.1 Tilton cutting

Location: 2 km east of Tilton on the Hill, East Leicestershire (SK764053 to SK761056), see Figure 1.

The site is a disused cutting along the line of an old railway. The development of the railway line revealed the presence of the ironstone and was used to transport ironstone from the workings which extended both east and west of the track. These workings, to the north of the Tilton-Oakham road, were operational from 1880-1961 (Tonks, 1992). At different points along the

cutting, it is possible to access a complete section from the Dryham Formation through the MRF to the overlying Whitby Mudstone Formation.

5.1.2 Brown's Quarry, Holwell

Location: 4 km north of Melton Mowbray, North-east Leicestershire (SK742234) (Figure 1).

These former ironstone workings are now a nature reserve. They also give a complete section from the Dyrham Formation, through the MRF, to the overlying Whitby Mudstone Formation. Workings around Holwell were in operation from 1879 to 1962, the quarry visited forming the most southerly part of an extensive area of opencast sites that included a small zone where ironstone was worked underground (Tonks, 1992). The Brown's Hill quarry was worked from 1879-81, 1917-1930, underground from 1931-43 and again, in the northern part, from 1953-56 (Tonks, 1992).

5.1.3 Branston

Location: Mid-way between Grantham and Melton Mowbray, North-east Leicestershire (SK814295) (Figure 1).

A working exposes a small section of the MRF and the underlying Dyrham Formation. The top of the MRF and the overlying beds are not exposed.

5.1.4 Eaton

Location: Mid-way between Grantham and Melton Mowbray, North-east Leicestershire (SK797295) (Figure 1).

Small exposures of the MRF, without the base or top of the formation being seen, were examined just south of Eaton. These form the south-eastern end (Windmill Hill Quarry) of the former ironstone workings of Eaton Ropeway Quarries (Tonks, 1992). Opencast operations lasted from 1914 until 1948 (Tonks, 1992).

Figure 1 Site Locations in the East Midlands where field investigation and sample collection were conducted in 2000 and 2003.

5.2 2003 FIELD STUDIES

In 2003, the work begun in 2000 was extended by examining three further sites in the MRF, and adding three field sites in the NSF to the study. Field work, of a similar nature to the previous work was carried out but suites of rock samples were additionally collected from each of the sites to conduct laboratory testing. The laboratory-based work was intended to build on the results of initial investigations carried out previously into the petrographic origins of radon in the NSF, in which core samples had been examined (Hodgkinson, 2002), and to relate this approach more closely to the field-based work being done on the ironstones. A large number of potential

sites were visited briefly to determine their practicability for study, based on access permissions and extent of exposure. The final six sites (Figure 1 and Figure 2) were chosen to represent the variation in radon potential across a geographical range, and to be as near as possible to areas of housing, where a radon risk would have the biggest potential impact. The six sites were as follows:

Marlstone Rock Formation (Figure 1)

Scalford Railway Cutting, northeast Leicestershire

Pickwell Village, field bank, east Leicestershire

Sauvey Castle, stream bank, east Leicestershire.

Northampton Sand Formation (Figure 2)

Twywell Gullet: disused quarry near Kettering, Northamptonshire

Pitsford Quarry: active quarry near Northampton

Harlestone Quarry: active quarry near Northampton

Fieldwork at these sites began in Summer 2003. At each site, the accessible extent of the ironstone was recorded on lithological logs, which are given in Appendix 1 together with photographs of the exposures in Appendix 2. *In situ* permeability tests were attempted at some sites using the Temco mini- permeameter but this was found to be impractical to use under field conditions and with the relatively low permeabilities encountered. Gamma spectrometry was successfully carried out at regular intervals down through the profile at each site, and also at regular intervals, rock samples were taken to give a representative selection of lithologies throughout the depth range (see sample lists, Appendix 3). These were then returned to the laboratories for further analysis. At one site (Twywell, NSF), the exposure was overlain by a soil profile and so soil gas testing was attempted here, but this was unsuccessful.

5.2.1 Scalford Railway Cutting - Marlstone Rock

Location: near Holwell, 5 km north of Melton Mowbray, East Leicestershire (SK 753 259) (Figure 1).

The site encompassed a disused cutting along the line of one of the railways used to transport ironstone from the point of extraction (Tonks, 1992). Short exposures (up to 3 m of continuous vertical section) occur periodically along the length of the cutting, none of which reach the top or the base of the formation. Some weathered surfaces are often coloured dark pink and there are subvertical fractures filled with a pale purple cement, presumed to be manganese and iron oxides. Rare subvertical fractures are filled with white calcite. The upper layers of the sections are broken up by extensive fracturing, so it is hard to tell if the top of the formation is exposed. Samples were taken and gamma measurements carried out on a discontinuous section representing about 4 m of the formation.

5.2.2 Pickwell Village - Marlstone Rock

Location: 8 km WNW of Oakham, East Leicestershire (SK 784 115) (Figure 1).

The exposure examined, in the old quarry on the north-west side of the village, consists of a bank around two sides of a field, several metres high and containing short sections of rock face exposing 1 to 2 m of the formation. Neither top nor base of the Formation are exposed. Samples and gamma measurements were taken from four different parts of the exposure.

5.2.3 Sauvey Castle - Marlstone Rock

Location: 15 km east of Leicester (SK 787 053) (Figure 1).

At this site the exposed rocks form a high bank over a stream. They comprise 3.5 m of the MRF, down to the basal beds and the Whitby Mudstone Formation below, which forms the stream bed at one point. Samples and gamma measurements were taken and a descriptive log made throughout the exposed section.

5.2.4 Twywell Gullet - Northampton Sand

Location: 5 km ESE of Kettering, Northamptonshire (SP 942 773) (Figure 2).

Twywell Country park follows the line of an old tramway to ironstone workings (the 'gullet', Tonks, 1991), with up to 2 m continuous exposure at numerous locations along the north side (see Plate 2). The section was logged, and gamma measurements and samples taken from one exposed section about 50 m northeast of the entrance to the gullet. The rock surfaces were highly weathered, and showed good examples of 'boxwork' style alteration typical of some areas of the NSF. This comprises a network of iron oxides, deposited in cavities and along fracture planes after the oxidation and leaching of the primary iron minerals. It indicates significant re-distribution of Fe, although the overall concentrations in the rock are not altered (Taylor, 1949).

5.2.5 Pitsford Quarry - Northampton Sand

Location: 1.5 km north of the northern outskirts of Northampton (SP 757 669) (Figure 2).

Pitsford Quarry is an active quarry, operated by Peter Bennie Ltd, for stone rather than iron, although close to former iron ore workings (Tonks, 1989). Exposures of ironstone are likely to change constantly as the quarry is worked. The basal beds and the underlying Liassic mudstones were exposed in two sections. Logging, gamma spectrometry and sampling were carried out on one 3 m section of freshly exposed and highly fractured Northampton Sand (not including the basal beds) and a nearby 2 m section of lower Northampton Sand, including the basal beds and passing into the Whitby Mudstone Formation.

5.2.6 Harlestone Quarry - Northampton Sand

Location: 0.6 km northwest of New Duston in the suburbs of Northampton (SP 708 635) (Figure 2).

This is another active quarry, also operated by Peter Bennie Ltd for stone but not its iron content. When visited, the exposures of Northampton Sand were in a large open pit area (about 10 x 35 m, see front cover of report) not being worked at that time, giving continuous exposure through the overlying Grantham Formation sands and down through over 7 m of the Northampton Sand Formation, but not reaching its base. Each quarry wall has continuous exposures tens of metres long and several metres high. Logging, gamma measurements and sampling were carried out on three sides of this pit in order to access the entire exposed vertical section.

Figure 2 Site Locations in the East Midlands where field investigation and sample collection were conducted in 2003.

5.3 GROUND-BASED GAMMA SPECTROMETRY

5.3.1 Methods

At each of the ten sites, a series of gamma spectrometry measurements were made through the exposed vertical profile of the ironstone and adjacent formations. Gamma spectrometry was carried out using an Exploranium GR-320 with a 76 x 76 mm NaI (Tl) detector. The GR-320 NaI (Tl) detector was internally stabilised with a small ^{133}Ba source. The position of the ^{133}Ba peak in the spectrum, the Full Width Half Maximum (FWHM) of the peak and the system gain were

tested at the start and end of each day of data collection to ensure the instrument was working correctly.

The detector was calibrated on the BGS radiometric calibration pads prior to, and after fieldwork. The four calibration pads comprise: 3 pads with known concentrations of K, U and Th and one 'blank' pad which allows the background contribution from the concrete to be subtracted. Measurements on each pad enable stripping ratios to be calculated which remove the influence of other radionuclides from each region of interest (ROI) therefore leaving only net counts of K, eU and eTh in their respective ROI. The sensitivity for each ROI (counts per second in each ROI per unit concentration of K, U and Th) can then be calculated from the known concentrations in each pad. Geometry correction must also be made, as the calibrations pads do not represent an infinite source. The background of the instrument itself is subtracted. This is obtained by measurements over a large water body from a boat.

The stripping ratios, the sensitivity, the geometric conversion factor and the instrument background are all taken into account during data processing in the Explore software (Grasty, *et al*, 1991) allowing counts to be converted to concentrations of K (%), eU (ppm) and eTh (ppm).

Typical count times were 30 s for each gamma measurement, with the detector placed against the rock face to minimise the field of view. This gives an effective sample of around 40-50 kg from a radius of about 40 cm and depth between 10-15 cm (Løvborg *et al*, 1974). As far as possible 2 π solid angle geometry was maintained between the detector and the rock face i.e. the detector was held perpendicular to the face where the rock surface was as close to a continuous flat surface as was possible.

In addition to the static measurement of ironstone exposures, the same instrument was used for a limited investigation of higher gamma response over the MRF observed in the HiRES-1 airborne geophysical survey (Peart et al, 2003). Some limited measurements in 2000 had failed to replicate airborne anomalies on the ground. In this work the GR320 spectrometer was mounted in a backpack and data were recorded into a Husky ruggedised PDA every 5 seconds whilst the operator walked slowly over the ground. Positions from a GPS, also linked to the PDA, were merged with each spectrometer point using a customised version of PocketGIS™ software. Data were calibrated in a similar way as for the static measurements using each 5 s data point as well as moving sums (created by adding together adjacent data points) to improve counting statistics.

In the case of all the gamma spectrometry measurements it should be noted that an equivalent uranium (eU) value is determined from the ^{214}Bi gamma peak and an equivalent thorium (eTh) value is determined from the ^{208}Tl gamma peak. This is because adequate gamma peaks cannot be recorded directly from U or Th themselves, so daughter products are used to determine an equivalent value and equilibrium with the parent U or Th is assumed.

5.3.2 Results; Marlstone Rock Formation

5.3.2.1 TILTON CUTTING

The results of gamma spectrometry are shown in Figure 3. They combine data from three different points in the cutting; the top part of the section (Whitby Mudstones) was measured around SK 76400 05300, the MRF and the upper part of the Dyrham Formation at SK 76225 05448 and the basal part of the exposure further north, near access to the cutting at SK 76135 05586. The MRF had generally higher total counts than the Whitby Mudstones or Dyrham Formation. This was reflected in consistently higher eTh, whilst eU showed some higher values and some that were within the range of those from the adjacent formations. On the other hand, K concentrations were generally lower in the MRF than the Whitby mudstone Formation.

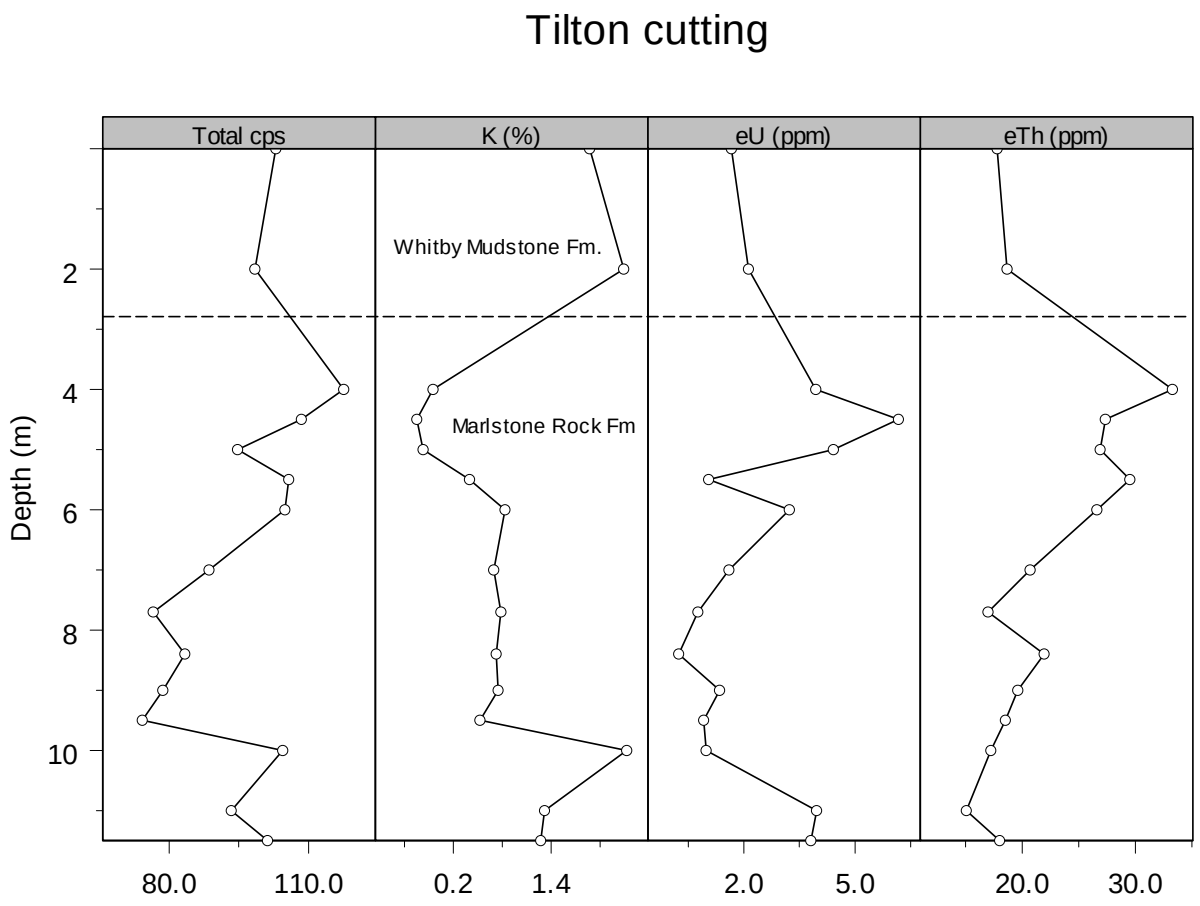

Figure 3 Tilton Cutting gamma spectrometry profiles showing total counts (cps), potassium (K, %), equivalent uranium (eU, ppm) and equivalent thorium (eTh, ppm) with depth down the exposed rock profile. Approximate boundaries between rock formations are shown.

5.3.2.2 BROWN'S QUARRY, HOLWELL (SK 74213 23372)

Gamma spectrometry data are given in

Figure 4. Total counts were consistently higher in the MRF, in spite of the K levels being always lower than the Whitby Mudstones or the Dyrham Formation. As at Tilton, eTh was always higher, if somewhat variable, in the MRF whilst eU was the most variable radioelement with a similar range of values in all three formations.

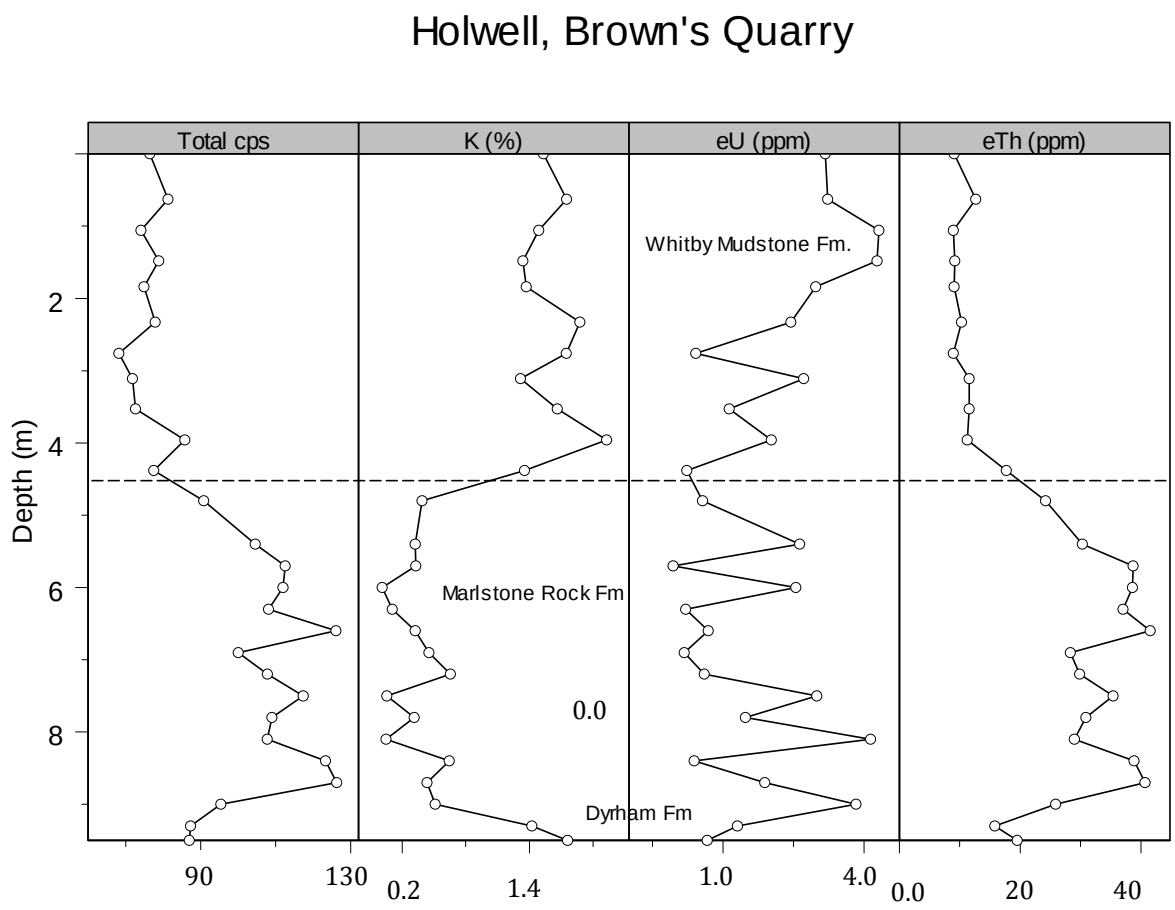

Figure 4 Brown's Quarry, Holwell. Gamma spectrometry profiles showing total counts (cps), potassium (K, %), equivalent uranium (eU, ppm) and equivalent thorium (eTh, ppm) with depth down the exposed rock profile. Approximate boundaries between rock formations are shown.

5.3.2.3 BRANSTON (SK 81350 29460)

Only the MRF and a small part of the Dyrham Formation were exposed in the Branston section (Figure 5) but the picture is similar to that at Holwell. Total count and eTh were higher in the MRF and K was lower, whereas eU values were not markedly different between the two formations.

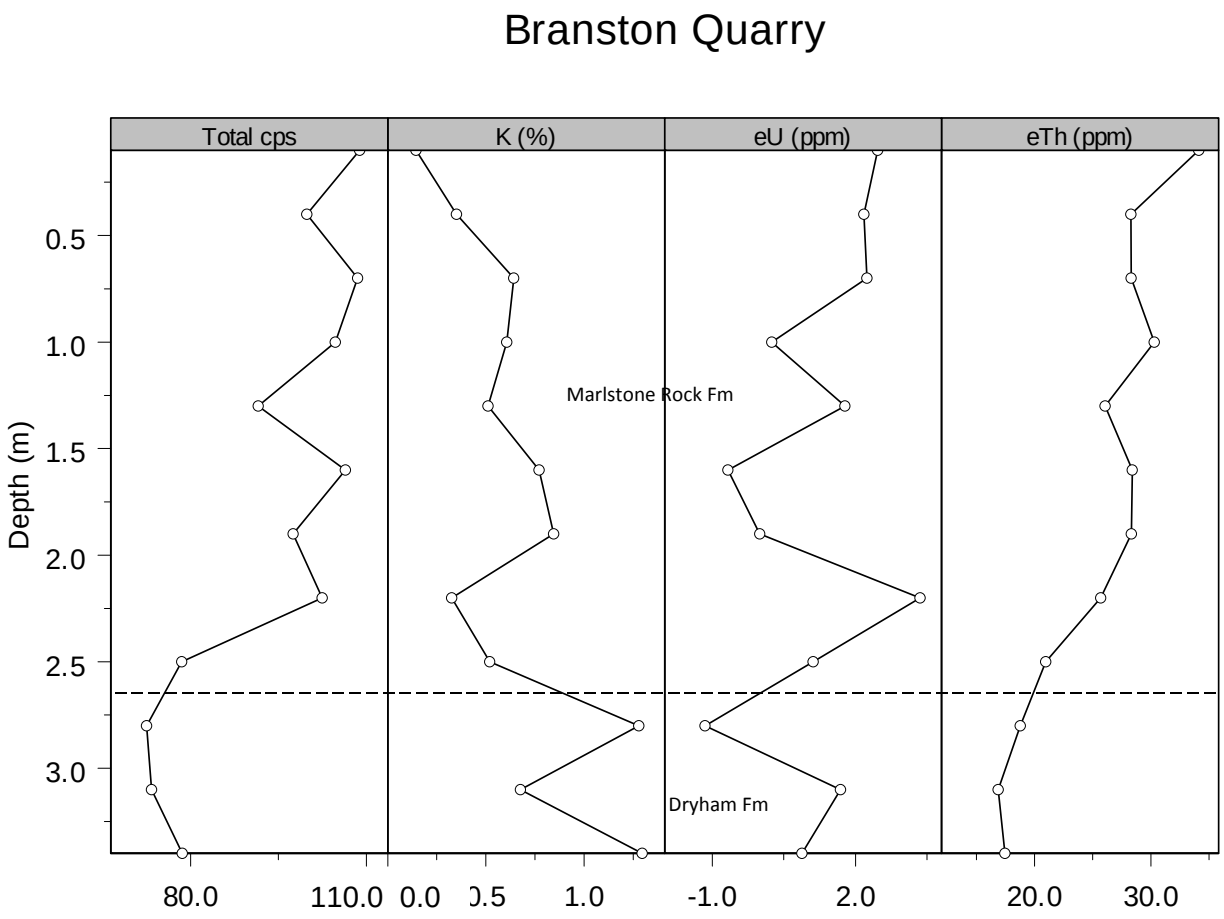

Figure 5 Branston Quarry gamma spectrometry profiles showing total counts (cps), potassium (K, %), equivalent uranium (eU, ppm) and equivalent thorium (eTh, ppm) with depth down the exposed rock profile. Approximate boundaries between rock formations are shown.

5.3.2.4 EATON (SK 79580 28330)

The old ironstone workings at Eaton, exposed only part of the MRF but the data (Figure 6) were consistent with the formation in other sections. Total counts were in the range 80-120 cps, K was below 1 %, eTh above 20 ppm and eU – the most variable of the three – in the range 0-5 ppm.

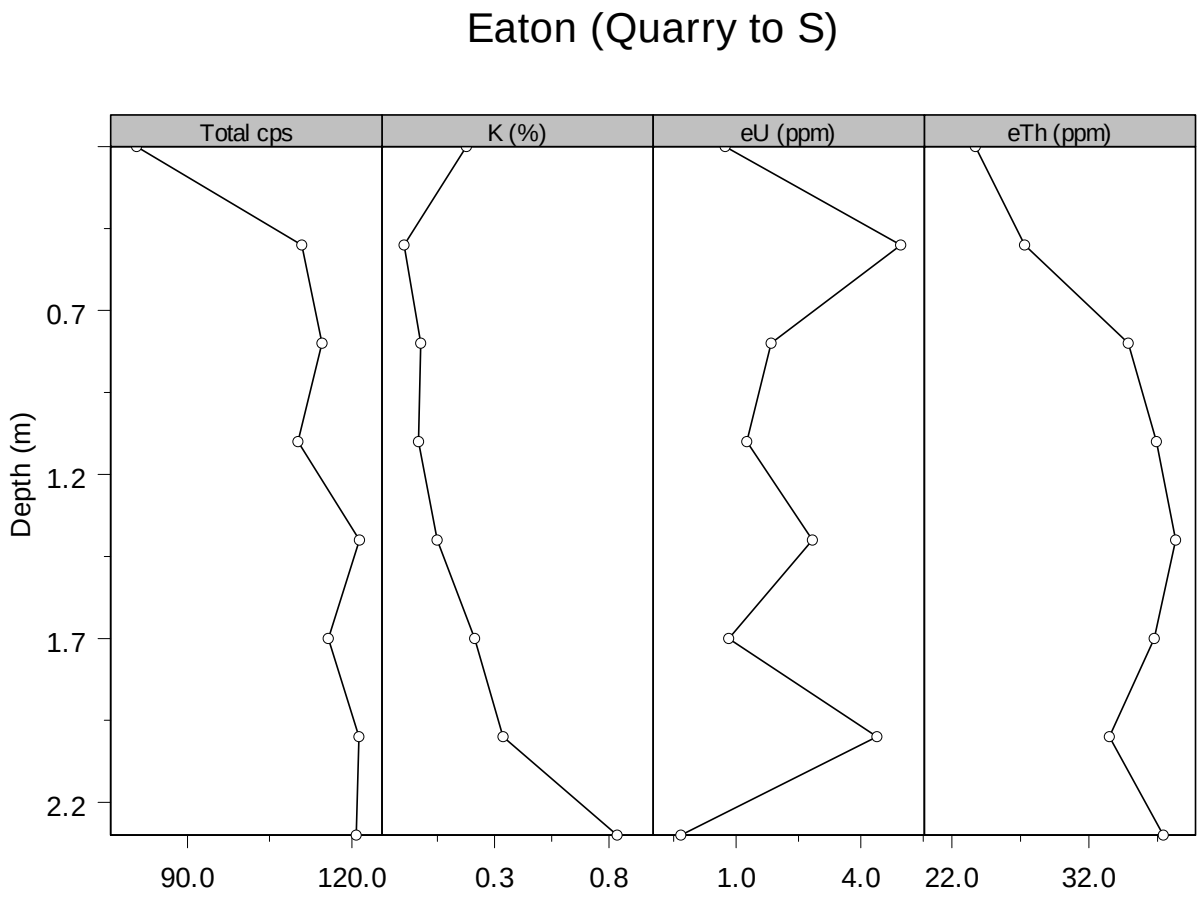

Figure 6 Eaton gamma spectrometry profiles showing total counts (cps), potassium (K, %), equivalent uranium (eU, ppm) and equivalent thorium (eTh, ppm) with depth down the exposed rock profile (MRF).

5.3.2.5 SCALFORD RAILWAY CUTTING (SK 75250 25900)

The gamma spectrometer readings were taken from two adjacent exposures some 5 m apart and are shown in Figure 7. As at Eaton, the over- and underlying formations were not exposed but a similar range of radioelement concentrations was observed here when compared to the other site profiles. As at Eaton and Holwell, there was a general increase of total counts and eTh with depth.

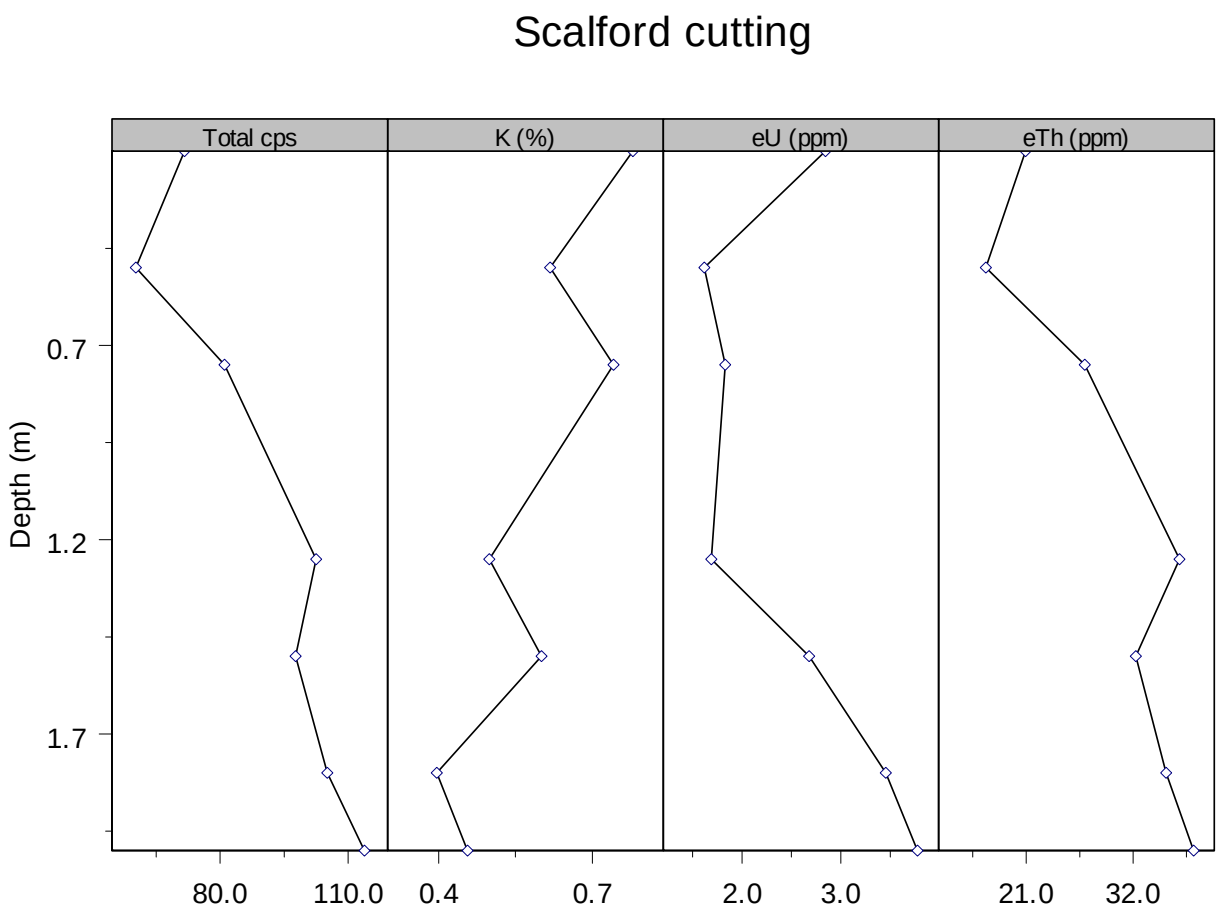

Figure 7 Scalford cutting gamma spectrometry profiles showing total counts (cps), potassium (K, %), equivalent uranium (eU, ppm) and equivalent thorium (eTh, ppm) with depth down the exposed rock profile (MRF).

5.3.2.6 PICKWELL VILLAGE (OLD QUARRY AT SK 78425 11515)

Gamma measurements were made at a number of points in the old quarry. Data from the two longest sections are presented in Figure 8. Ranges of total counts and concentrations of the radioelements are similar to those for the MRF from other sections.

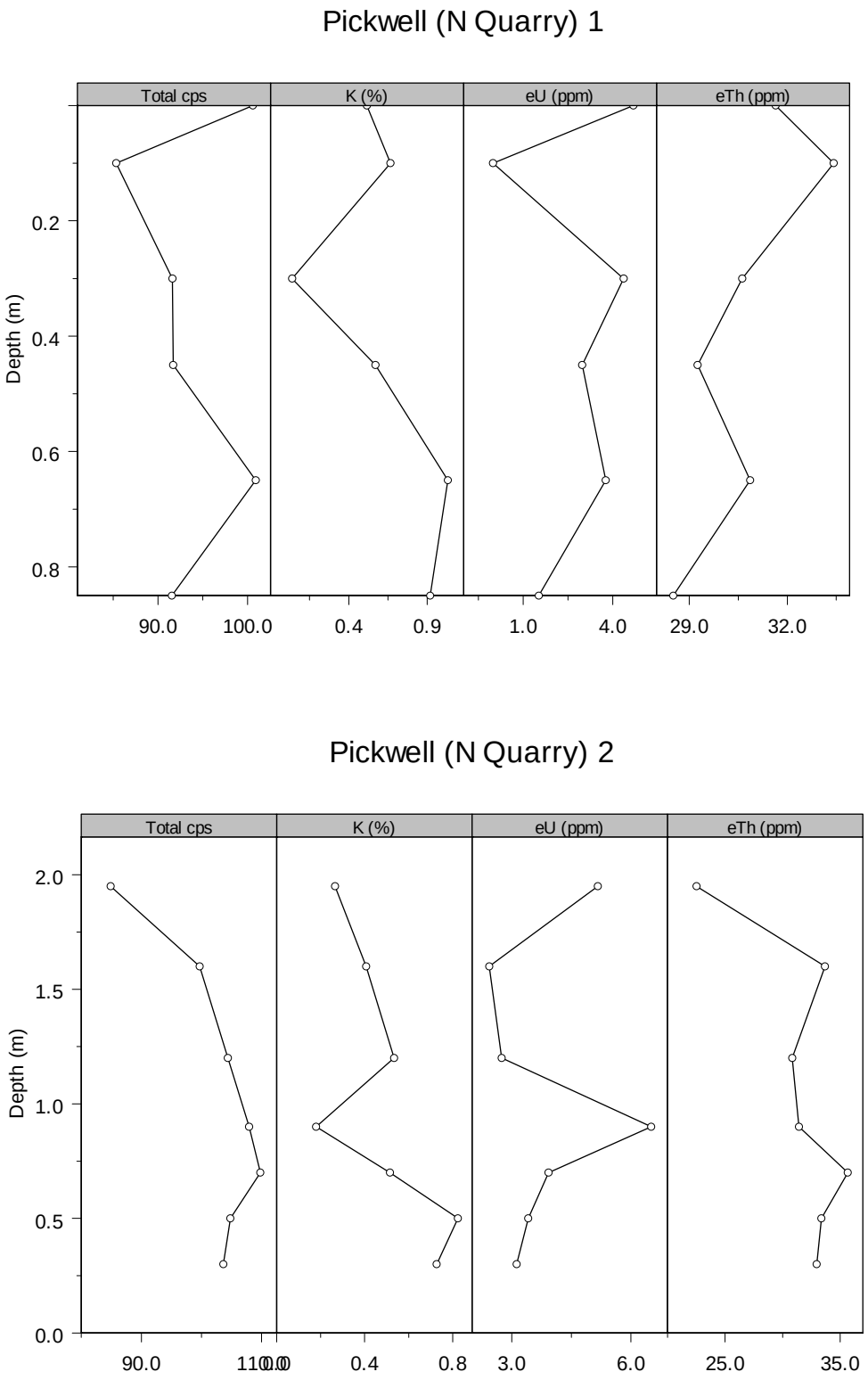

Figure 8 Pickwell gamma spectrometry profiles showing total counts (cps), potassium (K, %), equivalent uranium (eU, ppm) and equivalent thorium (eTh, ppm) with depth down the exposed rock profile (MRF).

5.3.2.7 SAUVEY CASTLE (SK 78535 05303)

The small stream section to the north of the castle was measured from the MRF down to the underlying mudstones of the Dyrham Formation that crop out in the stream bed. Total count declines generally from the top of the section towards the base from over 100 to around 70 cps, but then increases at the base and into the underlying beds to 90 cps (Figure 9). As elsewhere, eTh is consistently higher in the MRF. It shows a general decline with depth, as seen at Branston and one of the Pickwell sections, but not elsewhere. Potassium is once again lower in the MRF than the Dyrham Formation, whereas eU fluctuates with depth more than the other radioelements.

Figure 9 Sauvey Castle gamma spectrometry profiles showing total counts (cps), potassium (K, %), equivalent uranium (eU, ppm) and equivalent thorium (eTh, ppm) with depth down the exposed rock profile. Approximate boundaries between rock formations are shown.

5.3.3 Results; Northampton Sand Formation

5.3.3.1 TWYWELL GULLET (SP 94261 77309)

A section was logged through the exposed part of the Northampton Sand Formation and the gamma spectrometry results are presented in Figure 10. The data were remarkably similar to those from the MRF with similar ranges of values: total count 75-95 cps, K 0.2-0.8 %, eU approximately 2-4 ppm and eTh 22-32 ppm. No comparison was possible at this site with the over- and underlying formations due to the lack of bedrock exposure.

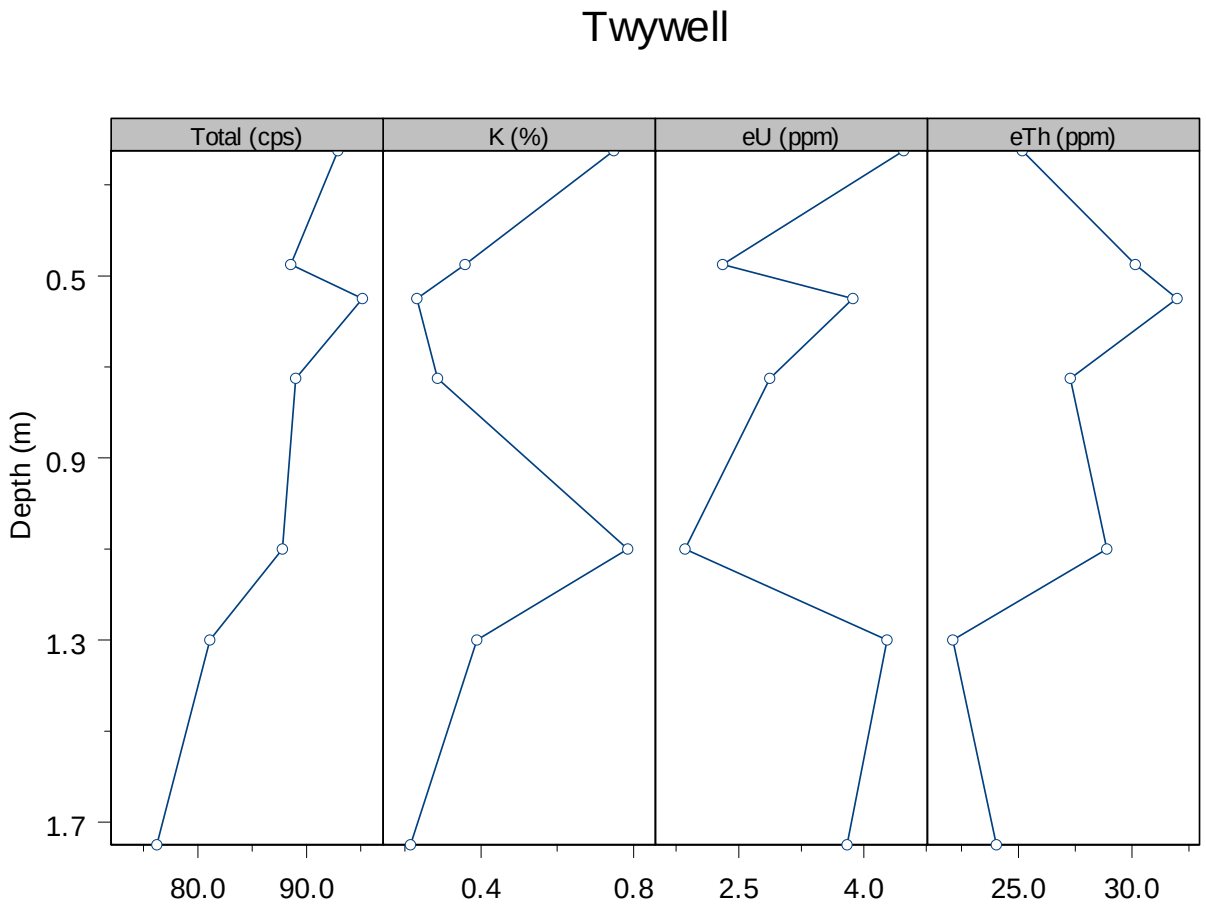

Figure 10 Tywell gamma spectrometry profiles showing total counts (cps), potassium (K, %), equivalent uranium (eU, ppm) and equivalent thorium (eTh, ppm) with depth down the exposed rock profile (NSF).

5.3.3.2 PITSFORD QUARRY (SP 75717 66891)

Figure 11 shows the combined measurements from the two separate exposures at Pitsford. In common with the MRF, the concentrations of K were lower in the NSF and eTh generally higher than values in the underlying Whitby Mudstone Formation. There appeared to be a general increase of eU and decrease in eTh with depth in the NSF. Radioelement concentrations were mostly similar to those at Twywell, although eTh was below 20 ppm in the lower part of the section.

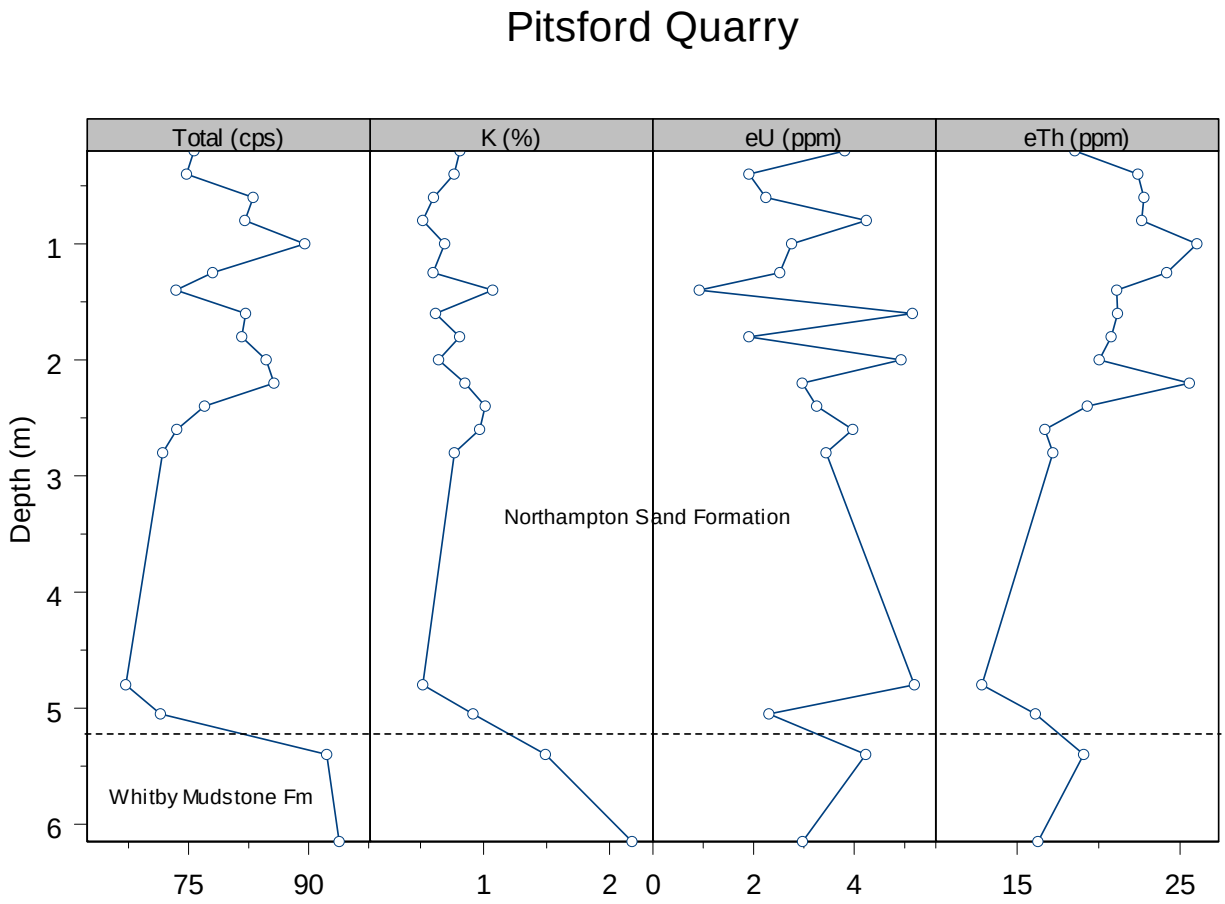

Figure 11 Pitsford Quarry gamma spectrometry profiles showing total counts (cps), potassium (K, %), equivalent uranium (eU, ppm) and equivalent thorium (eTh, ppm) with depth down the exposed rock profile. Approximate boundaries between rock formations are shown.

5.3.3.3 HARLESTONE QUARRY (SP 70761 63545)

Gamma spectrometry results from throughout the quarry have been compiled in Figure 12. The data from this locality are significantly different from those from other sections; concentrations of K are higher (almost all being above 1 %), eU and eTh are lower with values mostly less than 2 ppm and 15 ppm, respectively.

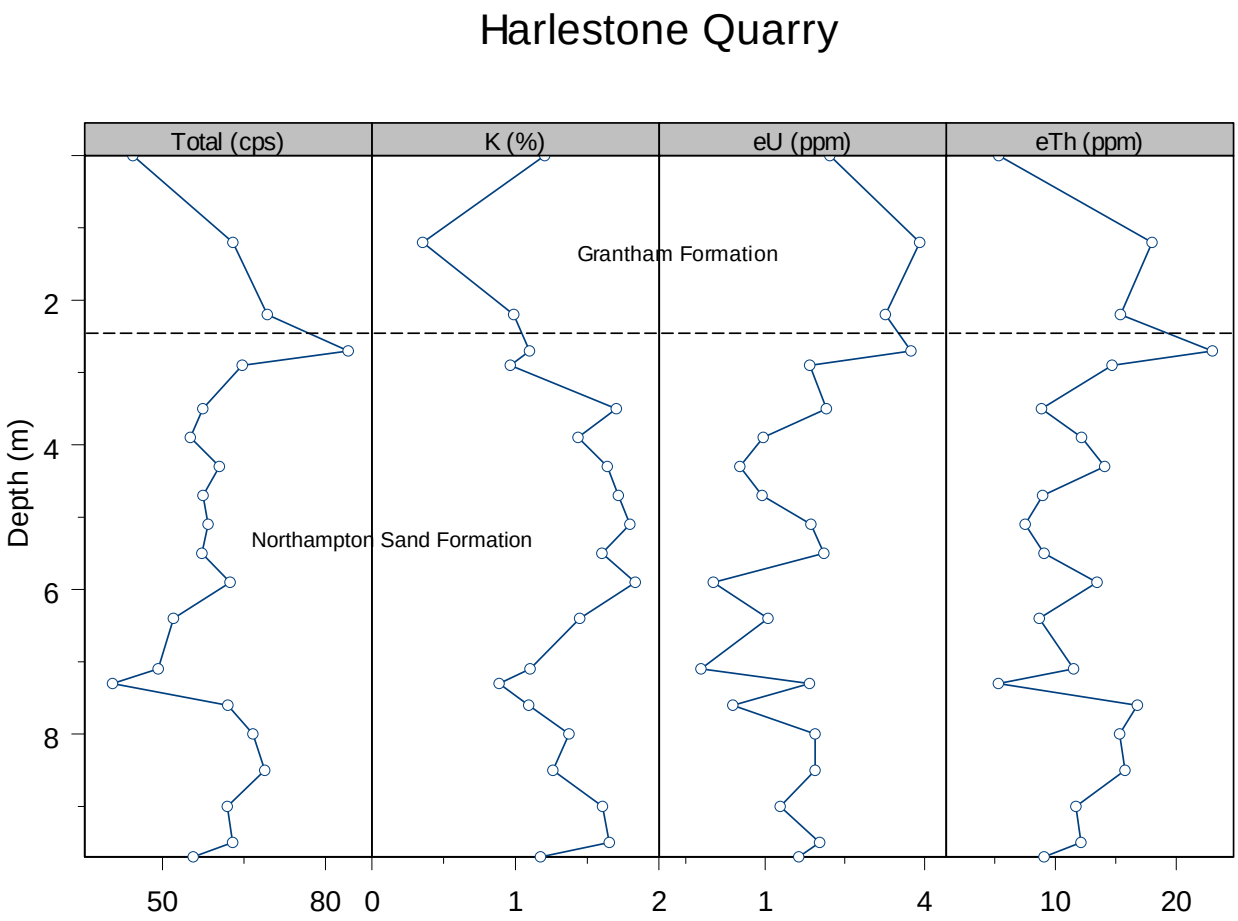

Figure 12 Harlestone Quarry gamma spectrometry profiles showing total counts (cps), potassium (K, %), equivalent uranium (eU, ppm) and equivalent thorium (eTh, ppm) with depth down the exposed rock profile. Approximate boundaries between rock formations are shown.

5.3.4 Results from ground follow up of airborne data

Mobile ground gamma data were collected in three separate areas:

- Holwell, Leicestershire; approximately 5 km NNE of Melton Mowbray (SK473500, 324000).
- Wycomb, Leicestershire; approximately 6 km NNW of Melton Mowbray (SK477400, 325300).
- Harston, Leicestershire; approximately 8 km SW of Grantham (SK483500, 332350)

These data are presented in Figure 13 to Figure 16. Earlier limited investigations at the most southerly site near Holwell had suggested there were problems matching the airborne anomalies on the ground. However, the larger set of measurements presented here indicate a good agreement between the airborne and ground eTh data (Figure 13a). There are differences in detail but this is to be expected given the large area over which the airborne data are averaged relative to the ground measurements and the more limited number of airborne points. Higher eTh values are seen to occur over areas of worked (and infilled) and unworked MRF, in the ground data (Figure 14), and the sandstones of the upper part of the Dyrham Formation ('Sandrock'). Potassium is rather variable over the infilled Marlstone workings (Figure 14) perhaps reflecting heterogeneous fill material. Potassium values are generally lower over the Dyrham Formation sandstones and higher on the siltstones and mudstones as would be anticipated.

The central site (near Wycomb) and northerly site also show very good agreement between airborne and ground eTh data (Figure 13b and c, respectively). At Wycomb the area is free of ironstone workings and the higher eTh values appear to correspond to the upper part of the Dyrham Formation and lower part of the MRF as mapped (Figure 15). This could, however reflect slippage of MRF debris downslope onto the Dyrham Formation.

The northerly site (near Harston) consists partly of worked ground (Figure 16), but unworked areas still show higher eTh levels. The data here show a good contrast with much lower levels of eTh and higher K concentrations on the underlying Dryham Formation and Charmouth Mudstone Formation (Figure 16). The eU data are more variable but generally higher on the Marlstone and thus comparable to the outcrop measurements.

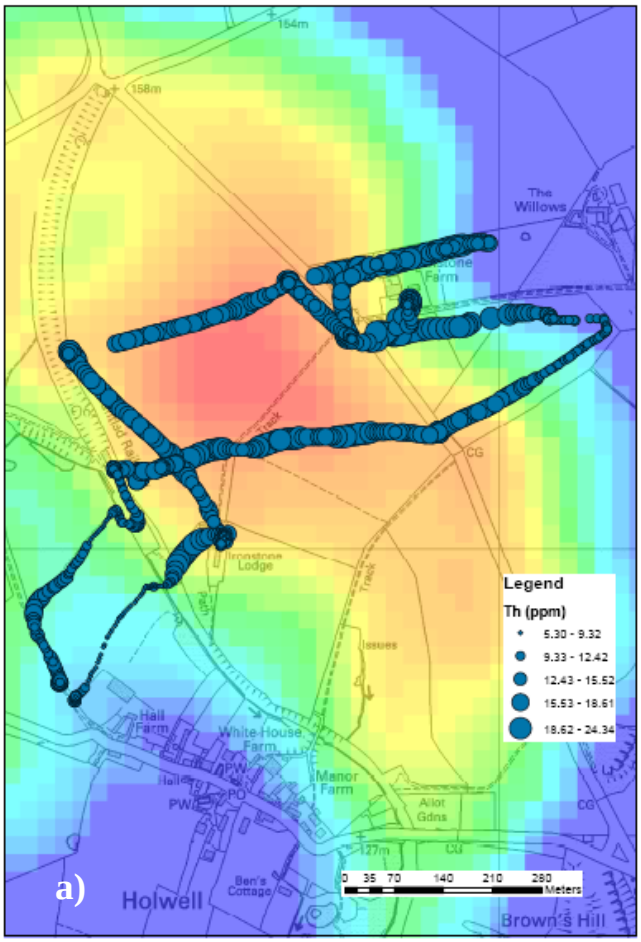

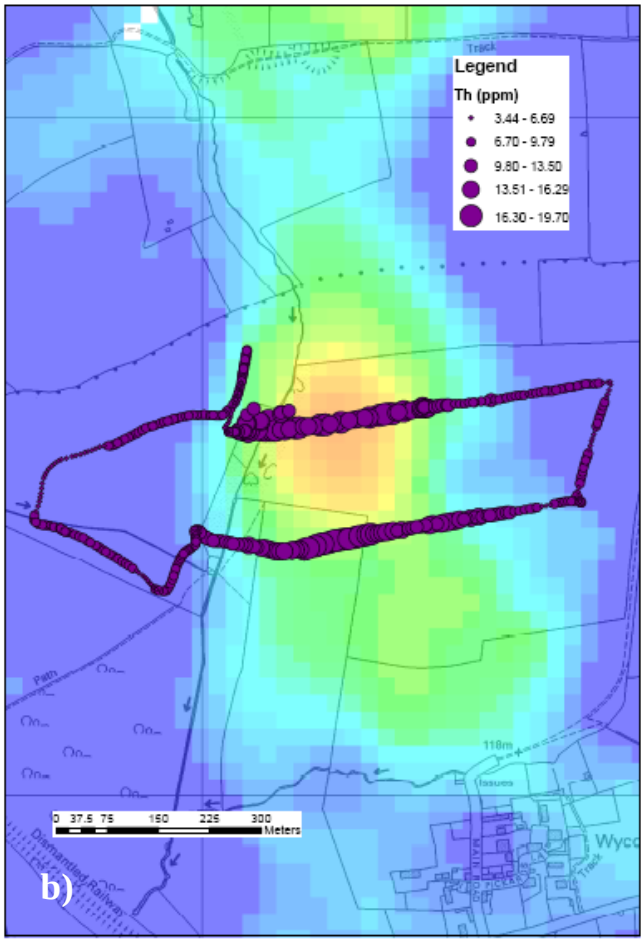

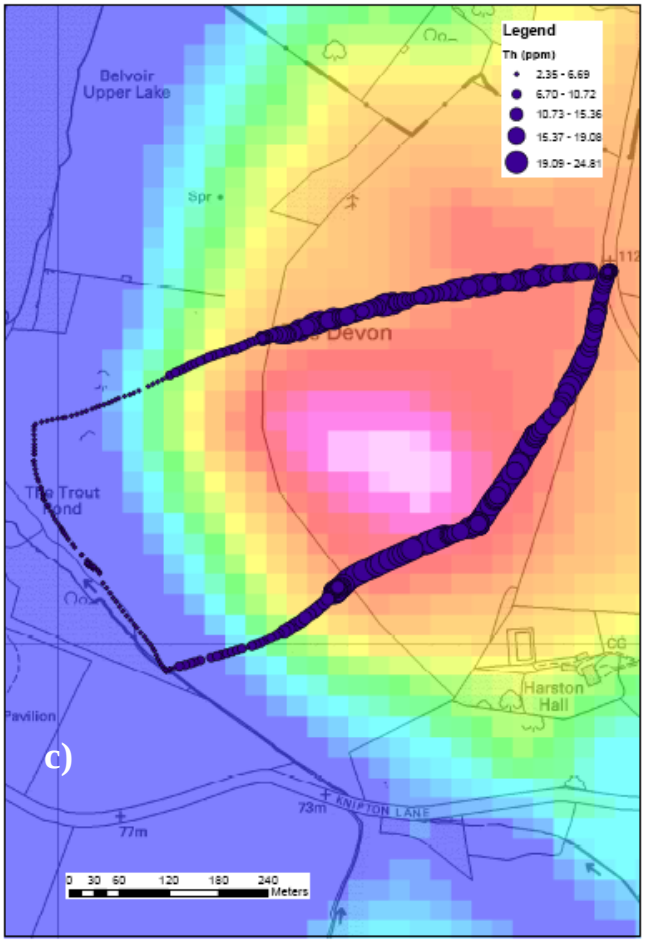

Airborne Survey eTh data

- ~21 – 22 ppm eTh
- ~20 – 21 ppm eTh
- ~ 19 – 20 ppm eTh
- ~15 – 18 ppm eTh
- ~ 12 – 14 ppm eTh
- ~10 – 12 ppm eTh
- < 10 ppm eTh

Figure 13 Mobile ground gamma spectrometry results for: a) Holwell, b) Wycombe and c) Harston superimposed on airborne gamma spectrometry data from the HiRES-1 survey.

5.3.5 Discussion of field gamma data

Certain general conclusions can be drawn from the field gamma spectrometry of outcrop sections and the mobile gamma data, where measurements were mostly on soil and/or superficial deposits over bedrock:

- The ironstones usually have higher total gamma and eTh and lower K than the adjacent beds above and below.
- The ironstone values for eU are quite variable but concentrations mostly are in the same range as the over- and underlying formations, but the range of values over the MRF is greater and includes higher values than the adjacent strata.
- The data for the NSF at Harlestone stand out as being different, with lower eTh and eU and higher K than other ironstone sections. This appears to be due to the presence of the 'Variable Beds' at the top of the NSF succession here, which have a different character to the other parts of the NSF.
- Gamma profiles through the MRF and NSF cannot be correlated between locations. This is consistent with a high degree of lateral variation within the formations. Whitehead et al (1952) could not recognise any definite divisions within the MRF that are of more than local significance. They describe lenses of highly fossiliferous calcareous stone and local non-sequences. The NSF is of similarly variable character; Hollingworth and Taylor (1951) show that within a broad overall stratigraphic scheme there are considerable lateral changes that are visible in individual exposures.

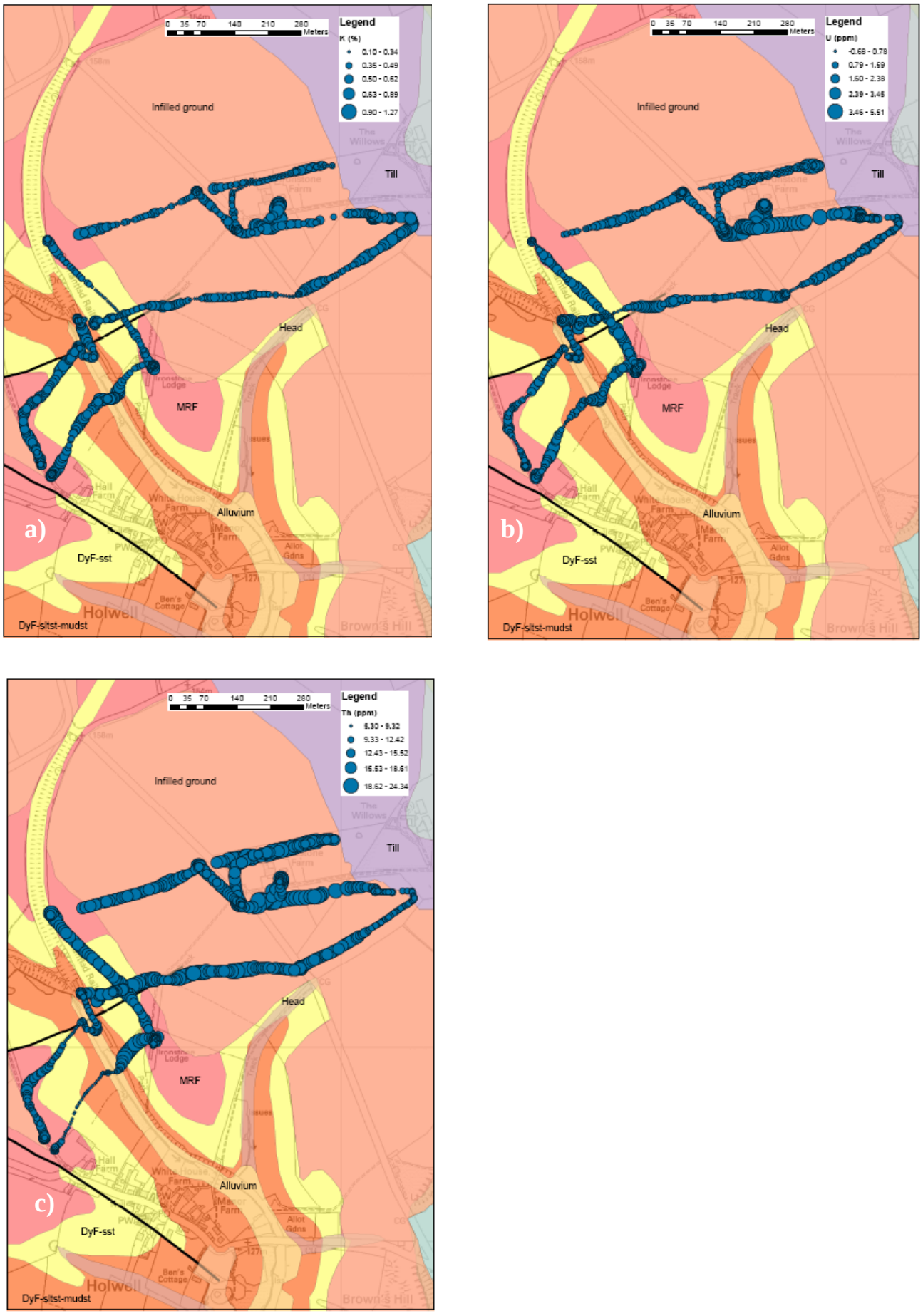

Figure 14 Mobile ground gamma spectrometry results for the Holwell area showing: a) K (%) b) eU (ppm) and c) eTh (ppm) superimposed on 1:50,000 scale bedrock and superficial geology.

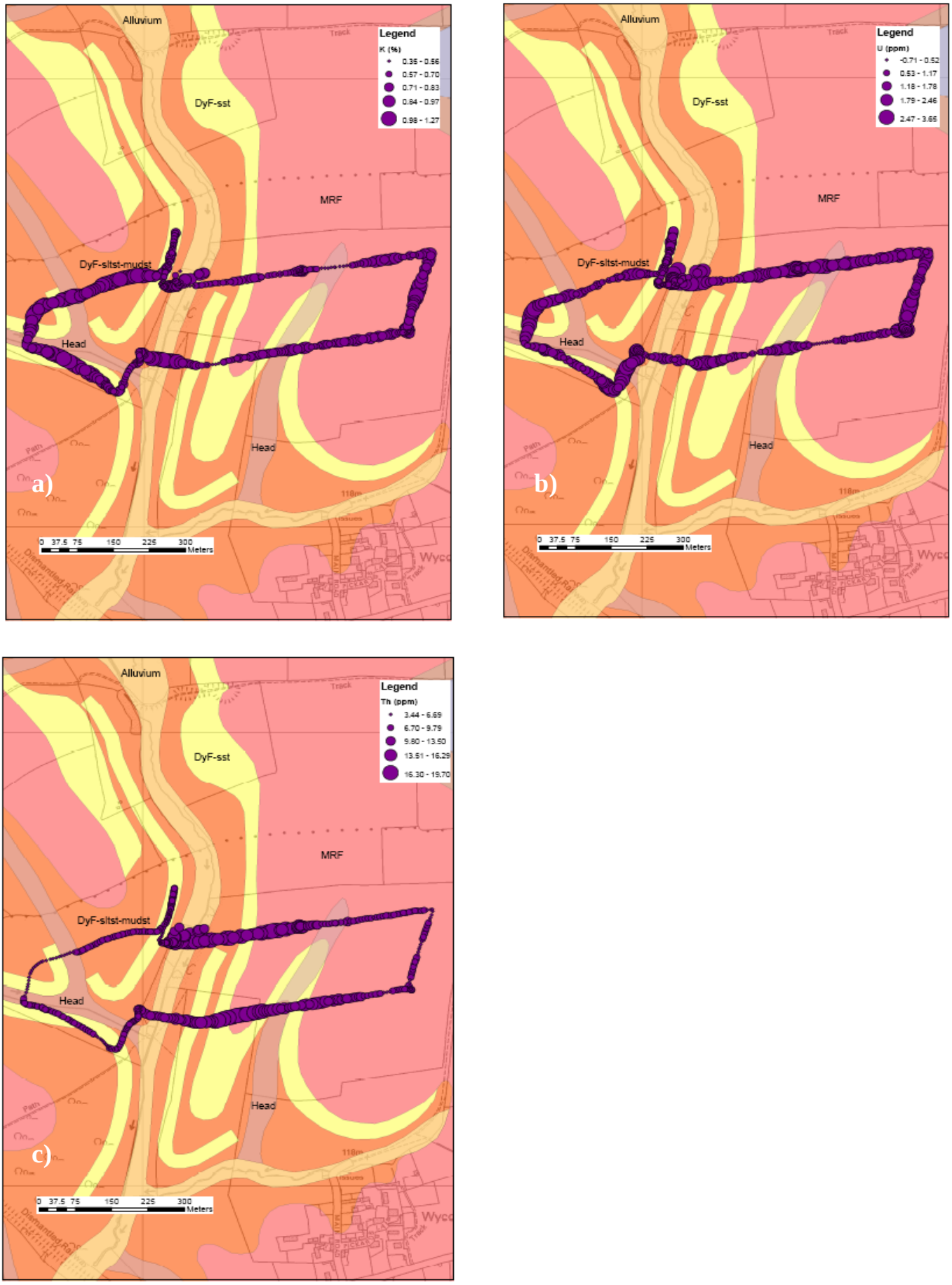

Figure 15 Mobile ground gamma spectrometry results for the Wycombe area showing: a) K (%) b) eU (ppm) and c) eTh (ppm) superimposed on 1:50,000 scale bedrock and superficial geology.

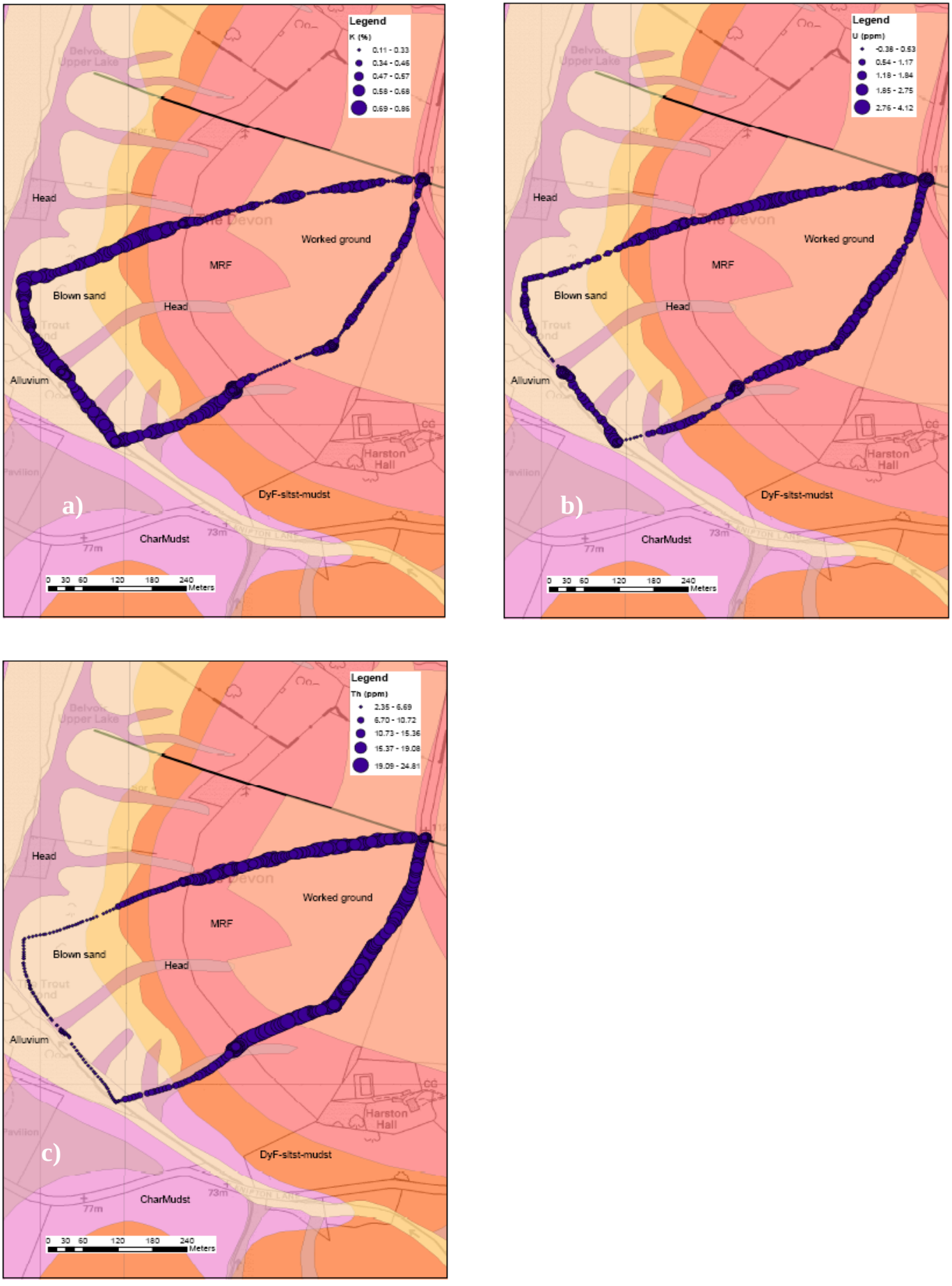

Figure 16 Mobile ground gamma spectrometry results for the Harston area showing: a) K (%) b) eU (ppm) and c) eTh (ppm) superimposed on 1:50,000 scale bedrock and superficial geology.

6 Laboratory-based studies

6.1 PETROGRAPHIC STUDIES: ALPHA RADIOGRAPHY AND SEM PETROGRAPHY

A sub-set of 57 field specimens were chosen for further analysis by petrographic methods (see sample list, Appendix 3). Autoradiographic registration of alpha-particle emission from geological materials makes it possible to locate, quickly and effectively, sources of high radioactivity prior to identification by chemical and/or mineralogical methods. At the time of this investigation, autoradiography could provide information only on the location and relative level of alpha particle emission in a specimen and as such must be considered a precursor, albeit an essential one, to a more detailed microscopic study. In this case, 37 samples were sliced and analysed by autoradiography. The radiographs were examined under an optical microscope to locate radiographic alpha particle 'hotspots'. Some of the samples were then prepared for more detailed examination by scanning electron microscopy, in order to confirm the petrographic and mineralogical identity of the radiographic hotspots located.

6.1.1 Methods

Each hand specimen was sliced so that it could be laid flat on a tray with another smooth, flat, horizontal surface lying uppermost. These slices ranged from about 3 x 5 cm up to about 10 x 20 cm in size. The uppermost surfaces of some of the specimens were polished for a few hours in order to ensure good contact with the radiography film. Alpha-particle autoradiography was carried out following the technique described by Basham (1981), using 'CR39' plastic film. This a highly sensitive thermoset polymer with particularly high optical qualities (transparent), with high track resolution and uniform response to alpha particles of energies up to 6 MeV created during radioactive decay of radioelements in the rock samples. Each specimen slice was first cleaned with ethanol to remove all traces of preparatory residues (e.g. rock-saw lubricants etc.) that could contaminate the CR39. A piece of CR39 film was then placed on it and attached with sticky tape. Close even contact was ensured by placing a piece of foam packaging sheet over the film and binding the assembly firmly between two rigid pieces of MDF. All the specimens were then placed in a drawer where they would not be physically disturbed, and left for about 7 weeks. After exposure the CR39 was carefully removed and cleaned with ethanol to remove any materials which may interfere with the etching process, such as residues from the sticky tape. The sheets of film were etched by suspension in a beaker containing an aqueous solution of 6N NaOH at 80 ºC in order to make the alpha tracks visible. During etching the film was periodically removed, rinsed with water, and placed under an optical microscope to monitor track-etch development. After 4-5 hours, the tracks were visible under a microscope and the film was rinsed with water and cleaned again with ethanol.

The films were examined under an optical microscope to identify alpha-particle tracks marks and observe their spatial distributions. These were broadly mapped out by marker pen onto the film and then matched back to the original slices in order to select interesting areas for further analysis by Scanning Electron Microscopy (SEM).

The areas selected for SEM analysis were prepared as much smaller (3 to 4 cm diameter) polished blocks, which were carbon-coated before examination in the SEM. A Leo 435 VP Scanning Electron Microscope was used to examine the blocks. It was operated in Back-Scattered Electron Imaging mode, which produces images whose brightness is related to average atomic density, thus allowing regions and phases of differing chemical composition to be distinguished. Semi-quantitative chemical analysis of individual phases was performed using an ISIS 300 Energy-Dispersive Spectrometer.

6.1.2 Results of alpha autoradiography and SEM

Some general comments on the distribution patterns of alpha tracks can be made. After etching, alpha tracks were visible on all the films and a number of patterns in their distribution were observed. The tracks generally were present in relatively low spatial density (compared to other BGS work with highly radiogenic materials). On many films, alpha tracks occurred in greater density *outside* the perimeter of the rock slices, i.e. where the film was only in contact with air! High track densities also occurred in the places adjacent to cavities in the specimens, where the rock matrix did not come into direct contact with the film. These tracks may originate from a combination of radon gas emitted from the specimens into the air, and possible extra sources from dust in the drawer, whose history of use was unknown but suspected to include radiogenic rock storage at some point in the past.

Calcite bioclasts and fracture fills have no alpha tracks at all, while the fine grained, iron-rich matrix of all the samples acts as a widespread, diffuse low-level alpha source. This diffuse background source sometimes marks out inter-grain boundaries, possibly because the sand-sized grains visible at this scale may be calcite. In some specimens though, the surface of an occasional sand-sized grain appears to actually be the source, producing a circle of single tracks that follows its perimeter. Point sources, often small and very intense, are found in most of the specimens and are distributed unevenly throughout the matrices of the specimens. Very occasionally, centimetre-sized diffuse sources are seen.

6.1.2.1 NSF - TWYWELL

The lithology here is oolitic, with clay/calcite ooliths in a originally clay-rich matrix now largely replaced by Fe oxides (e.g. Plate 8). Towards the top of the formation (TW01), the rock is heavily altered by replacement of both ooliths and matrix with Fe oxides, and by Fe oxide vein/fracture mineralisation (Plate 9). Here, most ooids have empty centres, surrounded by surviving layers of Fe-rich clay (Plate 10). The matrix in TW01 (including an earlier rhombic cement) is almost entirely replaced by Fe oxide.

Auto-radiography showed that the rock matrix in all samples is a source of diffuse, widespread alpha-tracks, occasionally visibly outlining intergrain boundaries. In one specimen (TW01) diffuse sources are concentrated into spots and patches, including patches where the matrix is a yellow ochre colour. These matrix sources are most likely to be associated with either Fe oxide (potentially goethite), and/or surviving primary clay matrix.

Slightly higher concentrations of alpha tracks sometimes occur parallel to bedding planes and along small cracks and iron oxide-filled veinlets, but not the thicker bands of Fe oxide cement which form the boxwork style alteration. Examination by SEM revealed the presence of phosphate pellets in TW04, generally small but rarely as large as 1 mm (Plate 11). These consist of a mixture of Ca-Al phosphate and Fe oxide with some detrital micas. They can be overgrown by phosphate cement, which also occurs as a late, local matrix cement (Plate 12). Both pellets and matrix cement occur along phosphate-rich mineralised bands, parallel to fractures, which may correspond to the lines of alpha sources seen. The large amounts of phosphate seen in sample TW04 correspond to this sample having the highest level of phosphate as determined by XRF (see Section 6.4).

Point sources were only seen in one specimen (TW01 - the uppermost); they are large and not particularly intense and appear in regions where zircons and monazites were identified as rare detrital components.

6.1.2.2 NSF - PITSFORD

The rock matrix is a source of diffuse, widespread alpha-tracks, often visibly outlining intergrain boundaries. Some patches of higher than average matrix tracks occur, but many of these may

correspond to cavities or places where the rock did not touch the film surface. Centimetre-sized diffuse sources are seen in three of the specimens (PI04, PI08 and PI10) and were confirmed by SEM to be pellets of pure Ca phosphate (e.g. Plate 13) but they are not particularly abundant.

The basal nodular bed (PI10) is not oolitic, but is a siliclastic sand with coarse calcareous bioclasts (Plate 14). It contains rare zircons which are likely to be point sources for alpha tracks; numerous point sources were identified by autoradiography in the uppermost and lowermost specimens (PI01 and PI11) but were rare elsewhere.

6.1.2.3 NSF - HARLESTONE

The upper parts of the Formation at Harlestone consist of a siliclastic sandstone with a minor oolitic content (e.g. Plate 15). The ooids and the matrix are of Fe-rich clay and an Fe oxide cement coats all grain surfaces in a meniscus style, leaving regions of vuggy, poorly interconnected porosity. The lower parts of the Formation are also of a siliclastic, ocasionally slightly oolitic sandstone, but are tightly cemented by sparry calcite (Plate 16). The concentration of alpha tracks is generally low for all these specimens. Alpha tracks associated with the rock matrix occur in higher concentrations in specimens from the upper levels (i.e. HQ03, HQ04 and HQ07) but the concentrations are very low in specimens from lower down in the formation. This may reflect the presence or absence of the calcite matrix cement, implying that the source of matrix alpha tracks is the Fe-rich clay and/or Fe oxide cement.

Relatively large point sources of alpha tracks occur in specimens from the upper levels (HQ03 to HQ09). They are most abundant in the uppermost specimen, HQ03, where zircons are relatively numerous amongst the detrital grains.

In the lower parts of the Formation (HQ09 and HQ12), the ooliths consist mainly of calcite and Fe-rich clay (probably a chlorite) with some kaolinite books. Small amounts of Ca phosphate are present in the form of occasional pellets (Plate 17), a fine grained cement forming narrow rings of inner oolite (Plate 18), and part of a late cement in association with Fe oxide (Plate 19). Auto-radiography revealed occasional sand grain-sized circular outlines of alpha tracks which may correspond to the occasional phosphate cement seen in ooliths here.

There are occasional bands of late, Fe-rich cement throughout the Formation. In the upper parts, one of these was seen to contain a fine grained, tabular Fe-Si-K-sulphate phase, possibly jarosite (Plate 20). Elsewhere, a late Fe oxide cement replaces pyrite and a rhombic phase (possibly siderite) and forms veinlets and wide mineralised bands. Diffuse alpha sources are occasionally concentrated along red-stained bedding planes and iron oxide-filled veinlets but are not associated with the thick, Fe oxide-mineralised bands.

6.1.2.4 MRF - SCALFORD

The lithology at Scalford consists of a mixture of coarse-grained calcareous bioclasts, siliclastic sand and clay ooliths, which vary in relative proportions throughout the formation (e.g. Plate 21, Plate 22, Plate 23). The matrix consists of Fe-rich clay partially replaced by variable proportions of calcite and Fe oxide cements. In all the specimens the matrix is a source of diffuse, widespread alpha-tracks, clearly outlining intergrain boundaries. They sometimes appear especially concentrated in regions particularly rich in coarse-grained calcareous bioclasts, although the bioclasts themselves are not sources.

One of the samples from the lower part of the formation (RC09) is highly siliclastic and includes many detrital zircons and monazites. Small, intense alpha point sources are present throughout all the specimens, sometimes positively identified as zircons.

The rocks have experienced variable degrees of alteration to Fe oxide, which in places is clearly associated with a surface weathering profile where the surface layer has been stained pink to a depth of about 5 mm. By SEM, it can be seen that some of the Fe oxide contains a small amount

of Mn which may be the source of diffuse concentrations of alpha tracks present along weathered margins, at alteration fronts and along fractures. In fact some late fractures associated with an alpha source in sample RC07 are filled with Mn oxide (Plate 24). However, some diffuse alpha sources are concentrated in patches with more Fe oxide cement than average but no Mn. No phosphate was identified in any of the samples.

6.1.2.5 MRF - PICKWELL

The lithology observed here is oolitic with coarse grained bioclasts (Plate 25). The ooliths are of clay and calcite and the matrix, originally of Fe-rich clay, has been partially replaced by several cementing phases: an early rhombic phase now completely replaced by Fe oxide, and a sparry calcite. This matrix is a source of diffuse, widespread alpha-tracks, clearly outlining intergrain boundaries in many places. Calcareous shell fragments are not alpha sources. The matrix alpha source is likely to be either the matrix clay and/or the Fe-oxide-replacing phase. There are also grain-shaped, diffuse alpha sources that can be quite intense in concentration, which were not identified by SEM as being associated with a particular phase. There are numerous small and intense point sources throughout the specimens which are presumed to be detrital materials such as zircons and monazites. No phosphates were identified during the SEM examinations.

6.1.2.6 MRF - SAUVEY CASTLE

The upper part of the formation consists of a calcite-cemented oolite (Plate 26). The ooliths are composed of Fe-rich clay and calcite, in a matrix of Fe clay. In many areas the clay matrix is mixed with very fine grained Ca phosphate (e.g. Plate 27). The rock matrix throughout all the specimens is a source of diffuse, widespread alpha-tracks, clearly outlining intergrain boundaries. However, more intense sources correspond to areas with the phosphate-rich matrix.

The basal, nodular and supposedly phosphatic beds are actually composed of siliclastic sand with calcareous bioclasts and a matrix cemented by calcite and late Fe oxide (Plate 28). Nodules of calcite are present in widely varying sizes and their interiors can be oolitic (e.g. Plate 29). There are a few sand-sized pellets of phosphate present but otherwise these beds are not phosphate-rich. Calcareous shell fragments and bioclasts are not alpha sources, and a large calcareous nodule sampled from the basal beds (SC06) is associated with a very low level of alpha tracks.

Point sources tend to be very small and are numerous in most specimens. They are presumed to be detrital components such as zircons and monazites. In the sample from the basal beds, zircons were found to be common and some of them demarcate the edge of a calcareous nodule.

6.2 XRD

The SEM petrographic examinations enabled most of the phases present in the ironstones to be identified, but the finer grained phases such as clays, iron oxides and phosphates were only identified by broad phase type. These phase types are all potentially significant in the control of uranium distribution in the rocks. It was therefore decided to use X-Ray Diffractometry (XRD) to identify the actual phases present. Seven samples were selected (Table 1) to represent a range of both lithologies and Fe contents, and were prepared for analysis by XRD.

Table 1 List of samples analysed by XRD

Site	Depth (m)	Field code	Lab code	Lithology	FeO (%)	Fe2O3 t (%)	FeO/Fe2O3 (%)
Northampton Sand:							
Twywell Gullet	0.15	TW01	J649		0.06	71.63	0.08
Pitsford Quarry	1.84	PI08	J662		0.2	46.36	0.43
Pitsford Quarry	4.05	PI10	J664	Nodular base	15.26	25.11	60.77
Harlestone Quarry	4.1	HQ12	J679	Oolite	0.69	3.09	22.33
Marlstone Rock:							
Pickwell Village	0	PV03	J693		0.78	21.51	3.63
Sauvey Castle	0.6	SC01	J697		1.45	29.91	4.85
Sauvey Castle	2.3	SC04	J700		2.1	6.09	34.48

6.2.1 Method

About 3 g of each powdered sample was back-loaded into a standard aluminium sample holder. XRD analysis was carried out using a Philips PW1700 series diffractometer equipped with a cobalt-target tube, operating at 45kV and 40mA. The whole-rock samples were scanned from 2-75 °2θ at 0.70°2θ/minute. Diffraction data were initially analysed using PANalytical X'Pert software coupled to an International Centre for Diffraction Data (ICDD) database running on a PC system.

6.2.2 Results

The resulting XRD traces are shown in Appendix 6. The phases identified are summarised in Table 2.

Table 2 Summary of XRD results (tentative identification marked with '?').

Site	Field code	Major	Minor	Trace
Northampton Sand:				
Twywell Gullet	TW01	Goethite	Quartz, lepidocrocite, ?chamosite, ?kaolinite	Woodhousite, ?calcite
Pitsford Quarry	PI08	Goethite, calcite, swelling clay	Apatite	
Pitsford Quarry	PI10	Calcite, quartz, siderite, Mg calcite	Mica, goethite, kaolinite	
Harlestone Quarry	HQ12	Quartz, Mg calcite	Orthoclase, ?mica, ?clay	
Marlstone Rock:				
Pickwell Village	PV03	(Mg?) calcite, goethite, swelling clay		
Sauvey Castle	SC01	Mg calcite, goethite, chlorite		
Sauvey Castle	SC04	(Mg?) calcite,	Quartz, chlorite	

XRD is a bulk method capable of identifying the major and minor crystalline phases in a sample. It may also be possible to identify more poorly ordered phases (in this case goethite) and sometimes phases present at trace levels may be identified.

The 'swelling clays' seen in samples PI08 and PV03 have not been identified but based on their XRD patterns are likely to be Fe-rich. The chlorite identified in sample SC01 may have a slight swelling component. Fe-rich clays are therefore present in all the MRF samples analysed, and at least one of the NSF samples.

Since phosphate has only been observed as a minor phase by SEM, it is not surprising that very little phosphate was identified by XRD, however apatite (at Pitsford) and possibly woodhouseite

($CaAl_3(PO_4)(SO_4)(OH)_6$; at Twywell) were both seen at minor to trace levels in NSF samples. This fits with the observations made by SEM of an Al-bearing phosphate cement at Twywell, and a pure phosphate cement at Pitsford and Harlestone

6.3 SUMMARY AND INTERPRETATION OF SEM, AUTORADIOGRAPHY AND XRD DATA

The ironstones consist mostly of varying proportions of carbonates, detrital silicates and Fe-rich phases. The latter, where primary, are present as Fe-rich clay ooliths and matrix but both have often been altered to fine grained Fe oxides, especially towards the surface and where they have been exposed for longer. XRD was used to identify the major Fe oxide phase as goethite.

The carbonates, whether they occur as coarse bioclasts (common) or as sparry matrix, are clearly not a source of alpha particles. The carbonate cements all appear to greatly reduce both porosity and matrix permeability in the rocks and are therefore expected to have a significant effect on the ability of radon to migrate through the system. In the NSF, the carbonate cement appears to be restricted to the lower levels at Harlestone; possibly corresponding to the 'Variable Beds'. The difference between the upper and lower beds at Harlestone can be seen by comparing Plates 10 (upper) and 11 (lower). In the MRF it is ubiquitous although developed to varying degrees, occurring at all the sites sampled. Sparry calcite cement was also observed to be a common feature in MRF samples examined using optical microscopy from Holwell, Tilton Cutting and Branston (Lott, 2001) with poorly developed porosity as a result.

The detrital silicate-based components include detrital zircons and occasionally monazites, and these act as small, intense point sources of alpha particles. However, these are no more concentrated in number than in many sedimentary rocks and are not likely to be the main source of radon.

The fine grained Fe-rich matrix in these rocks acts as a diffuse source of alpha particles. The detected alpha particle density from the matrix is far lower than from the detrital zircons and monazites, but volumetrically it represents a far greater alpha source. Furthermore, this matrix is fine grained and has a high porosity and is therefore likely to be far more accessible as a source of radon than any point sources in the rocks. This matrix appears to consist mostly of a mixture of mainly Fe-rich clays (chlorites and possible Fe-rich swelling clays) and, where alteration has occurred, Fe oxide (goethite). As the matrix is very fine grained, it was not possible to tell which phase was responsible for the alpha particles. However the Fe-rich clays, when present within ooliths, do not appear to be a significant identified source of alpha particles.

Occasional mineralized bands are present. These are a darker red than the altered matrix and may be haematite. They are not associated with alpha emissions.

Phosphate is present and is always associated with alpha emissions. It occurs mainly as pellets but also forms a minor matrix cement and rarely a veinfill. The pellets are rare and tightly cemented, and so are not likely to be the main contributor to radon, when compared to the more volumetrically significant fine-grained matrix. Moreover, the phosphate was not identified by SEM as a widespread matrix cement, and therefore it is not likely be the source of most of the observed, matrix radioactivity. In most samples this phase was pure Ca phosphate, but an Al-bearing phosphate (woodhouseite) was observed in material from Twywell.

Some Mn oxide veinfill was identified at one site in the Marlstone Rock (Scalford), where there is also a characteristic pink weathering surface. The Mn oxide is clearly associated with alpha radioactivity but is quite rare even at this one site.

In summary, Ca phosphate cement is one of the sources of radioactivity. However, it is restricted in extent and does not appear to be highly accessible to emanate radon. Secondary phases, i.e. Fe (and Mn) oxides, are far more widely distributed throughout the matrix and are less tightly cemented, providing a far more accessible potential source of radon. One possibility

is that uranium and/or radium in the phosphate phase may have migrated into these fine grained oxides (by precipitation or sorption) during alteration and the latter may now be acting as the more significant radon source.

6.4 BULK CHEMICAL ANALYSIS

Initially, XRFS was used to determine the major and minor elemental compositions of 43 the samples (see Appendix 3). It was intended to combine this dataset with other numerical analyses and determine correlations between different analytes; however the uranium data obtained by XRFS were very low in value and too close to the detection limits to be used in constructing correlations. It was therefore decided to carry out repeat analyses of uranium concentration using ICP-MS following a mixed acid digest ($HF/HClO_4/HNO_3$). This was performed for 40 of the 43 XRF samples. These same digested solutions were then also used to carry out analysis for radium concentration by alpha particle liquid scintillation counting (LSC). Lastly, the reduced Fe concentration in 12 selected samples was investigated using a wet chemical titration method. The results for all these analyses are presented in Appendix 4, Table 5 -Table 9.

6.4.1 Analysis by XRFS: qualifications to the chemical data

The results for all the XRFS bulk chemical analyses are shown together in Table 5 - Table 8 (in Appendix 4). All the data should be considered accurate to no more than three significant figures. For many elements, concentrations were lower than the detection limits of the method. However, for the purposes of correlation the actual figures for those elements below detection limits were used in data analysis.

In the datasets obtained by XRFS, Fe_2O_3t represents total iron expressed as Fe_2O_3. SO_3 represents sulphur retained in the fused bead after fusion at 1200°C. In some samples, the determined Sr and/or Zr concentrations were found to be above the calibration limit for the programme used (1000 ppm for both Sr and Zr). For high Sr, this will affect the trace element data for Ni, Cu, Zn, Ga, Ge, As, Se, Br, Rb, Sr, Y, Zr, Hf, Ta, W, Tl, Pb, Bi, Th, U data and possibly other elements. For high Zr, this will affect the trace element data for Ni, Cu, Zn, Ga, Ge, As, Se, Br, Rb, Sr, Y, Zr, Nb, Mo, Hf, Ta, W, Tl, Pb, Bi, Th, U data and possibly other elements. The specified trace element data were not corrected for this effect.

Sample J662 was fused with a reduced sample mass of 0.8464 g rather than 0.9000 g as standard. Sample J655 gave a low total (95.02%) which on repeated testing continued to fall outside the normal accepted range (99-101%). This was thought to be due to the chemistry of the samples or the presence of other elements that were not quantified.

6.4.2 Method for 226-Ra analysis by liquid scintillation counting (LSC)

The 10 ml aliquot of each digested solution was placed in a low background glass LSC vial and 10 ml of a toluene-based LSC cocktail was added. Prior to counting, each vial was shaken to extract the radon into the organic layer. The sample activity was then counted on an LBK Wallac Rackbeta liquid scintillation counter using pulse shape analysis to differentiate alpha and beta scintillation events. The samples were initially screened for unsupported radon (^{222}Rn). Samples were then stored for a period of time calculated from the initial ^{222}Rn activity to allow unsupported ^{222}Rn to decay. ^{226}Ra was then determined by analysing the residual concentration of ^{222}Rn, since the activity of the two radionuclides should have reached equilibrium. The time required for equilibrium of supported Rn, assuming minimal initial unsupported Rn, is 8 half-lives (approximately 30 days). In the unlikely event of excessive initial unsupported Rn, samples may require a period of greater than 8 half-lives before counting.

Duplicates, standards, and blank samples were included in each batch. The results are calibrated using an in-house radium standard solution. At an activity of 1 Bq/l, analytical error (2σ) is

typically of the order of 5 – 10 %, for a 1 hour count time, though it will vary slightly depending on the characteristics of the sample such as salinity and discolouration. The results are presented in Appendix 4, Table 9.

6.4.3 Determination of reduced Fe by titration

The reduced Fe technique uses an H_2SO_4/HF digest, followed by wet chemical titration. It is designed for use with silicate matrices and has not been tested on ironstones. There were no suitable calibration reference materials available so, in addition to the usual silicate matrix standard, a Basic Slag (BCS 381) was analysed. A recovery of 82% was achieved. The certificated value had been obtained using a different digest to the one used by the BGS method so the recovery level could be affected by the different digestion and/or matrix. The results are presented in Appendix 4, Table 9.

6.4.4 Discussion

The uranium concentrations obtained by ICP-MS and XRFS compare well, with a significant correlation between them, although the data obtained by XRFS are at slightly higher levels than by ICP-MS (Figure 17). This could be because of an incomplete acid digestion of the sample, whereas with XRFS the whole sample is analysed. Overall, the amounts are low, with means of 3 ppm in both Formations. Th levels are high in comparison, with means of 13 ppm in the NSF and 18 ppm in the MRF.

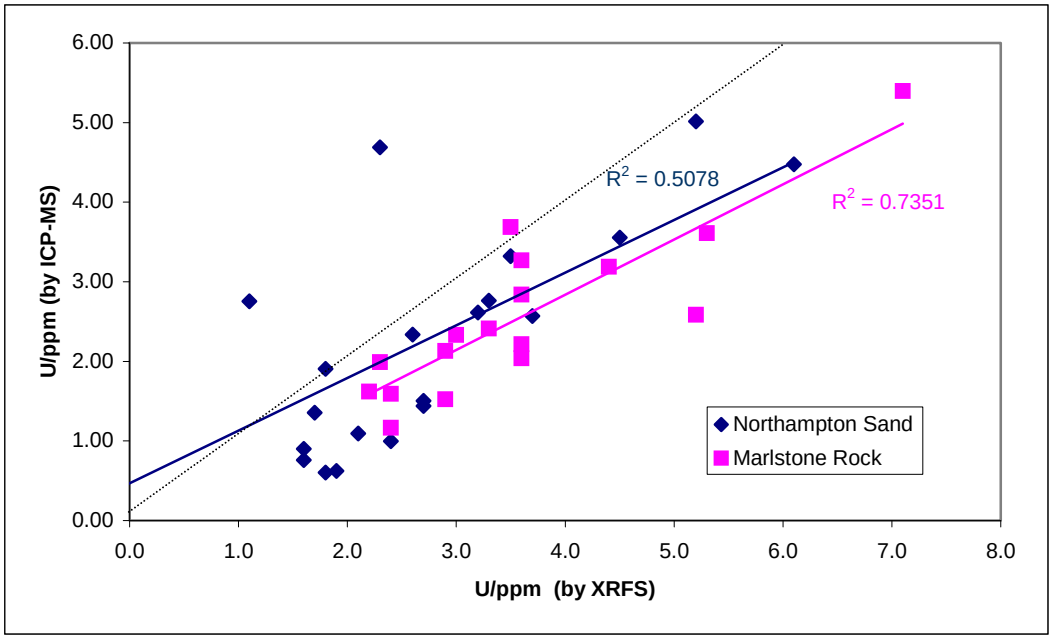

Figure 17 Uranium concentration determined by two different methods: ICP-MS following acid digest, and XRFS of solid sample.

From the XRFS data it can be seen that the majority of the samples consist of the following oxides/analytes: SiO_2, Fe_2O_3, CaO and LOI (the latter representing $H_2O + CO_2$). Between them these elements total between 84 and 95 wt% of the rock mass. The LOI is assumed to be made up of a combination of H_2O from Fe oxy-hydroxides, and CO_2 from calcium carbonates. The samples are plotted on a ternary plot with SiO_2, Fe_2O_3 and CaO at the three apices, to represent the silicate, Fe oxide and carbonate components of the rock respectively (Figure 18). This shows

that most of the MRF material from all sites plots in the same region, with a relatively low Si content and varying ratio between Ca and Fe. In contrast, each site of the NSF has a distinct major element signature (and hence lithology). All the Twywell material has an extremely high Fe content, far higher than any of the other sampled ironstones. Pitsford material plots in a similar area to the MRF data, and Harlestone quarry can be divided into upper material (three datapoints with almost no Ca, from the upper 1 m) and lower, 'Variable Beds' material which has a more substantial Ca content. This agrees with the petrographic observations of a Ca carbonate cement in the lower parts of the exposed NSF at Harlestone. Interestingly, the lower parts of the MRF (4 m at Scalford and the basal bed at Sauvey Castle) plot in the same area as the 'Variable Beds' at Harlestone.

After the components represented in Figure 18 (with LOI), the next most abundant components are Al_2O_3 and P_2O_5. The phosphate is presumed to come from the phosphate cements and pellets associated with significant radioactivity. Phosphate levels in the ironstones lie between 0 and 3 wt% P2O5, with a mean of 1 wt% in both the NSF and the MRF. These levels compare well with a previous study by Sutherland (1991) of the NSF, except that Sutherland sampled a basal phosphatic (francolite) pebble-bed and found up to 55 ppm U and over 30 wt% phosphate in the pebbles in temporary exposures created by road building (Sutherland Sharman, 1996). This bed was not seen in the present study. A pebbly basal unit was sample in the MRF (at Pitsford and Sauvey Castle) but the pebbles were mostly carbonate and elevated phosphate or U were not found.

In the NSF, Al and phosphate correlate with each other to a surprisingly high degree, with R = 0.70 for the whole NSF dataset (Figure 19). This does not necessarily mean they are both present in the same phase, and Al also correlates to a slightly lesser degree of significance with Fe. Petrographic observations suggest that most of the Al is present in Fe-rich clays, although some is also present in the phosphate phase at Twywell. The correlation coefficient for Al_2O_3 and P_2O_5 in the MRF is much lower, R= 0.41, although there is clearly a relationship as Figure 19 shows.

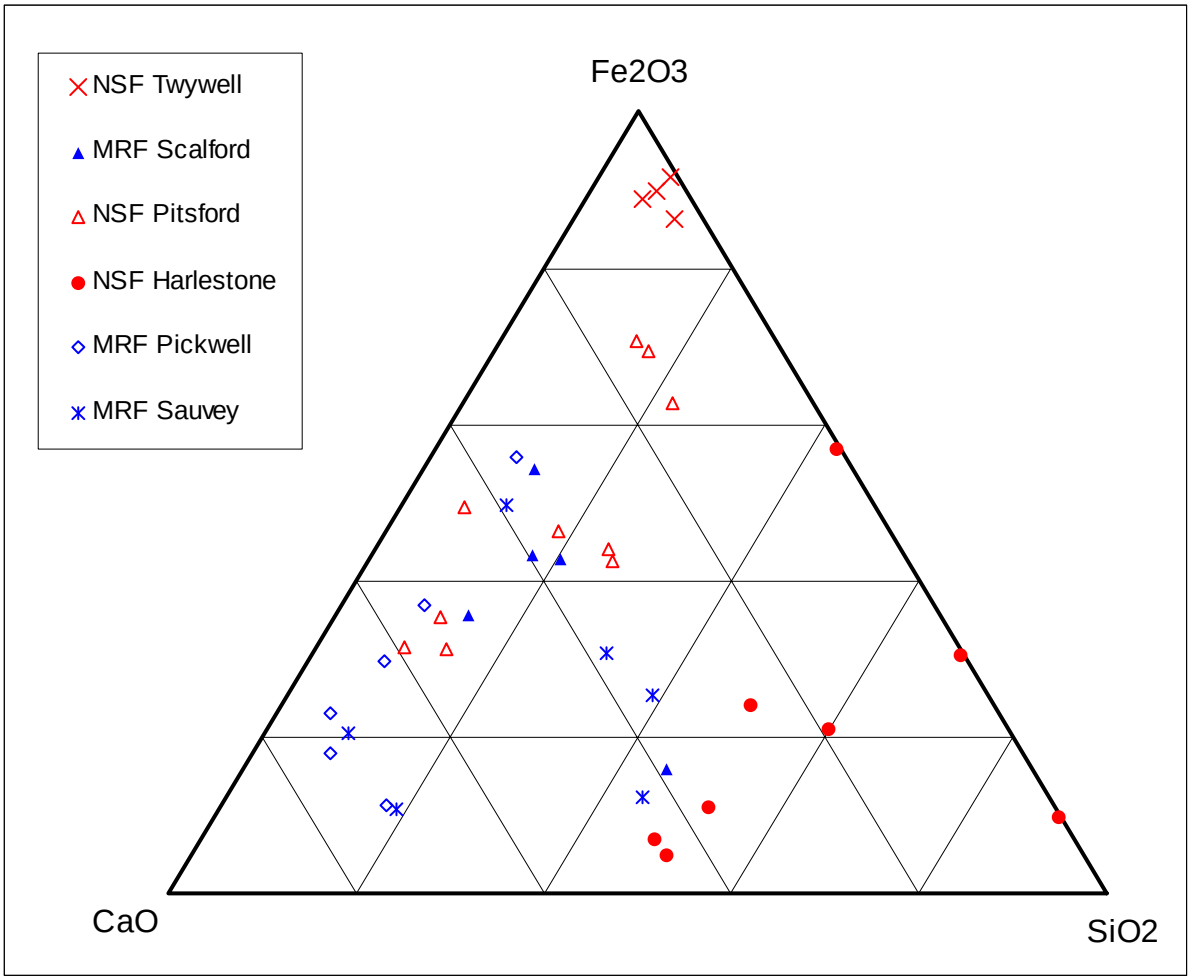

Figure 18 Ternary element oxide plot calculated from XRFS data.

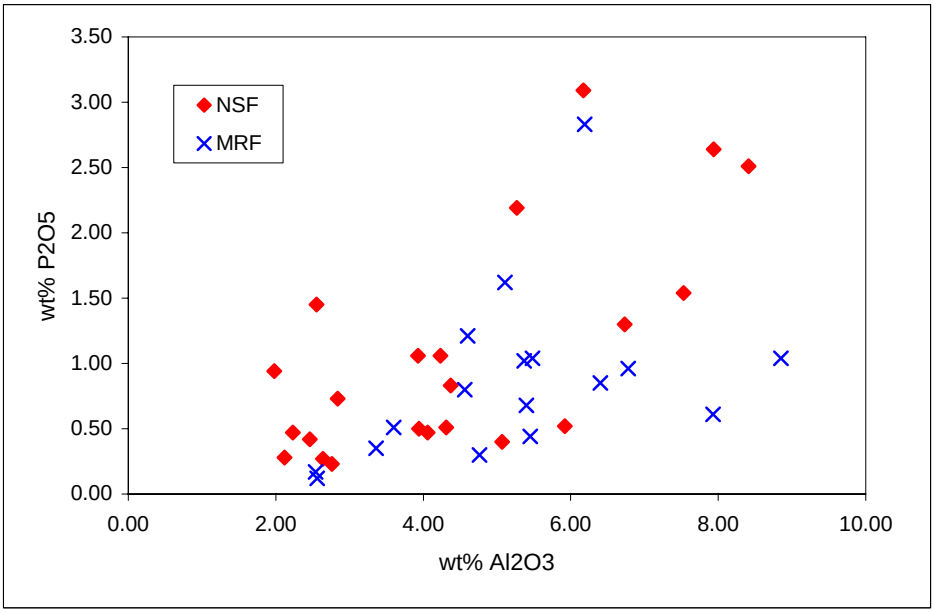

Figure 19 Relationship between Al_2O_3 and P_2O_5 in the ironstones, as determined by XRFS.

There are some interesting relationships between Al, phosphate, U and Th, as illustrated in Figure 20 and Figure 21. All four of these components correlate with each other to some degree in some of the ironstones. In the NSF, Th has a very strong relationship with Al_2O_3 (R = 0.87; Figure 22). Also in the NSF, U has a strong relationship with phosphate (R = 0.75) *except at Twywell*, where there is no significant relationship (Figure 20). Perhaps the high degree of alteration at Twywell has caused U and phosphate to respond differently. In the MRF, U does not have a significant relationship with either Al or phosphate, but Th still has a strong relationship with Al_2O_3 (R = 0.81). It is important to note that strong correlation between elements does not necessarily mean they are present in the same mineralogical phase; these are highly likely to all be present in the matrix mixture of clay, iron oxide and minor phosphate cement, rather than in the detrital or carbonate components and this association is probably strong enough to result in high correlation coefficients.

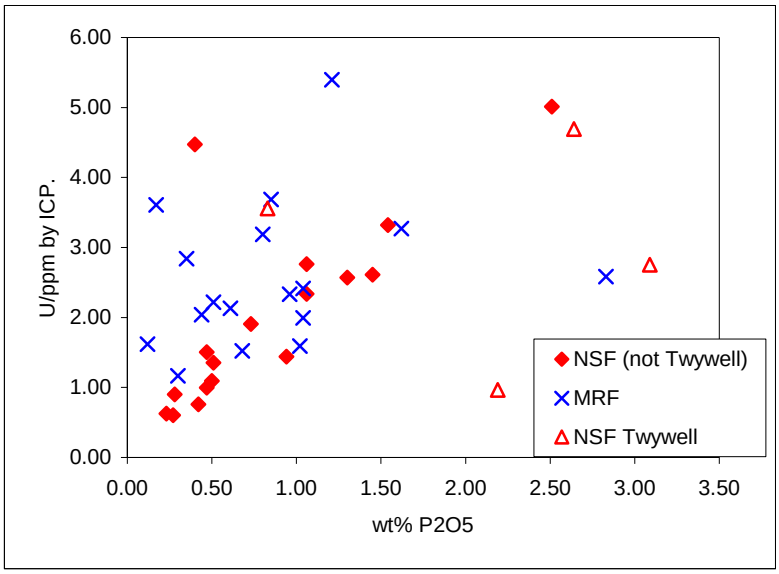

Figure 20 Relationship between U (determined by ICP-MS) and phosphate (determined by XRFS) in the ironstones.

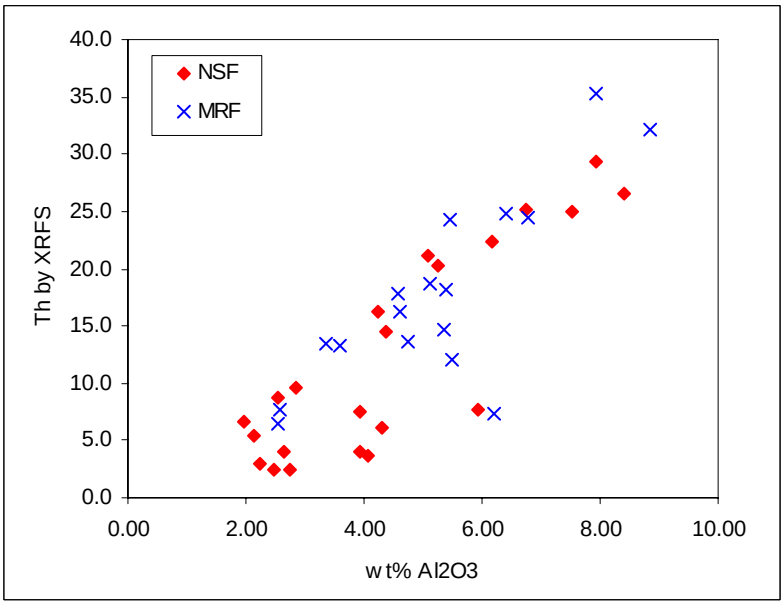

Figure 21 Relationship between Th (ppm) and Al_2O_3 (determined by XRFS) in the ironstones.

Uranium and ^{226}Ra correlate very strongly in both the NSF (R = 0.879) and the MRF (R = 0.836) (Figure 22) showing that there is no apparent disequilibrium.

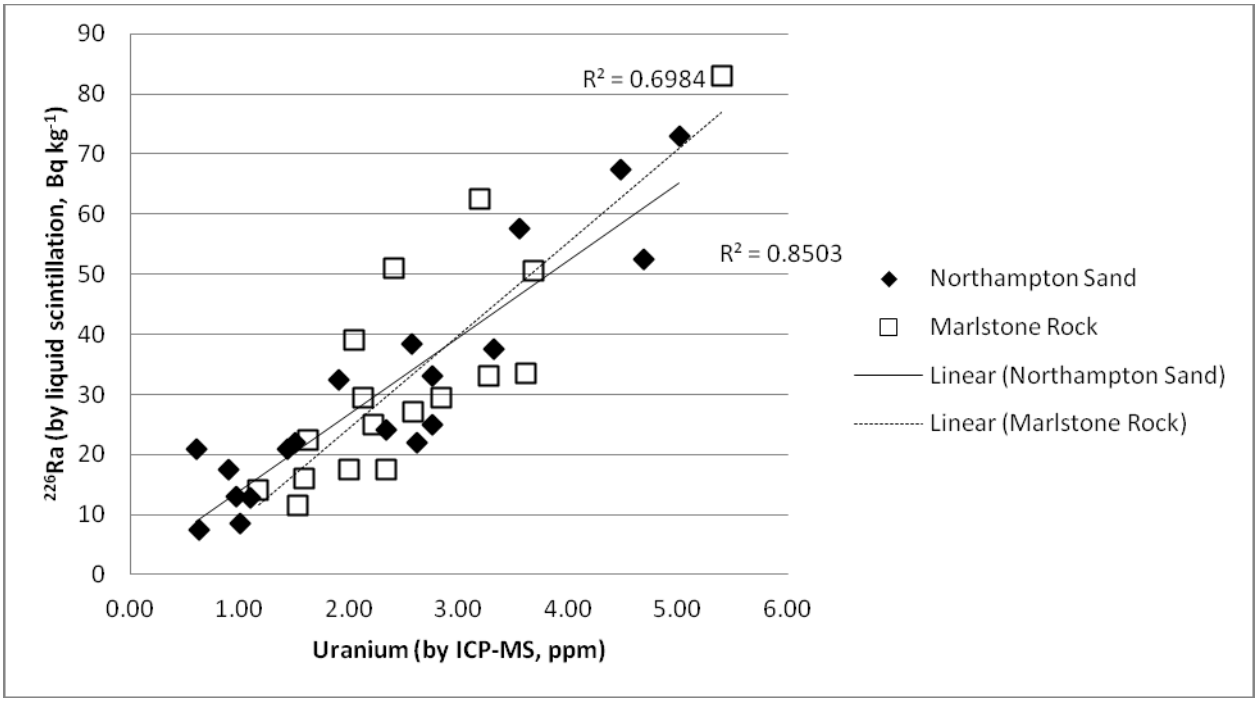

Figure 22 Relationship between ^{226}Ra (determined by LSC) and U (determined by ICP-MS) in the ironstones.

In Section 7, these data are compared further with data obtained by gamma spectrometry and radon emanation experiments conducted on the same samples. This is in order to determine whether there is a relationship between the amounts of radiogenic material present and the amount of radon actually escaping from the rocks on a hand specimen scale.

6.5 GAMMA SPECTROMETRY

Laboratory-based gamma spectrometry was carried out on 40 samples which had been crushed and milled to a fine powder and placed in 150 ml polystyrene pots with polyethylene snap lids. Analysis was conducted using high purity germanium detectors in a low background counting facility (10 cm of Pb shielding with a Cu-Cd lining). Counting times were 24 hours on a 35% efficiency detector and 48 hours on a 17.4% efficiency detector with data analysis using Genie 2000 software (Canberra Industries, Inc.) with efficiency calibration through the mathematical calibration software, LabSOCS (Bronson et al, 1998; 2000). XRF data were used to create appropriate LABSOCS models in terms of the composition for each sample. The effect of varying the composition of the samples, particularly the Fe content, on the calibration was investigated but was not found to be critical. Significant variations (i.e greater than the reported 1 sigma errors) were only seen when the modelled and actual compositions were widely divergent (e.g. a 10 % Fe_2O_3 model used for a sample with 60%).

6.5.1 Results

The results are shown in Table 10 and Table 11 in Appendix 4. The sample pots were not fully sealed, so there is a possibility that radon could have escaped leading to reduced levels of radon daughters, such as ^{214}Bi and ^{214}Pb in the analyses. There is a strong correlation between eU,

derived from the radon daughter results, assuming secular equilibrium in the ^{238}U decay series, and total U by ICP-MS (

Figure 23), but the eU values are systematically lower, which suggest that radon loss may have occurred. However, calibration effects (relating to the sourceless calibration) are an alternative explanation for this discrepancy.

The gamma spectrometry results showed that the thorium series radionuclides were generally higher in the MRF, uranium was also slightly higher in the MRF but the NSF was generally more K-rich (Table 10 and Table 11).

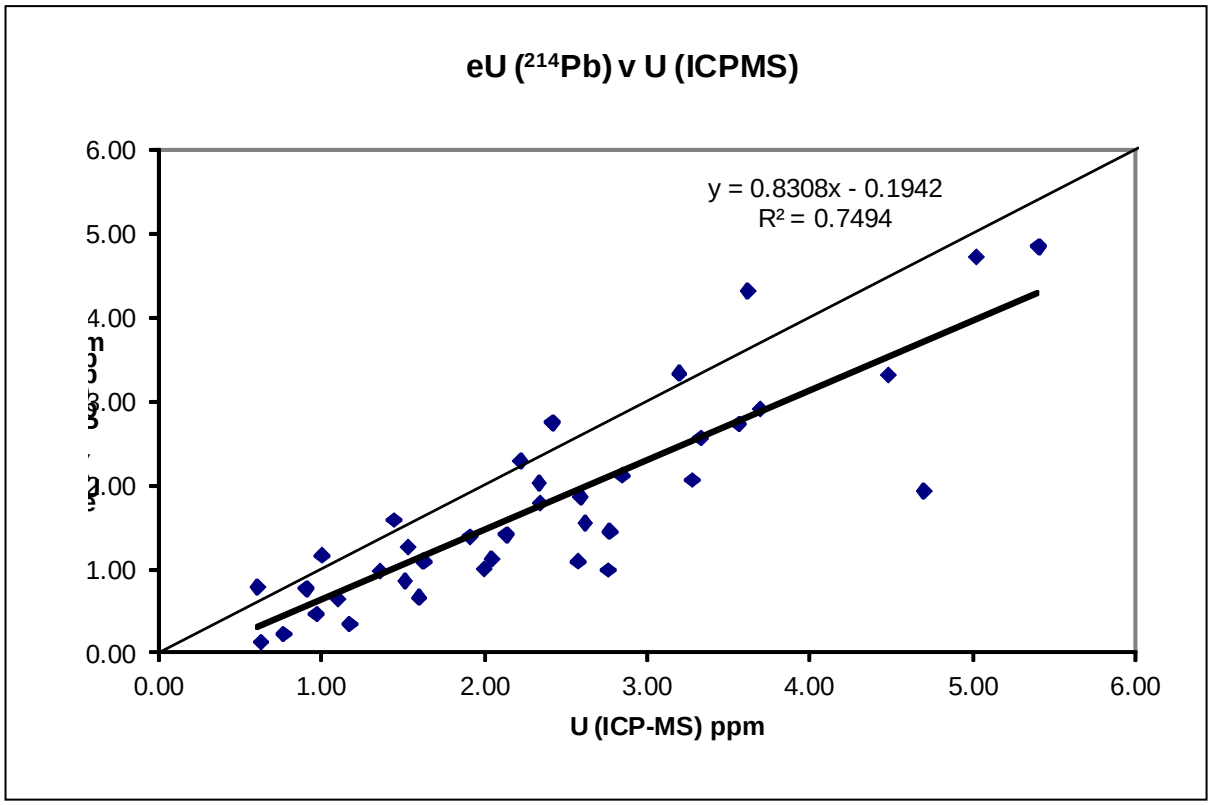

Figure 23 Comparison of total U (ICP-MS) and e U (^{214}Bi, ppm on Y axix) by gamma spectrometry with 1:1 line shown.

6.6 RADON EMANATION EXPERIMENTS

6.6.1 Method

Forty five samples of the ironstone were selected for radon emanation measurements. Many of the ironstone samples consisted of multiple small pieces of rock, while only a few were present as sufficiently large single hand specimens, so for many samples, multiple rock pieces were used in the tests. The rock samples were first cut with a rock saw to give flat surfaces on all faces. This enabled easier surface area (SA) measurements. The SA for each sample was then calculated. As this method could only give an approximation of SA, measurements were calculated to the nearest $5cm^2$.

The dry sample volume (V_d, i.e. the solid volume occupied by all the pieces assuming them to be nonporous) was then determined by displacement in water after first sealing the samples with cling film to prevent any ingress of water into the rock via fractures or pores. Cling film was chosen because it would produce negligible increase in sample volume. Sample volumes varied considerably, between 22 and 330 cm^3.

The volume of the internal porosity ($V_{i,}$) of each sample, to the nearest 1 ml, was then determined by measuring the difference in water displacement between a cling film covered sample and one without cling film after 24 hours immersion.

After calculation of the external and pore volume of each sample, the rocks were placed in glass Kilner jars with rubber seals. The jars were filled with reverse osmosis water, ensuring that when the jar was sealed shut, a minimal air space was present between the water level and the lid. This was essential in order to maximise the radon concentration in the water. The volume of water in each jar was calculated by subtracting the sample displacement volume ($V_d - V_i$) from the total volume of the jar (0.5,1 & 2 litres depending on sample size).

The jars were then sealed and allowed to stand for 25 days to allow the radon to reach secular equilibrium. After this period, duplicate 10 ml aliquots of the water were taken by syringe from the sample container and placed in a low background glass Liquid Scintillation Counting (LSC) vial, which already contained 10 ml of a toluene-based LSC cocktail. Immediately prior to analysis each vial was shaken to extract the radon into the organic layer. The samples were counted on an LBK Wallac Rackbeta liquid scintillation counter using pulse shape analysis to differentiate alpha and beta scintillation events. Duplicates, standards, and blank samples were included in each batch.

At an activity of 1 Bq/l, analytical error (2σ) is typically of the order of 5 – 10 %, for a 1 hour count time, though it will vary slightly depending on physical characteristics of the sample (such as salinity and discolouration). The results are calibrated using an in-house radium standard solution. With its long half life (1602 years) radium provides a stable source of radon. The radium solution has been compared to a certified standard solution at Central Mining Institute, Poland and to a certified standard solution in the Water Authority of Jordan (Certificate No. 425-56-3, Isotope Products Laboratory, Burbank, California, USA).

6.6.2 Results

The results of the radon emanation experiments are given in Table 12 in Appendix 4.

Many negative values were obtained from the liquid scintillation counting; these are given as <0 in the table. Furthermore, there was frequently a wide divergence between duplicate measurements in the LSC results, resulting in very high final errors. These wide variations in measurements may be due to the method used to extract radon from the jars; it was observed that during extraction of water by syringe, gas bubbles formed within the syringe. The bubbles may have contained radon exsolving from solution in water under the negative pressures experienced during expansion of the syringe. If the radon did exsolve, significant amounts of it would not

therefore be transferred to the counting vials. This would lead to underestimates of the radon emanation.

Correlation coefficients between mean activity per litre, and surface area or rock volume, were –0.23 and –0.26, respectively indicating no significant relationship between detected activity concentration and either surface area or volume of rock. This suggests a more complex relationship is involved than mere emanation volume/area or the potential sampling problems referred to above having a major impact.

In Figure 24 to Figure 27, the relationship between radon emanation measurements, and uranium and radium, are illustrated for both ironstones. In the NSF, there is a strong linear correlation between radon emanation and uranium (Figure 24; R ~0.9), as well as between radon emanation and radium (Figure 26; R = 0.9). However, in the MRF, there is no significant relationship between radon emanation levels and either uranium (R ~0.3, Figure 25) or radium (R = 0.3, Figure 26). The possible explanations for, and implications of these observations are examined further in Section 7.

Lastly, radon also has a relationship with phosphate levels in the NSF (R = 0.9) as shown in Figure 27. This *could* mean that the radon is being emitted by a phosphate phase, but it does not necessarily mean this; the fine grained matrix in the NSF is a mixture of iron-rich clays and iron oxides; the phosphate cement is a minor component present within this mixture.

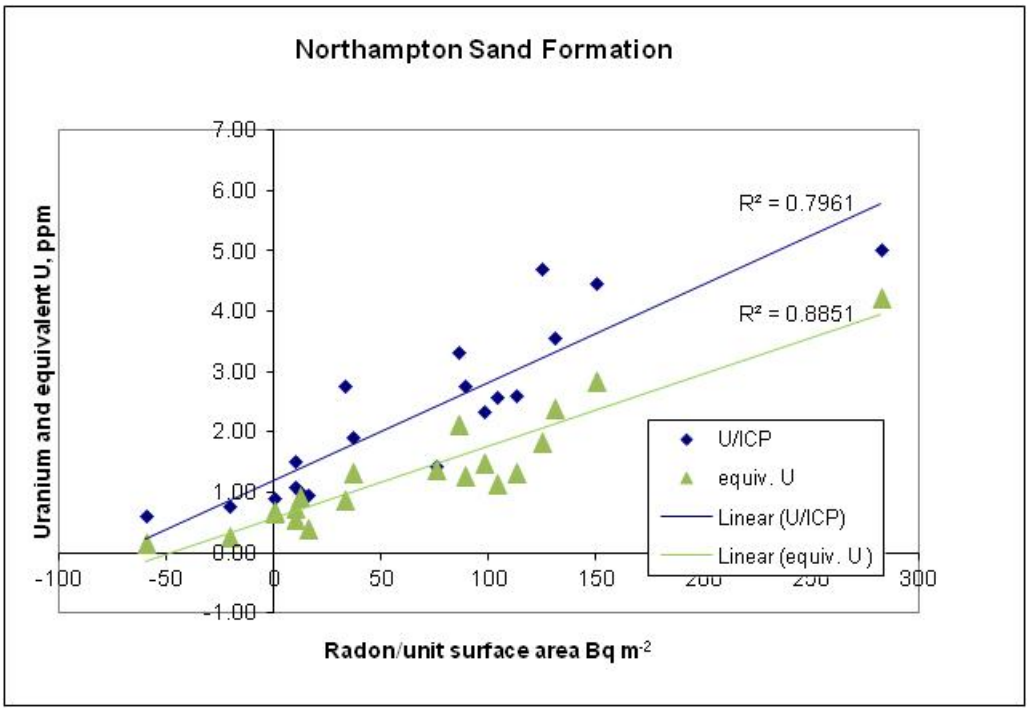

Figure 24 Northampton Sand Formation: Relationship between radon emanation measurements (per unit area) and uranium. 'U/ICP' is uranium concentration as determined by ICP-MS and 'equiv U' is uranium concentrations as determined by gamma spectrometry.

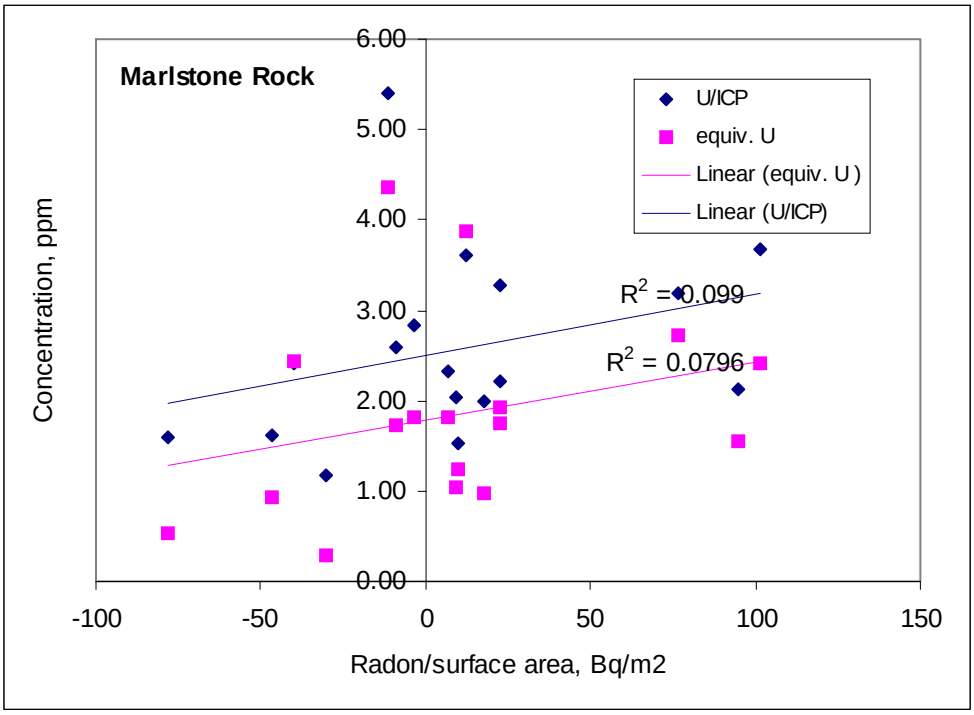

Figure 25 Marlstone Rock Formation: Relationship between radon emanation measurements (per unit area) and uranium. 'U/ICP' is uranium concentration as determined by ICP-MS; 'equiv U' is uranium concentrations as determined by gamma spectrometry.

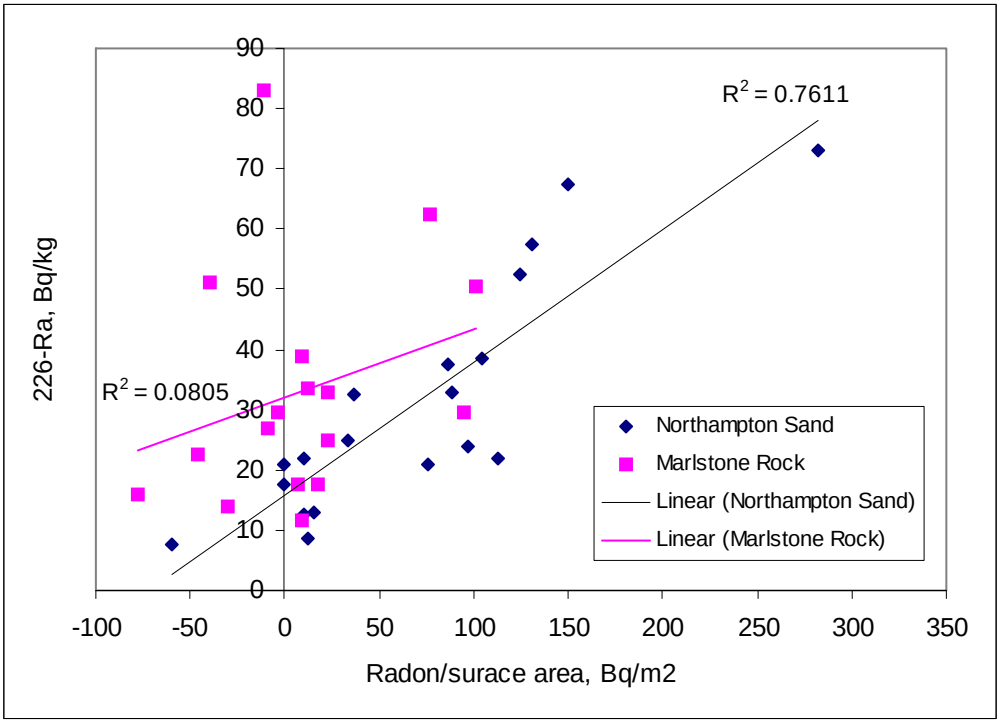

Figure 26 Relationship between radon emanation measurements (per unit area) and ^{226}Ra as determined by liquid scintillation counting of bulk sample digests.

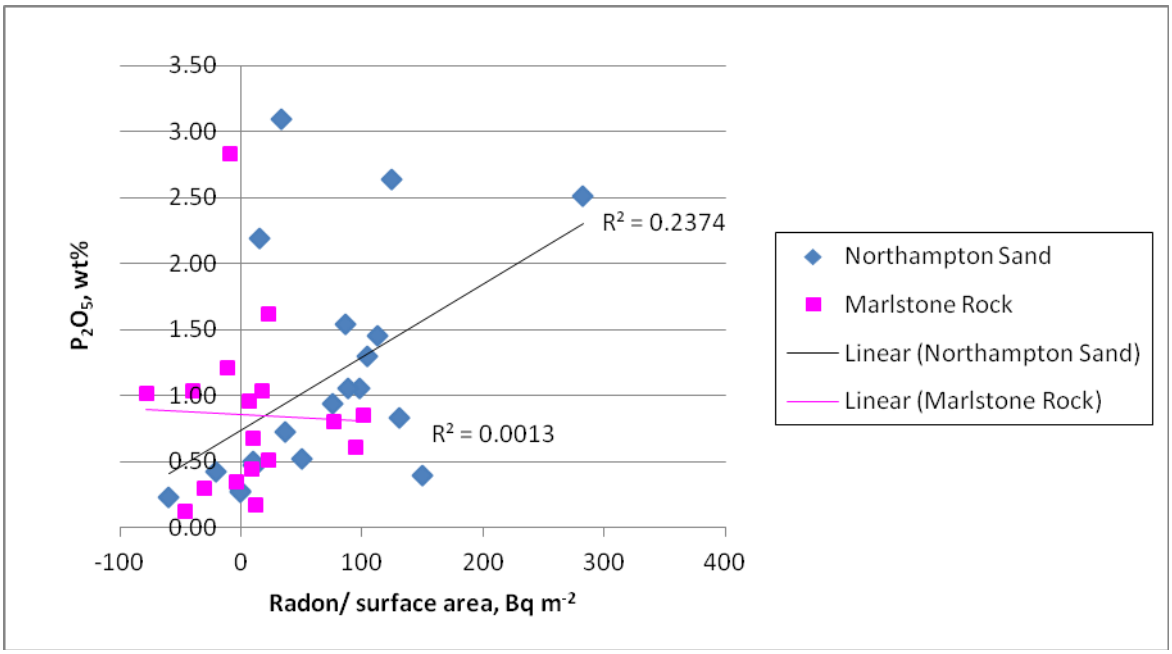

Figure 27 Relationship between radon emanation measurements (per unit area) and phosphate (wt% P_2O_5) as determined by XRFS of bulk samples.

7 Interpretation and discussion

7.1 PETROGRAPHIC AND ALPHA RADIOGRAPHY OBSERVATIONS

In terms of broad lithology, the chief differences between these two formations are that the MRF consists predominantly of well-cemented calcareous beds while the NSF comprises mainly berthierine/siderite ironstones which are much lower in carbonate and are less tightly cemented. The NSF has also extensive 'boxwork' style weathering in which Fe-rich clays and carbonates have been largely altered to a mixture of permeable goethite and haematite.

High concentrations of alpha tracks are associated with 3 main types of source:

(i) High-density point sources from zircon and monazite grains, representing terrestrial detrital components. These are ubiquitous but not present in much greater quantities than in many typical sedimentary rocks. Volumetrically they probably do not represent the biggest source of alpha emissions.

(ii) Phosphates, either of pure Ca or Ca-Al, present as pellets and sometimes as a late matrix cement. These have low interior permeability and are not common although present in many samples examined. In the NSF, phosphate occurs as rare pellets at Twywell, Pitsford and in the lower parts of Harlestone (below 1 m). In the MRF, phosphate is only seen where the basal beds are exposed (at Sauvey Castle), in the form of occasional pellets and occasional matrix cement.

(iii) Altered matrix material, consisting of goethite and some surviving Fe-rich clay (chlorite). Petrographic observations imply high permeability in this matrix, i.e. the interconnected porosity is high. An altered, goethitic matrix is well-developed in the NSF, especially at Twywell and the upper horizons at Harlestone – but this matrix is not seen in the lower parts of Harlestone. An alpha-emitting, goethitic matrix is also present in the MRF, with major chlorite, and also with some phosphate in the basal beds (at Sauvey Castle).

All three of these sources of alpha emissions are radon emitters but in order for any of them to make a significant contribution to the radon emitted at surface, they must emit a substantial total amount of radon (through a combination of mass and density), but they must also do so in a way that makes it accessible and mobile. Radon can travel by diffusion in solid matter but is extremely limited in its range, thus only emitters very close to pore space will contribute to the bulk radon emission of the rock mass. And then, unless the porosity is interconnected, the radon will not be able to travel out of the parent rock and to the surface, either as a gas of dissolved in the groundwater.

In view of this, the detrital monazites and zircons are unlikely to be a significant source because they are few in number and are present as dense single grains. The phosphates have lower alpha track densities than the detrital grains but are volumetrically more significant; however they occur mostly as tightly cemented sparry cement which would have little opportunity to release radon into the pore spaces. Some of the fine grained phosphatic cement within the matrix may be more significant but it only occurs in the MRF at Sauvey Castle. Lastly, the iron-rich matrix had a lower alpha-track density than the other two sources but takes up a far higher volume. It also is very fine grained and has a high permeability in most locations. It is therefore likely to be the major source of the radon that escapes from the rock formations.

SEM petrographic observations, visual observations of hand specimens, field observations and attempts to measure permeability all suggest that the matrix is far more permeable and less consolidated in the NSF, where the iron-rich matrix predominates, than in the MRF which is mostly tightly cemented by sparry calcite. The poor consolidation in the NSF may be related to the degree of alteration, with the maximum degree of alteration at Twywell, slightly less at Pitsford and none for most of the beds at Harlestone.

7.2 RELATIONSHIP BETWEEN U AND RADON EMANATION

In the NSF, there is a strong linear correlation between bulk uranium concentration and the measured radon emanation levels (R ~0.9, see Figure 24). However, there is no significant equivalent relationship in the MRF (R ~0.3, Figure 25). Furthermore, even though both Formations have similar concentrations of uranium, the amount of radon escaping from hand specimens of NSF is far higher than that escaping from the MRF specimens: this value reaches a maximum of 250-300 Bq/m^2 in the NSF compared to only 150 Bq/m^2 in the MRF.

Therefore it seems that the escape of radon is impeded from the MRF, relative to the NSF. The most likely explanation for this is a difference in permeability. Permeability on a hand specimen (or any) scale has not been directly measured in this study but petrogrphic observations have shown that the MRF is tightly cemented by sparry carbonate throughout most of its extent, whereas the NSF has a fine grained, more permeable and often more altered matrix.

7.3 RELATIONSHIP BETWEEN PHOSPHATE AND RADON

Phosphate levels correlate weakly with radon emanation in the NSF but do not correlate in the MRF. Phosphate increases from 0.4 wt% at Harlestone to over 2 wt% at Twywell following the same pattern of geographical variation as Fe and U. However, this does not necessarily mean that most of the uranium is present within a mineralogical phosphate phase, or that most of the accessible radon is being emitted from a phosphate phase. Petrographic observations show that the phosphate cement is a minor component, always present within the fine grained matrix. This matrix also contains iron-rich clays and iron oxides and was shown by autoradiography to be a significant alpha-emitter. All that can be concluded is that in the NSF, the accessible radon (on hand specimen scale) is being produced by the fine grained matrix, but it is not possible to identify which phase within that matrix most of this radon is coming from.

7.4 NSF SUMMARY

Radon emanation correlates well with both uranium and radium, showing that permeability is not a limiting factor in this rock type and this is supported by petrographic observations. The most significant source of alpha emitters is likely to be the fine grained iron-rich matrix, consisting of iron-rich clays and, where altered, goethite. Phosphate cements are also likely to be a second radon source but of less significance because of their restricted extent and largely sparry, tightly cemented form. Note that a phosphatic basal bed studied by Sutherland (1991) was not seen or sampled in this report and could make a further and potentially more significant contribution to radon levels than the main beds of the Formation; though probably only on a very localised scale (the P basal bed only forming a small part of the NSF). This warrants further investigation.

When the ironstone was worked the basal part of the formation, including the phosphatic bed, was left in place as it was not of workable quality (Hollingworth and Taylor, 1951) and provided a firm surface for large excavators and rail or road vehicles used to transport the ore (e.g. Tonks, 1992). It is possible that the permeable nature of any backfill used after working ceased may be in part responsible for the higher radon levels in houses associated with worked-out areas of ironstone (see Table 3).

Studies of NSF core samples (Hodgkinson, 2002) showed that these were quite tightly cemented compared to the surface samples studied here. The iron minerals in the cores (berthierine, chamosite and siderite partly altered to Fe and Mn oxides) weather to goethite and haematite in the near surface environment and it is likely that these phases are much more efficient radon emanators than their precursors. Intergranular films precipitated onto grains surfaces are much more likely to release radon into the pore space than well-crystallised minerals (Appleton and Ball, 1995; Semkow, 1990). Near surface weathering of the ironstones is therefore probably very important in enhancing their radon potential.

The development of the 'Variable Beds' in the upper part of the NSF succession near Northampton (Hollingworth and Taylor, 1951) potentially plays a part in the lower radon potential of this area (Figure 28). These form a thick sequence overlying what were workable ironstones or building stone. As seen at Harlestone for example, not only are the variable beds lower in Fe, but also in P_2O_5 and U when compared to the other NSF localities studied here and the worked parts of the ironstone (Taylor, 1949; Hollingworth and Taylor, 1951).

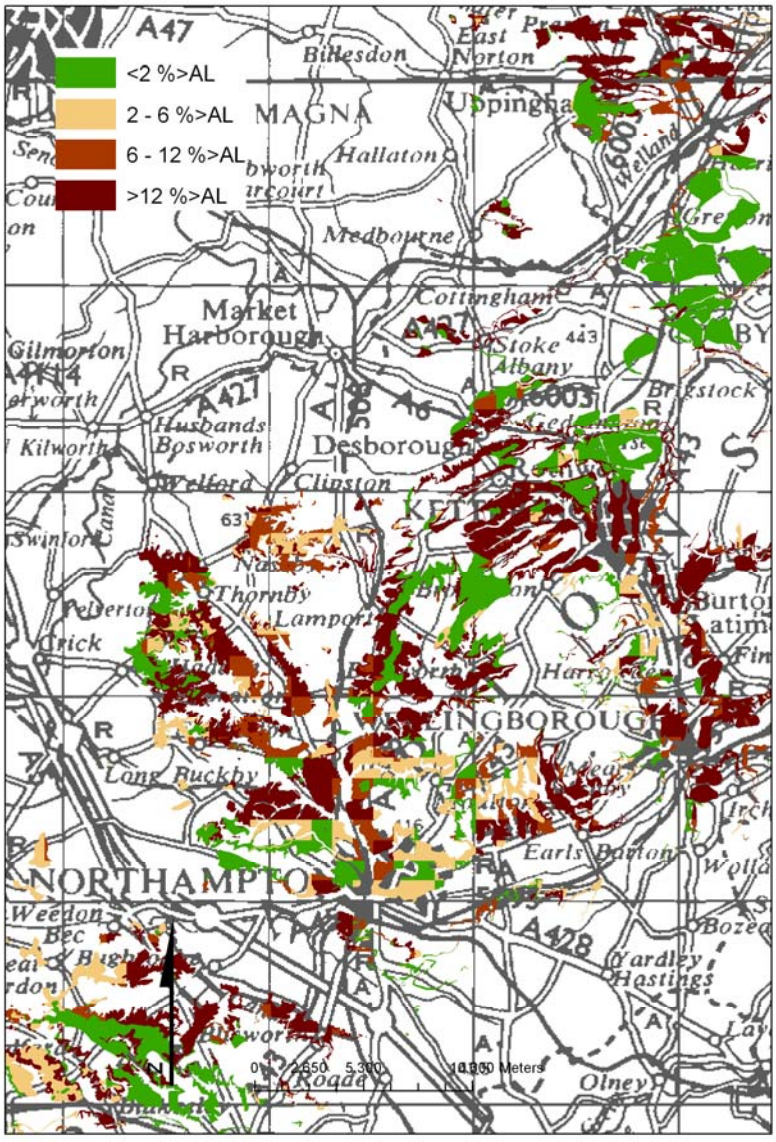

Figure 28 Radon potential map of the Northampton Sand Formation (grouped as Inferior Oolite Group (INONS)) showing the percentage of homes estimated to exceed the radon action level of 200 Bq m^{-3}.

7.5 MRF SUMMARY

Radon emanation is at lower levels and does not correlate with uranium or radium, suggesting its escape is impeded, and this is supported by petrographic observations that the MRF is mostly tightly cemented by sparry calcite. The source of radon is likely to be a mixture of fine grained iron-rich matrix phases and (to a lesser extent) phosphatic cements.

Since permeability is clearly an important factor, it is worth noting that at the field scale, the MRF is highly fractured, particularly along bedding and cross-bedding planes (see field photos).

These fractures may well control large scale permeability and hence radon migration. Matrix permeability has not been measured in this study and so its variability is not known. Variations in permeability at both hand specimen and field scale could be important in understanding variations in radon levels over the MRF.

7.6 ASSESSMENT OF FIELD DATA IN RELATION TO RADON POTENTIAL MAP

The majority of the outcrop of both the NSF and the MRF occur within the 100-km grid squares SK and SP (Figure 29 and Figure 30, respectively) in the English Midlands. Radon potential data for each bedrock unit, and where applicable with superficial geology, are detailed in Table 3.

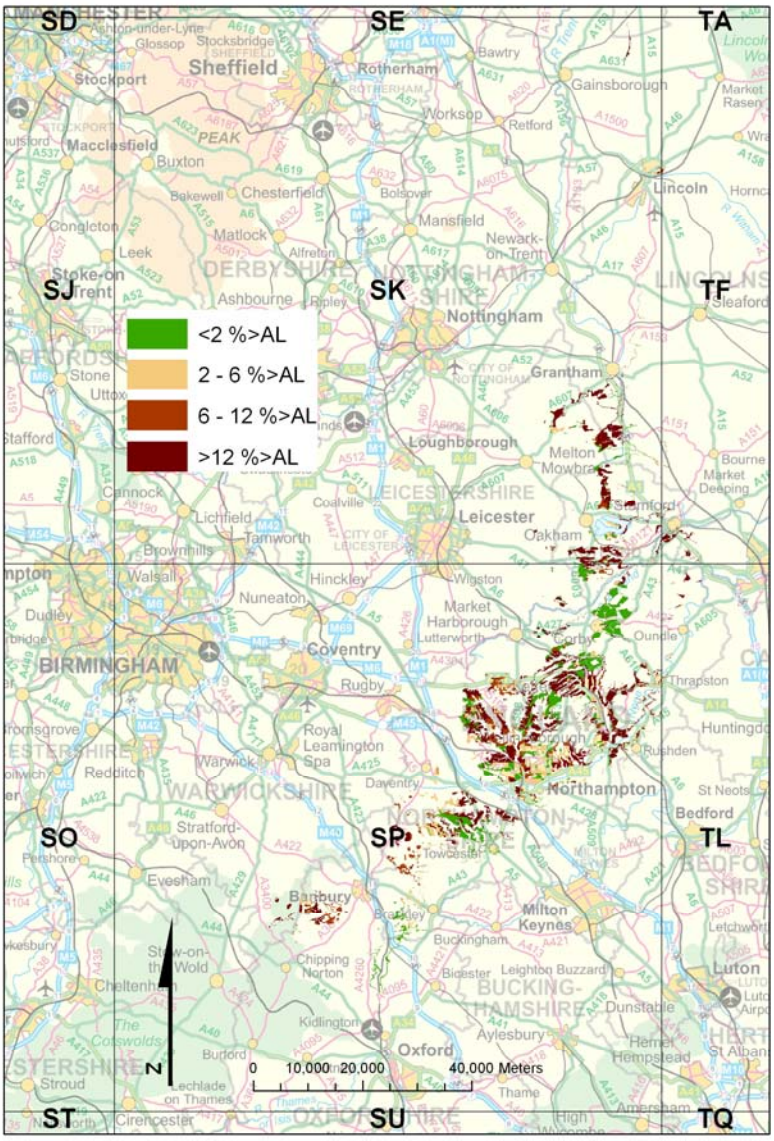

Figure 29 Radon potential map of the Northampton Sand Formation (grouped as Inferior Oolite Group (INONS)) showing the percentage of homes estimated to exceed the radon action level of 200 Bq m^{-3} for the SP and SK 100-km grid squares in Central England.

As a whole, the NSF exhibits a high average radon potential of 15.5 %>AL (number of indoor radon measurements conducted by the Health Protection Agency (n)= 27032) and ranges up to 86.9 %>AL. This means that up to 86.9 % of homes on this geological combination are estimated

to exceed the radon Action Level. Indoor radon measurements in excess of 4000 Bq m^{-3} have been recorded on this bedrock formation. Where the bedrock is covered with diamicton (DMTN), radon potential is very much lowered (Table 3) and less so by cover of sand and gravel (SAGR). This probably reflects the relative permeability of the superficial geology units; sand and gravel being of higher permeability than the diamicton and therefore impeding the flow of radon less than diamicton. Showing the reverse trend is where the NSF is covered by worked ground. This artificial ground classification, used as a pseudo-superficial unit, significantly increases the radon potential relative to bedrock.

There are less indoor measurements on the MRF, but this also displays a high average radon potential of 15.8 %>AL (n= 5311) ranging up to 90.8%>AL (Table 3). This indicates that potentially the highly fractured nature of the Marlstone observed at the field scale increases permeability such that radon can emanate to a similar degree as in the NSF, despite unweathered rock being more tightly cemented and radon emanation being lower at the hand-specimen scale.

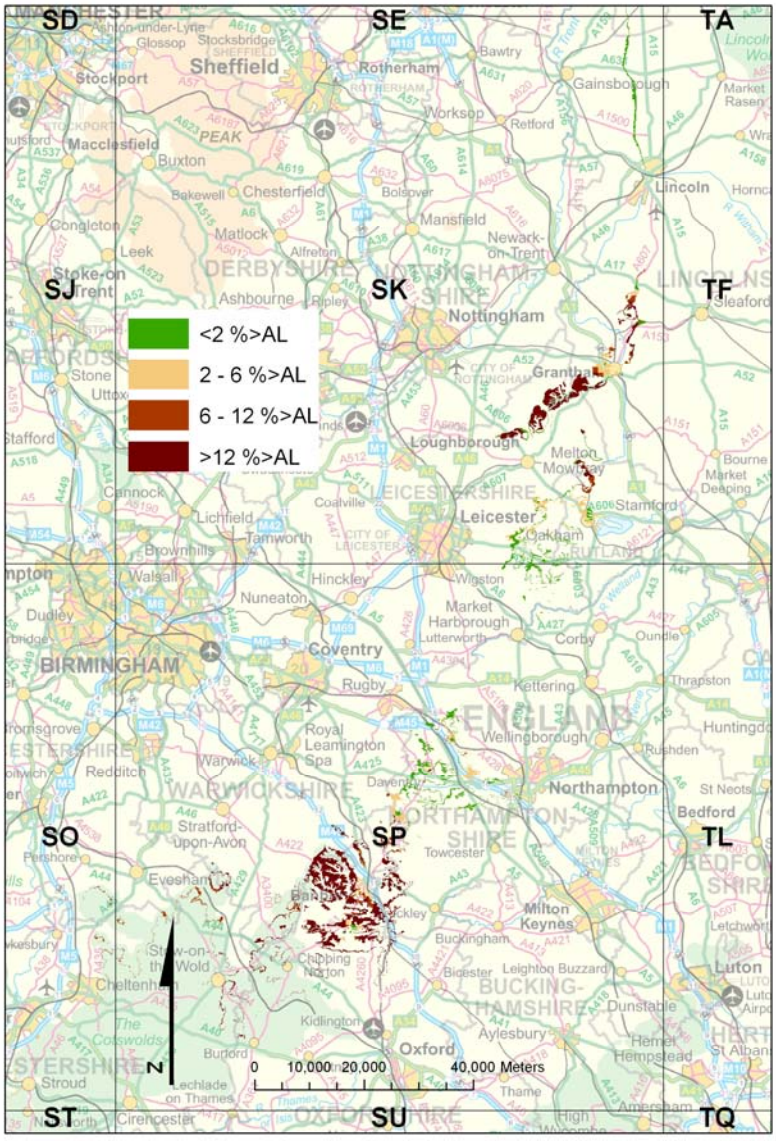

Figure 30 Radon potential map of the Marlstone Rock Formation (for the radon potential map, grouped as MRB) showing the percentage of homes estimated to exceed the radon action level of 200 Bq m^{-3} for the SP and SK 100-km grid squares in Central England.

Bedrock code	Superficial[#] code	100 km Grd-squ.	No:	GM	%>AL	100 km Grd-squ.	No:	GM	%>AL
Northampton Sand Formation (INONS)	-	SK	1211	84	17.9 %	SP	25633	66	12.9 %
Northampton Sand Formation (INONS)	DMTN	SK	59	28	0.3 %	SP	1065	33	2.4 %
Northampton Sand Formation (INONS)	SAGR	SK	12	52	6.6 %	SP	343	59	4.5 %
Northampton Sand Formation (INONS)	WGR	SK	42	189	46.5 %	SP	1332	88	21.6 %
Marlstone Rock Formation (MRB)	-	SK	626	82	18.7 %	SP	4613	86	19.2 %

Table 3 Radon potential data of the Northampton Sand Formation (grouped as Inferior Oolite Group (INONS)) and the Marlstone Rock Formation (grouped as MRB) showing: the 100-km grid square; the number of indoor radon measurements (No:); the Geometric Mean indoor radon (GM) in Bq m^{-3}; and the percentage of homes estimated to exceed the radon Action Level of 200 Bq m^{-3} (%>AL) for the SP and SK 100-km grid squares in Central England.

[#] Artificial geology code (WGR; worked ground) used as a pseudo-superficial geology layer (Ford *et al*., 2010). Other superficial geology codes are: DMTN, diamicton and SAGR, sand and gravel.

Since the field sites were selected in 2003, the radon potential dataset has been updated and re-published using more detailed digital geology and a method that combines both grid-square and geological radon potential mapping resulting in intra- and inter-geological unit interpolation (Miles *et al*., 2007; Miles and Appleton, 2005). This map is more accurate than either of the maps previously published. However, some of the field site selection done in 2003 before the detailed data was available are mismatched with this updated radon map (e.g. Sauvey Castle, Table 4).

Twywell Gullet (Table 4) falls within a high radon potential category, where full radon protective measures would be required in new buildings and extensions to existing buildings. This possibly reflects, as previously discussed, the higher permeability of the worked, made ground but also may reflect the slightly higher uranium and radium results than elsewhere on the Northampton Sand Formation (Table 4 and Table 9). The Scalford Railway cutting area has a cover of diamicton and exhibits a lower radon potential category than Pickwell village which also displays slightly higher U and ^{226}Ra content (Table 4).

Overall it is evident that detailed-scale processes, such as cementing, effect radon emanation at the hand-specimen type scale but those wider-spread processes like surface alteration, fracturing and worked ground make a greater difference to radon risk as a whole. Whilst reducing radon risk to people in homes remains the main motivation for investigation of radon, measurements in homes are the best source of data since these measurements incorporate small-scale and larger scale geological processes, house-specific factors and ultimately are the variable which determines human exposure to radon in the home.

Site name	Bedrock geology	Superficial geology	Mean U by ICP-MS, mg kg^{-1} (Std Err 2 s)	Mean ^{226}Ra Bq kg^{-1}, by LSC (Std Err, 2 s)	Radon potential category at site (%>AL)
Twywell Gullet	INONS	WMGR	2.99 (1.57) n=4	37 (21) n=4	10-30 %AL
Pitsford Quarry	INONS	-	2.61 (0.73) n=9	34 (11) n=9	5-10 %>AL
Harlestone Quarry	GOGRLM		1.35 (0.91) n=8	21 (15) n=8	<1 %>AL
Scalford Railway cutting	MRB	DMTN	2.38 (0.73) n=5	27 (13) n=5	<1 %>AL
Pickwell village	MRB	-	2.90 (1.11) n=6	39 (18) n=6	1-3 %>AL
Sauvey Castle	MLI	-	2.38 (0.75) n=6	32 (17) n=6	<1 %>AL

Table 4 Radon Potential categories and selected laboratory results for sites that underwent laboratory examination. For more information on laboratory samples consult Table 9. Bedrock codes: INON, Northampton Sand Formation (grouped as Inferior Oolite Group); GOGRLM, Great Oolite Group (Rutland Limestone Fm.); MRB, Marlstone Rock Formation; MLI, Middle Lias sandstone, siltstone, ironstone and limestone. Superficial or artificial geology codes: WMGR, Worked, made ground; DMTN, diamicton.

8 Conclusions

- In the Northampton Sand Formation, radon emanation correlates well with both uranium and radium, showing that permeability is not a limiting factor in this rock type. This is supported by petrographic observations. The most significant source of alpha emitters is likely to be the fine grained iron-rich matrix, consisting of iron-rich clays and, where altered, goethite. Phosphate cements are also likely to be a second radon source but of less significance because of their restricted extent and largely sparry, tightly cemented form.
- Areas of the Northampton Sand Formation that were formerly worked, and are now covered by worked ground exhibit increased radon potential. It is possible that the permeable nature of backfill used after working ceased may be in part responsible for the higher radon levels in houses associated with worked-out areas of ironstone.
- The Northampton Sand Formation exhibits a high average radon potential of 15.5 %>AL (n= 27032) but this is decreased by cover of superficial deposits. Diamicton, which is of lower permeability than sand and gravel, reduces the radon potential the most but sand and gravel also has a suppressing effect on radon potential in this case.
- Investigation of the Marlstone Rock Formation reveals that radon emanation is at lower levels than in the Northampton Sand Formation, and does not correlate with uranium or

radium suggesting its escape is impeded. This is supported by petrographic observations that this unit is mostly tightly cemented by sparry calcite. The source of radon is likely to be a mixture of fine grained iron-rich matrix phases and (to a lesser extent) phosphatic cements.

- At the field scale, the Marlstone Rock Formation is highly fractured. These fractures may control large-scale permeability and hence radon migration rather than matrix permeability, which was not measured in this study.
- The Marlstone Rock Formation also exhibits a high average radon potential of 15.8 %>AL (n= 5311). This suggest that the highly fractured nature of the Marlstone Rock observed at the field scale increases permeability such that radon can emanate to a similar degree as in the Northampton Sand Formation, despite unweathered rock being more tightly cemented and radon emanation being lower at the hand-specimen scale.
- Near surface weathering of the ironstones is likely to be very important in enhancing radon potential since weathered mineral phases emanate radon more efficiently.
- Whilst reducing radon risk to people in homes remains the main motivation for investigation of radon, measurements in homes are the best source of data since these measurements incorporate small-scale and larger scale geological processes, house-specific factors and ultimately are the variable which determines human exposure to radon in the home.

Appendix 1 Core logs - fieldwork 2003

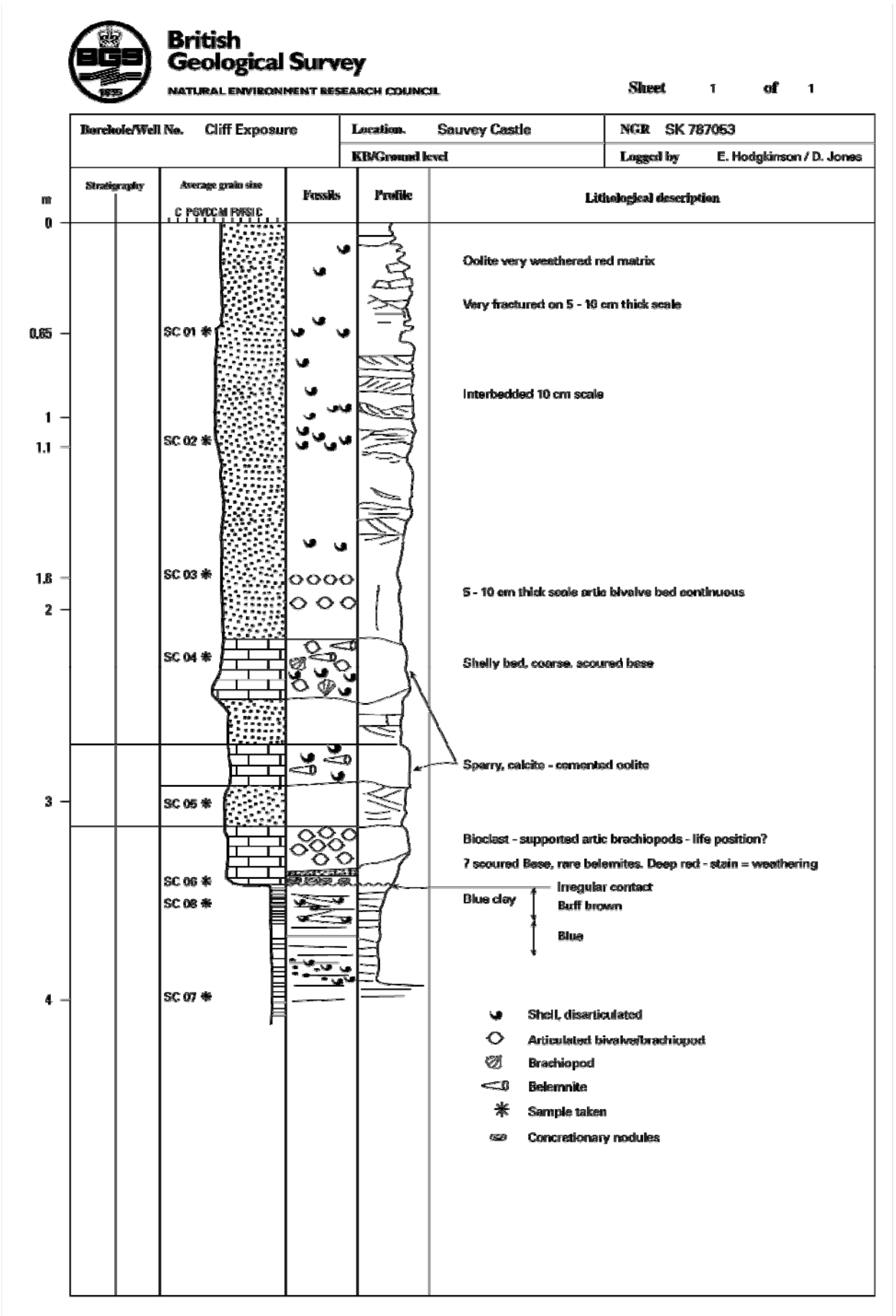

British Geological Survey

NATURAL ENVIRONMENT RESEARCH COUNCIL

Northampton Sandstone

Sheet of

Borehole/Well JH	Location. Twywell C.P. - Gullet	NGR SP 94261 77309
Surface Exposure	KB/Ground level	Logged by E. Hodgkinson / D. Jones 16/7/2003

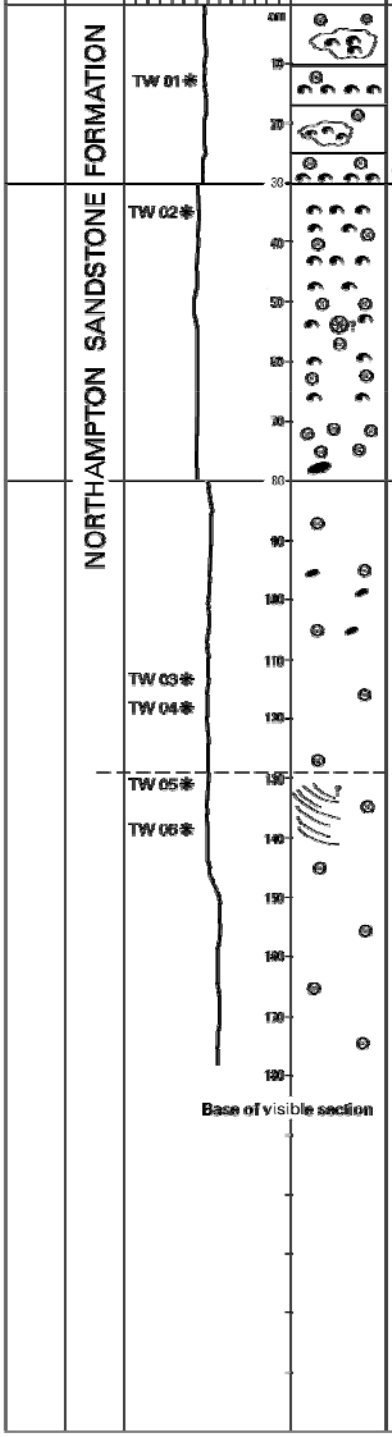

Lithological description

Highly altered, ferruginous, weathered oolitic grainstone.
Shell frags (bivalve) concentrated at certain horizons and in patches sphaeroidal/box-work weathering. Thick surface alteration (0.5-1m) purple, on surface, ochreous orange inside - matrix oolid replacement.

Coarse sandy, oolithic grainstone. Massive bed upper 40cm, shelly throughout (broken and whole bivalves). Box work weathering, ferruginous, becoming more highly developed towards the base occasional coral: pellets (near base) some plucked out at surface and replaced.

Medium ground, oolitic grainstone (ferruginous)
Top 5.0 cm non-fossiliferous, but whitish peloids a few mm ooids.

banded purple/orange weathering around central blocks

Highly weathered with v.well developed box-work structures.
Purplish (Mn?) layers possible cross-bedded unit (discontinuous)
some bivalve framents

Slightly fine grained, morebroken up towards base of section

Key

- Ooids
- Shells
- Coral
- Pellets
- Cross-bedding

British Geological Survey
NATURAL ENVIRONMENT RESEARCH COUNCIL

Sheet 1 of 2

Borehole/Well No.	Location.	NGR	
Surface Exposure	Pitsford Quarry	SP 75717 66891	
	KB/Ground level	Logged by	E. Hodgkinson / D. Jones 17/7/2003

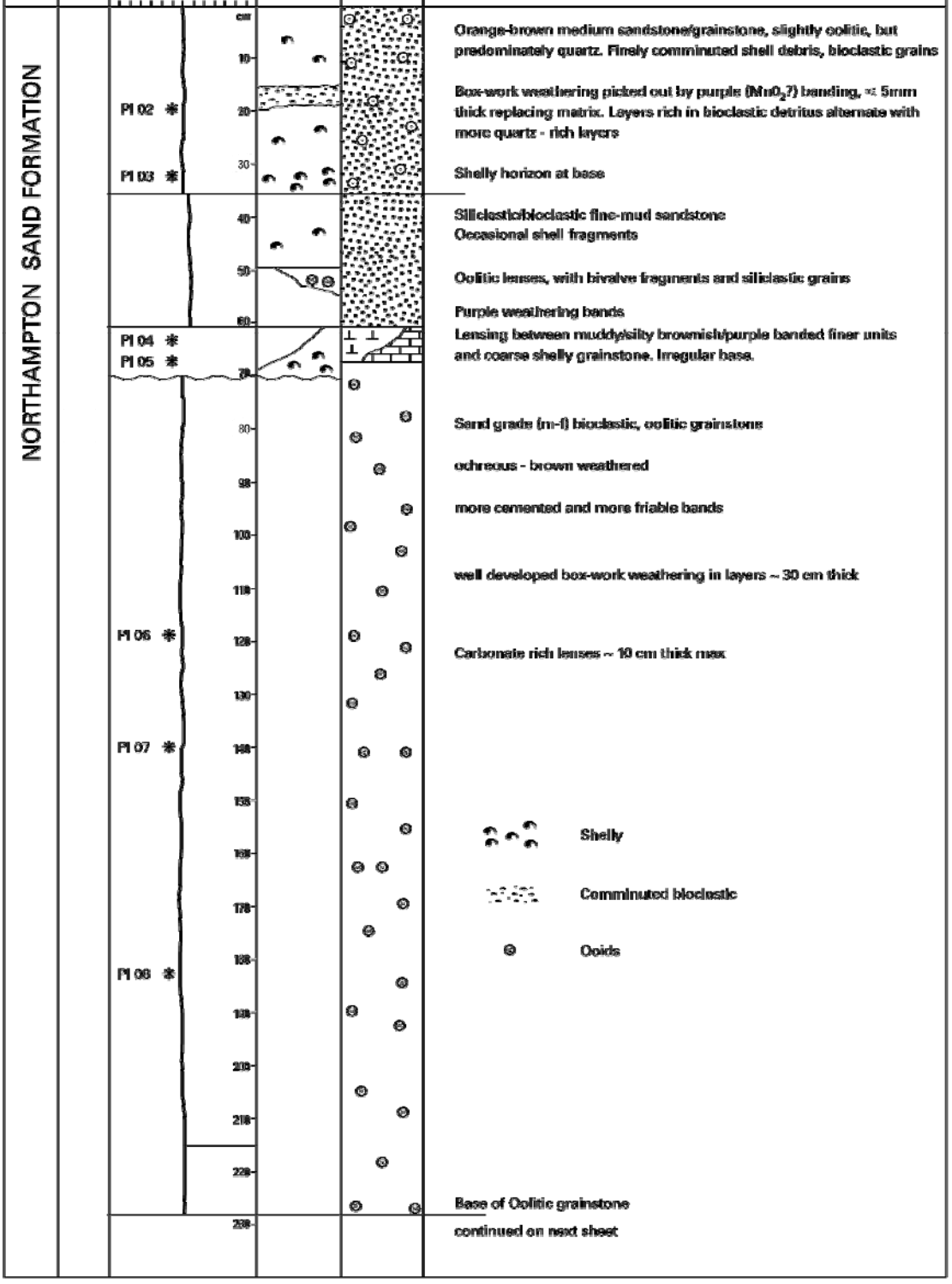

British Geological Survey
NATURAL ENVIRONMENT RESEARCH COUNCIL

Sheet 2 of 2

Borehole/Well No.	Location.	NGR
Surface Exposure	Pitsford Quarry	SP 75717 66891
	KB/Ground level	Logged by E. Hodgkinson / D. Jones 17/7/2003

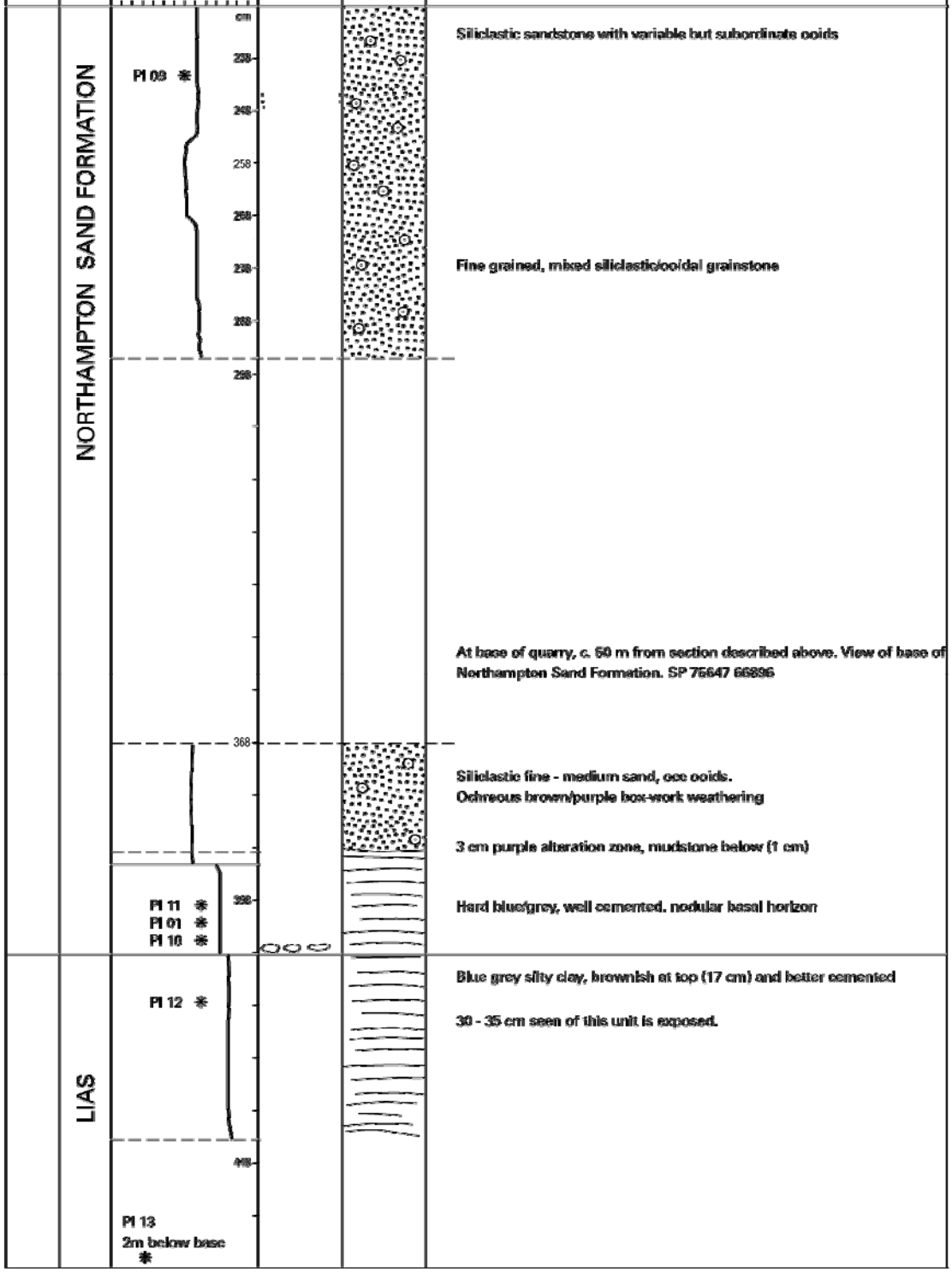

British Geological Survey
NATURAL ENVIRONMENT RESEARCH COUNCIL

Sheet 1 of 4

Borehole/Well No.	Location.	NGR
Surface Exposure, N of Northampton	Harlestone Quarry	SP 70761 63545 to 70778 63529
	KB/Ground level	Logged by E. Hodgkinson / D. Jones 16/7/2003

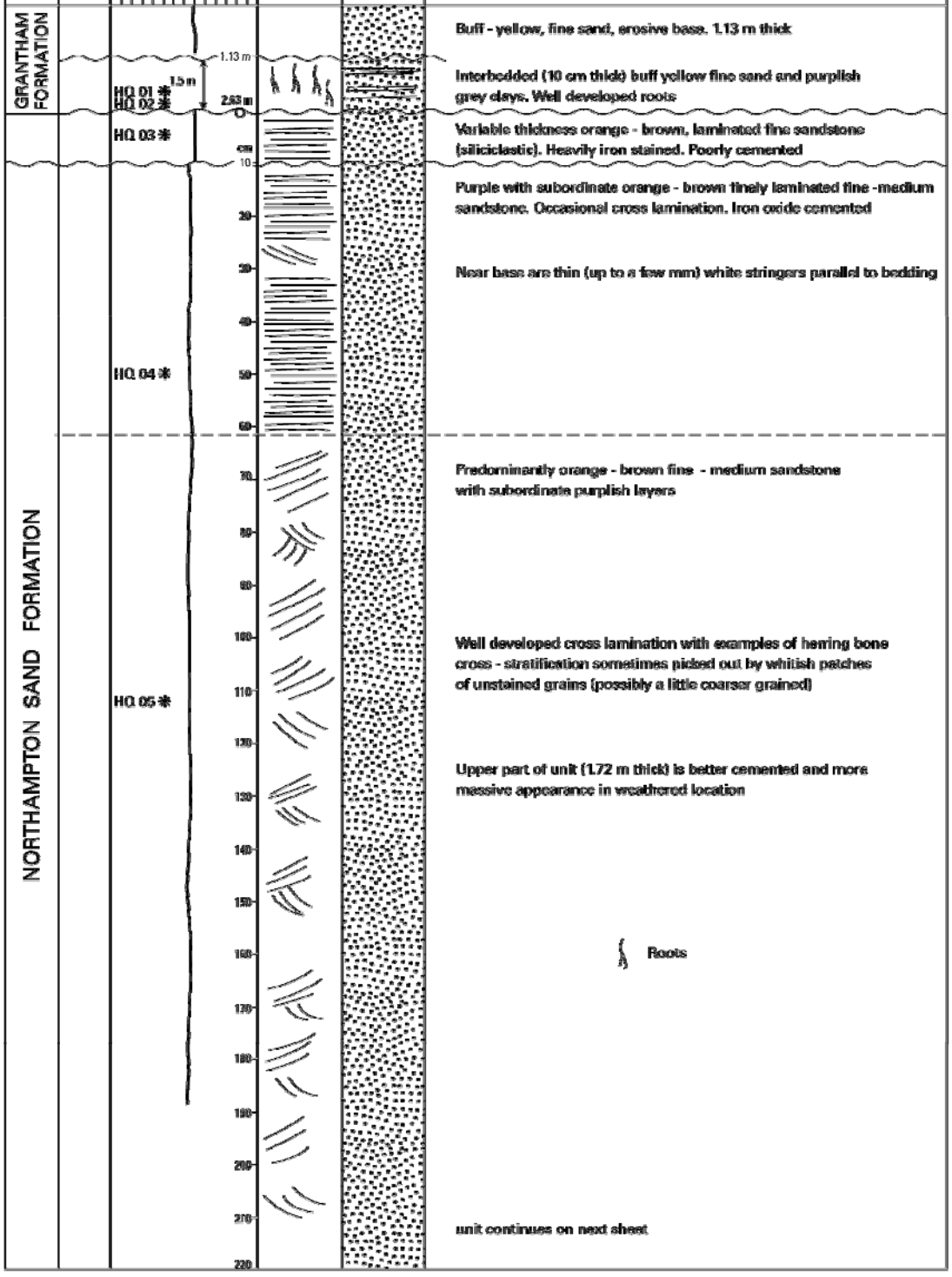

British Geological Survey
NATURAL ENVIRONMENT RESEARCH COUNCIL

Sheet 2 of 4

Borehole/Well No.	Location.	NGR
Surface Exposure, N of Northampton	Harlestone Quarry	SP 70761 63545 to 70778 63529
	KB/Ground level	Logged by E. Hodgkinson / D. Jones 18/7/2003

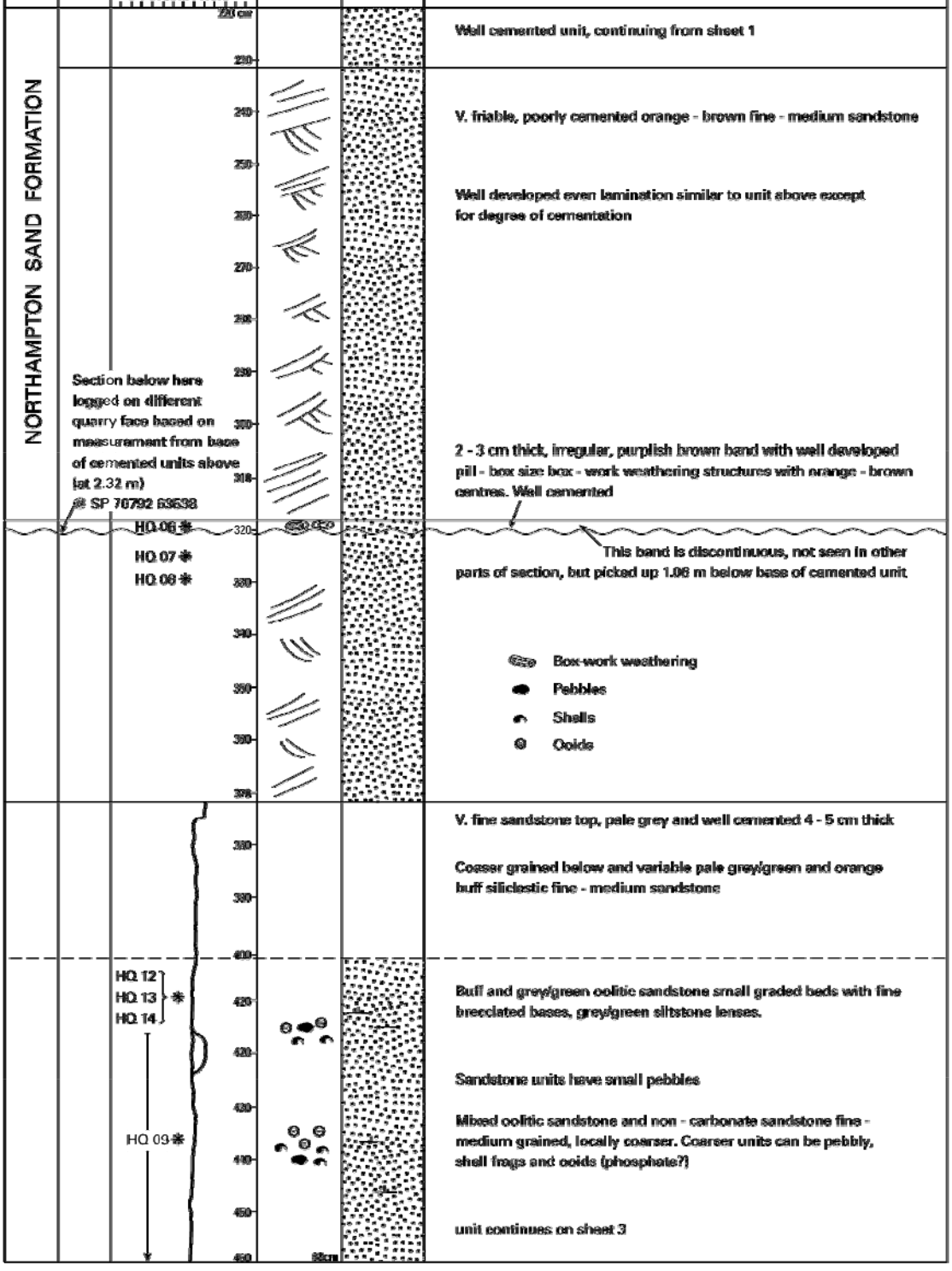

British Geological Survey
NATURAL ENVIRONMENT RESEARCH COUNCIL

Sheet 3 of 4

Borehole/Well No.	Location. Harlestone Quarry	NGR
	KB/Ground level	Logged by E. Hodgkinson / D. Jones

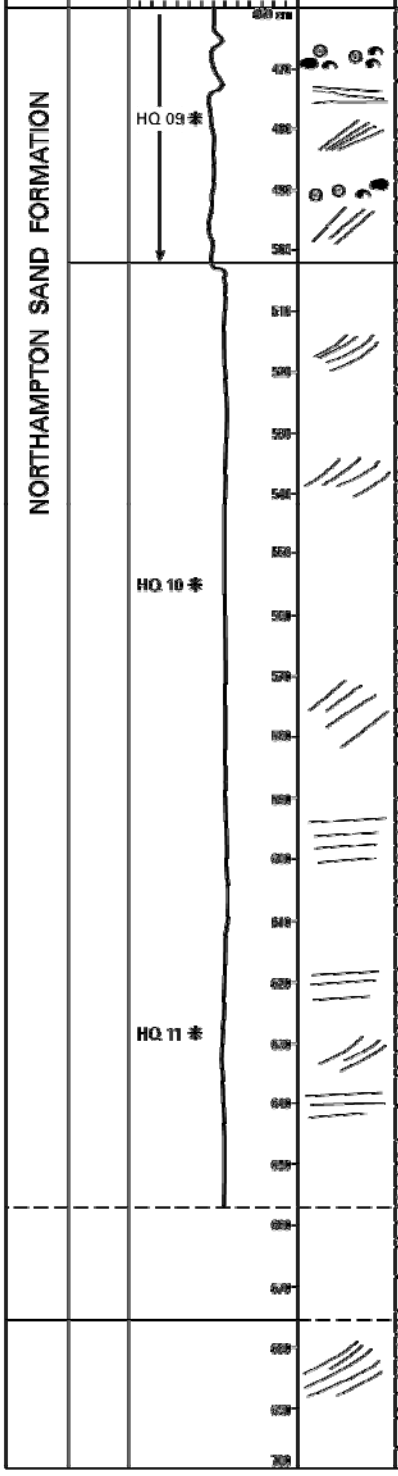

Lithological description

Mixed oolitic sandstone (m grained) and finer siliclastic sandstones. (as above) pale grey/green patches preserved within purplish oxide rims, otherwise orange - brown.

Possible lignite fragment associated with coarse oolitic band below finer lens

Orange brown fine sandstone

Cross lamination visible in places, other areas may be horizontally laminated

Locally developed box-work structure but not weathered out. Rock is moderately well cemented

Cross lamination
Pebbles
Shells
Oolds

Locally more cemented, very hard fine sandstone unit with pale grey/green patches inside a purplish rim

Orange brown fine sandstone, moderately well cemented. Cross bedded

British Geological Survey
NATURAL ENVIRONMENT RESEARCH COUNCIL

Sheet 4 of 4

Borehole/Well No.	Location.	NGR
Surface Exposure	Harlestone Quarry	SP
	KB/Ground level	Logged by E. Hodgkinson / D. Jones

Stratigraphy	Average grain size (C F VC C M F VF SI C)	Sedimentary structures	Graphic lithology	Lithological description
NORTHAMPTON SAND FORMATION	cm 710 720			Orange brown fine sandstone Cross bedded
	730 740			Well cemented fine sandstone, locally grey/green to grey with orange - brown ?????
				Base of observed section (water)

SP 70793 63564 SP 70778 63529

Rough extent of working logged

SP 70793 63564 SP 70761 63545

Appendix 2 Field photographs

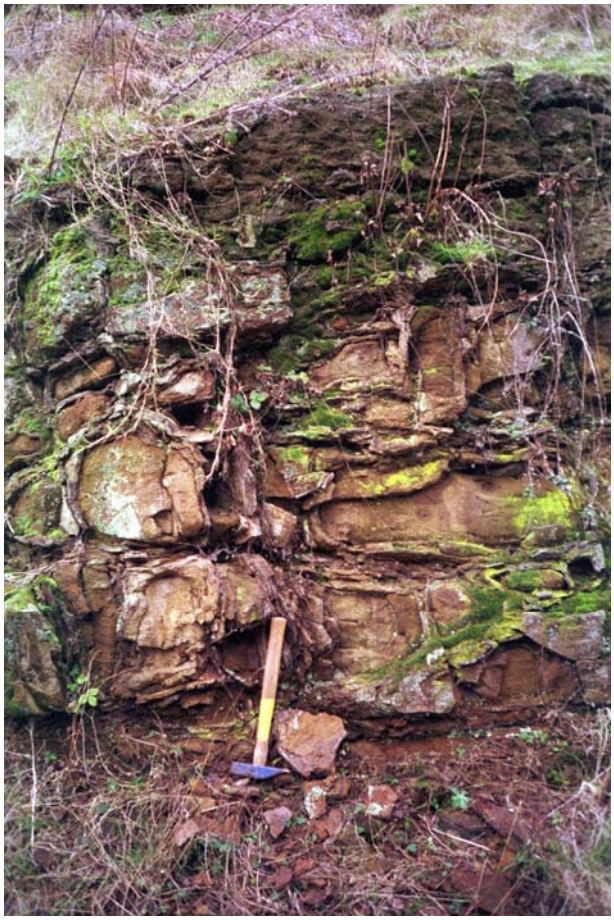

Plate 1 Typical boxwork weathering patterns of the NSF, seen in exposed section at Woodford disused quarry, near Twywell (Grid reference SP 947 768).

Plate 2 Typical exposed section of highly weathered NSF at Twywell Gullet, with boxwork style alteration in the lower part of the section.

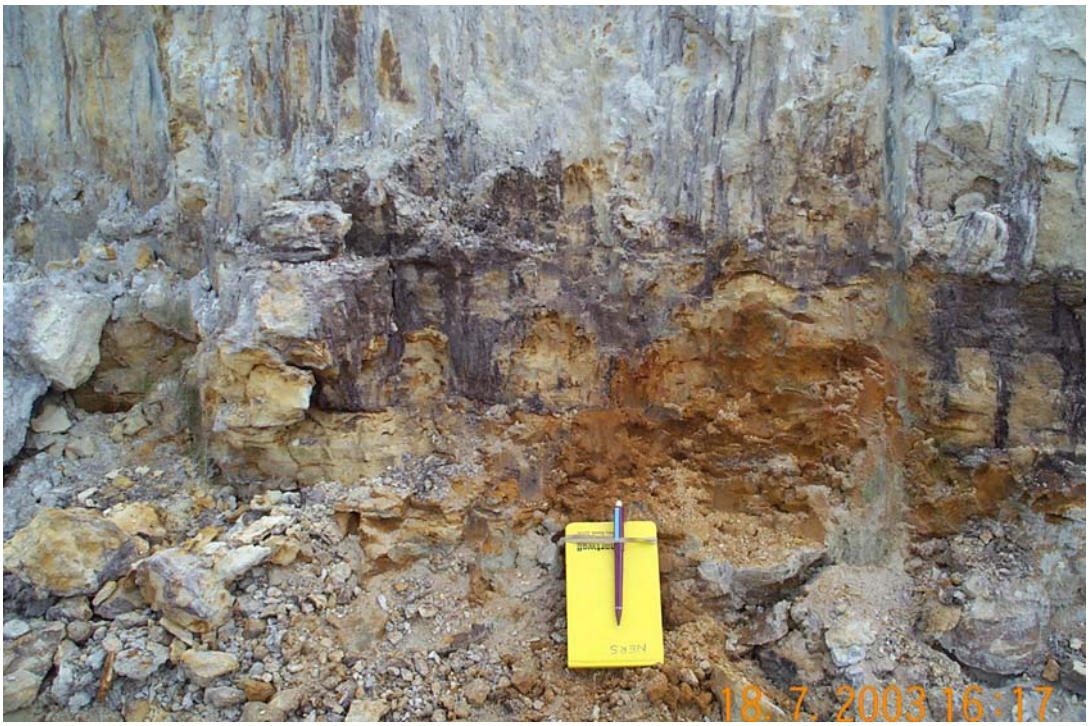

Plate 3 Monitoring exposed section of the NSF at Harlestone quarry (Grid reference SP 70761 63545).

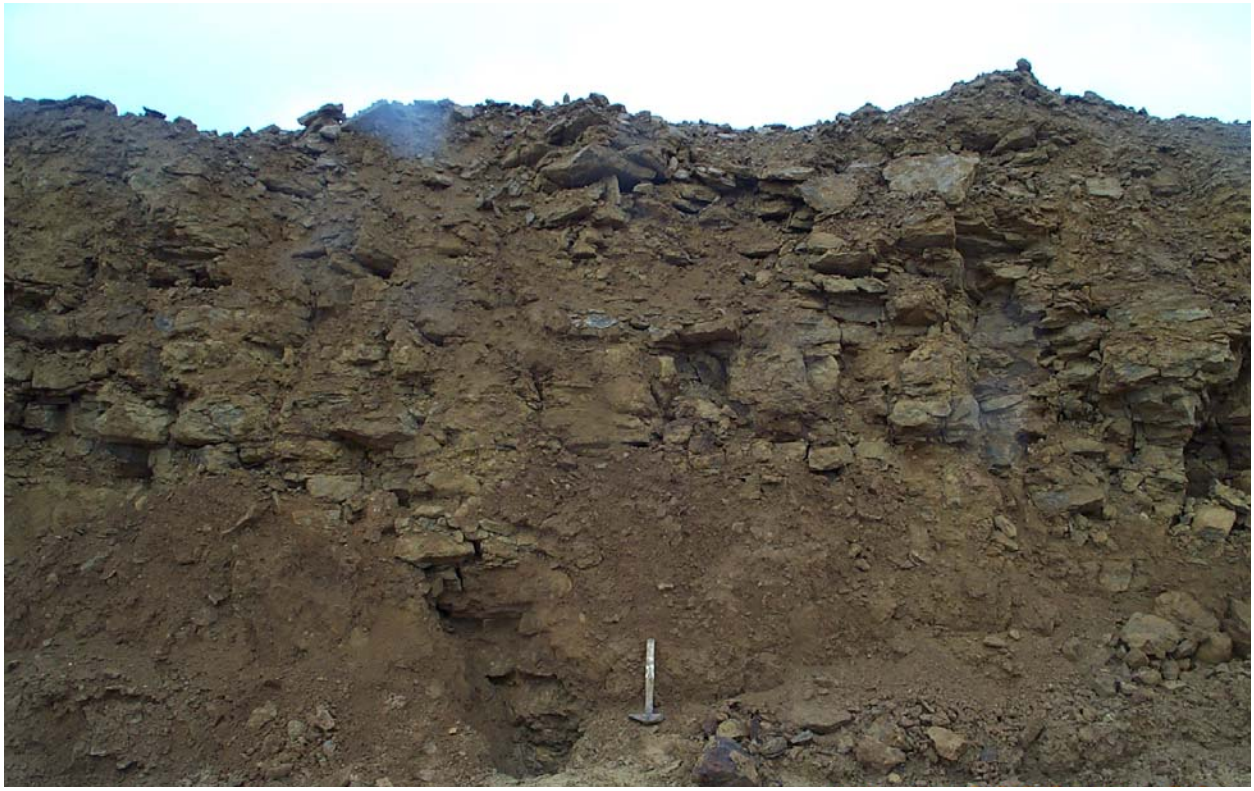

Plate 4 Exposed section of the NSF at Pitsford Quarry (Grid Reference SP 757 669).

Plate 5 Close-up of the MRF at Pickwell (Grid reference SK 784 115) with exposed shells.

Plate 6 A weathered exposure of the MRF at Sauvey Castle (Grid reference SK 787 053).

Plate 7 A close-up of bivalve bed in the MRF at Sauvey Castle.

Appendix 3 List of samples and analyses

Depth from top of ironstone (m)	Field code	MPL no.	Gamma spectrometry	ICP-MS - uranium	XRF	Radium	Radon emanation	Reduced Fe	XRD	Auto-radiography	Permeability
NORTHAMPTON SAND FORMATION											
Twywell Gullet											
0.1-0.2	TW01	J649	X	X	X	X	X	X	X	X	X
0.35	TW02	J650									
1.15	TW03	J651					X				X
1.16-1.23	TW04	J652	X	X	X	X	X	X			
1.3	TW05	J653	X	X	X	X	X			X	X
1.4	TW06	J654	X	X	X	X	X			X	
Pitsford Quarry											
0.17-0.24	PI02	J656	X	X	X	X	X			X	X
0.3-0.35	PI03	J657	X	X	X	X	X			X	
0.6-0.7	PI04	J658	X	X	X	X	X			?	
0.6.0.7	PI05	J659									
1.15-1.2	PI06	J660	X	X	X	X	X				
1.4-1.45	PI07	J661	X	X	X	X	X			X	X
1.8-1.88	PI08	J662	X	X	X	X	X	X	X	X	X
2.4-2.45	PI09	J663	X	X	X	X	X			X	
4	PI11	J665	X	X	X	X	X			X	
4-4.1	PI01	J655			X		X			X	X
4-4.1	PI10	J664	X	X	X	X	X	X	X	X	X
Clay (0.1)	PI12	J666	X	X	X	X					
Clay (2.0)	PI13	J667			X						
Harlestone Quarry											
-0.18-0.12	HQ01	J668	X	X	X	X	X				
-0.05-0	HQ02	J669					X				
0-0.1	HQ03	J670	X	X		X	X			X	?
0.45-0.57	HQ04	J671	X	X	X	X	X			X	X
1.1-1.2	HQ05	J672	X	X	X	X	X				
3.2?	HQ06	J673					X				
3.25?	HQ07	J674					X				
3.25-3.3?	HQ08	J675	X	X	X	X	X			X	
4-4.2	HQ12	J679	X	X	X	X	X	X	X	X	
4-4.2	HQ13	J680									
4-4.2	HQ14	J681									
4 -> 5	HQ09	J676	X	X	X	X	X			X	X
5.5-5.6	HQ10	J677	X	X	X	X		X		X	
6.3	HQ11	J678	X	X	X	X	X			X	X

Depth from top of ironstone (m)	Field code	MPL no.	Gamma spectrometry	ICP-MS - uranium	XRF	Radium	Radon emanation	Reduced Fe	XRD	Auto-radiography	Permeability
MARLSTONE ROCK FORMATION											
Scalford											
-	RC04	J685				X					
0-1	RC02	J683									
0.6	RC05	J686	X	X	X	X	X			X	
1.2	RC03	J684					X				
1.6	RC06	J687	X	X	X	X	X			X	
1.8??	RC01	J682					X				
1.8	RC07	J688	X	X	X	X	X	X		X	
2	RC08	J689	X	X	X	X	X	X		X	
~4	RC09	J690	X	X	X	X	X			X	
Pickwell											
0	PV02	J692	X	X	X	X	X			?	
0	PV03	J693	X	X	X	X	X	X	X	X	
0.4	PV06	J696	X	X	X	X	X			X	X
0.5	PV04	J694	X	X	X	X	X	X		X	X
1	PV01	J691	X	X	X	X	X			X	X
1.5	PV05	J695	X	X	X	X	X			X	
Sauvey Castle											
0.6	SC01	J697	X	X	X	X	X	X	X	X	
1.1	SC02	J698	X	X	X	X	X			X	
1.8	SC03	J699	X	X	X	X	X			X	
2.3?	SC04	J700	X	X	X	X	X	X	X	X	
3	SC05	J701	X	X	X	X	X			X	
3.3-3.4	SC06	J702	X	X	X	X	X			X	
3.5	SC08	J704			X						
4	SC07	J703			X						

Appendix 4 Chemical and other numerical laboratory data

On the following pages the bulk chemical data for the ironstones are presented in Tables 3 to 7. They data include major and trace elements obtained by XRFS, uranium measured by ICP-MS, ^{226}Ra measured by liquid scintillation counting and reduced Fe content determined by titration.

Table 5 Major element bulk chemical data for Northampton Sand Formation, by XRFS.

Depth in	Field	Sample	SiO2	TiO2	Al2O3	Fe2O3t	Mn3O4	MgO	CaO	Na2O	K2O	P2O5	SO3	Cr2O3	SrO	ZrO2	BaO	NiO	CuO	ZnO	PbO	LOI	Total
ironstone (m)	code	no.	%	%	%	%	%	%	%	%	%	%	%	%	%	%	%	%	%	%	%	%	%
Twywell Gullet:																							
0.15	TW01	J649	7.19	0.18	4.37	71.63	0.45	0.37	0.55	0.00	0.26	0.83	<0.1	0.04	0.07	<0.02	0.02	0.03	<0.01	0.04	0.01	13.63	99.64
1.2	TW04	J652	6.41	0.25	6.17	64.38	0.21	0.73	2.13	0.00	0.36	3.09	0.1	0.04	0.73	<0.02	0.04	0.02	<0.01	0.03	0.01	14.52	99.22
1.3	TW05	J653	9.40	0.35	7.94	59.08	0.20	0.84	1.96	0.00	0.48	2.64	0.1	0.07	0.84	0.03	0.05	0.02	<0.01	0.04	<0.01	15.06	99.10
1.4	TW06	J654	5.57	0.22	5.27	57.48	0.20	1.57	3.22	0.00	0.29	2.19	0.4	0.04	0.55	<0.02	0.03	0.02	<0.01	0.03	0.01	22.98	100.07
		Mean	*7.14*	*0.25*	*5.94*	*63.14*	*0.27*	*0.88*	*1.97*	*0.00*	*0.35*	*2.19*	*<0.18*	*0.05*	*0.55*	*<0.02*	*0.04*	*0.02*	*<0.01*	*0.04*	*<0.01*	*16.55*	*99.51*
	Std error (2 s)		*1.42*	*0.06*	*1.32*	*5.53*	*0.11*	*0.44*	*0.95*	*0.00*	*0.08*	*0.85*		*0.01*	*0.29*		*0.01*	*0.00*		*0.00*		*3.75*	*0.38*
Pitsford Quarry:																							
0.2	PI02	J656	12.58	0.15	2.84	18.87	0.12	0.22	33.12	0.10	0.45	0.73	<0.1	0.02	0.02	<0.02	0.03	0.01	<0.01	0.02	<0.01	29.84	99.13
0.33	PI03	J657	8.67	0.09	1.98	19.12	0.11	0.26	35.77	0.09	0.32	0.94	<0.1	0.01	0.03	<0.02	0.03	0.01	<0.01	0.03	<0.01	31.56	99.03
0.65	PI04	J658	10.19	0.21	4.23	21.26	0.24	0.33	32.11	0.02	0.34	1.06	<0.1	0.03	0.03	<0.02	0.04	0.02	<0.01	0.05	0.01	29.31	99.49
1.18	PI06	J660	6.34	0.11	2.55	32.02	0.13	0.31	28.21	0.09	0.32	1.45	<0.1	0.02	0.02	<0.02	0.02	0.01	<0.01	0.03	<0.01	27.56	99.20
1.43	PI07	J661	12.61	0.29	7.53	48.42	0.14	0.82	10.08	0.01	0.40	1.54	<0.1	0.06	0.02	0.02	0.02	0.02	<0.01	0.02	<0.01	17.89	99.89
1.84	PI08	J662	14.10	0.34	8.41	46.36	0.12	0.85	9.41	0.05	0.36	2.51	<0.1	0.06	0.03	<0.02	0.04	0.02	<0.01	0.03	<0.01	16.87	99.57
2.43	PI09	J663	15.58	0.28	6.73	28.61	0.10	0.71	21.62	0.12	0.67	1.30	<0.1	0.04	0.03	0.02	0.03	0.01	<0.01	0.02	<0.01	23.24	99.11
4.0	PI11	J665	20.29	0.25	3.93	45.90	0.15	0.36	10.84	0.07	0.75	1.06	<0.1	0.01	0.02	0.02	0.02	0.01	<0.01	0.01	<0.01	16.02	99.71
4.05 (base)	PI01	J655	21.35	0.31	5.92	24.21	0.14	2.08	17.92	0.12	0.88	0.52	0.5	0.02	0.03	0.02	0.02	0.01	<0.01	0.01	<0.01	20.96	95.02
4.05 (base)	PI10	J664	20.91	0.26	4.06	25.11	0.18	2.74	17.69	0.13	0.80	0.47	0.3	0.01	0.02	0.02	0.02	<0.01	<0.01	0.02	<0.01	26.42	99.16
		Mean	*14.26*	*0.23*	*4.82*	*30.99*	*0.14*	*0.87*	*21.68*	*0.08*	*0.53*	*1.16*	*<0.16*	*0.03*	*0.03*	*<0.02*	*0.03*	*0.01*	*<0.01*	*0.02*	*<0.01*	*23.97*	*98.93*
	Std error (2 s)		*3.32*	*0.05*	*1.40*	*7.40*	*0.03*	*0.54*	*6.37*	*0.03*	*0.14*	*0.38*		*0.01*	*0.00*		*0.01*	*0.00*		*0.01*		*3.65*	*0.89*
Lias (0.1)	PI12	J666	26.80	0.48	9.23	30.55	0.14	2.78	6.54	0.12	1.42	1.73	0.4	0.01	0.02	0.02	0.03	0.01	0.01	0.01	<0.01	18.84	99.14
Lias (2.0)	PI13	J667	58.76	1.02	18.58	6.05	0.02	1.54	0.83	0.36	2.98	0.17	0.3	0.02	0.01	0.03	0.05	0.01	<0.01	0.01	<0.01	8.73	99.47
Harlestone Quarry:																							
Grantham Fm	HQ01	J668	81.42	1.14	7.19	3.62	0.02	0.12	0.16	0.12	1.16	0.05	0.3	0.03	0.01	0.08	0.04	<0.01	<0.01	<0.01	<0.01	3.57	99.03
0.05	HQ03	J670	37.79	1.52	5.07	43.51	0.05	0.14	0.35	0.00	0.54	0.40	0.2	0.05	<0.01	0.17	0.02	<0.01	<0.01	0.02	<0.01	9.82	99.65
0.51	HQ04	J671	63.17	0.35	2.12	25.32	0.06	0.08	0.14	0.13	0.90	0.28	0.6	0.02	0.01	0.03	0.03	0.01	<0.01	0.03	<0.01	5.88	99.16
1.15	HQ05	J672	82.99	0.08	2.64	8.60	0.02	0.04	0.10	0.15	1.52	0.27	0.3	<0.01	0.02	<0.02	0.05	<0.01	0.01	<0.01	<0.01	2.46	99.26
3.28	HQ08	J675	42.89	0.06	2.76	6.93	0.05	0.38	22.88	0.28	1.20	0.23	0.5	0.01	0.04	<0.02	0.04	<0.01	<0.01	<0.01	<0.01	20.80	99.05
4.10	HQ12	J679	41.76	0.06	2.46	3.09	0.05	0.23	27.40	0.27	1.09	0.42	0.1	0.01	0.04	<0.02	0.04	<0.01	<0.01	<0.01	<0.01	22.48	99.51
4.50	HQ09	J676	40.16	0.08	2.23	4.39	0.05	0.29	27.46	0.22	0.93	0.47	0.2	<0.01	0.04	<0.02	0.03	<0.01	<0.01	<0.01	<0.01	22.60	99.15
5.55	HQ10	J677	50.34	0.30	4.31	14.64	0.05	0.24	13.38	0.31	1.19	0.51	<0.1	0.02	0.02	0.03	0.04	0.01	<0.01	0.01	<0.01	13.67	99.07
6.30	HQ11	J678	42.10	0.32	3.94	16.14	0.08	0.41	17.35	0.23	0.95	0.50	<0.1	0.02	0.03	0.03	0.03	0.01	<0.01	0.01	<0.01	17.21	99.36
		Mean	*50.15*	*0.35*	*3.19*	*15.33*	*0.05*	*0.22*	*13.63*	*0.20*	*1.04*	*0.39*	*<0.26*	*0.02*	*0.03*	*<0.04*	*0.04*	*<0.01*	*<0.01*	*<0.01*	*<0.01*	*14.37*	*99.28*
	Std error (2 s)		*10.98*	*0.35*	*0.78*	*9.56*	*0.01*		*8.54*	*0.07*	*0.20*	*0.08*		*0.01*	*0.01*		*0.01*					*5.46*	*0.15*
AVERAGE NORTHAMPTON SAND:																							
Mean			**26.02**	**0.28**	**4.43**	**31.14**	**0.13**	**0.64**	**15.17**	**0.11**	**0.68**	**1.06**	**<0.2**	**0.03**	**0.14**	**<0.03**	**0.03**	**0.01**	**<0.01**	**0.02**	**<0.01**	**19.26**	**99.16**
Std error (2 s)			**9.03**	**0.13**	**0.84**	**8.69**	**0.04**	**0.29**	**5.16**	**0.04**	**0.15**	**0.36**		**0.01**	**0.11**		**0.00**	**0.00**		**0.00**		**3.21**	**0.41**
Maximum			**82.99**	**1.52**	**8.41**	**71.63**	**0.45**	**2.74**	**35.77**	**0.31**	**1.52**	**3.09**	**0.60**	**0.07**	**0.84**	**0.17**	**0.05**	**0.02**	**0.01**	**0.05**	**0.01**	**31.56**	**100.07**
Minimum			**6**	**0**	**2**	**3**	**0**	**0**	**0**	**0**	**0**	**0**	**0**	**0**	**0**	**0**	**0**	**0**	**0**	**0**	**0**	**2**	**95**

Table 6 Major element bulk chemical data for Marlstone Rock Formation, by XRFS.

Depth in	Field	Sample	SiO_2	TiO_2	Al_2O_3	Fe_2O_3t	Mn_3O_4	MgO	CaO	Na_2O	K_2O	P_2O_5	SO_3	Cr_2O_3	SrO	ZrO_2	BaO	NiO	CuO	ZnO	PbO	LOI	Total
ironstone (m)	code	no.	%	%	%	%	%	%	%	%	%	%	%	%	%	%	%	%	%	%	%	%	%
MARLSTONE ROCK:																							
Scalford railway cutting																							
0.6	RC05	J686	14.71	0.25	5.40	26.62	0.27	0.65	24.28	0.17	0.49	0.68	<0.1	0.05	0.03	0.02	0.02	0.01	<0.01	0.02	<0.01	25.52	99.19
1.6	RC06	J687	16.66	0.42	8.85	25.20	0.21	1.03	21.62	0.14	0.74	1.04	<0.1	0.08	0.06	0.03	0.02	0.02	<0.01	0.04	<0.01	23.65	99.81
1.8	RC07	J688	11.67	0.33	7.93	19.84	0.28	0.87	28.02	0.14	0.36	0.61	<0.1	0.06	0.05	0.02	0.02	0.02	<0.01	0.03	<0.01	28.81	99.06
2.0	RC08	J689	10.31	0.28	6.40	34.96	0.44	0.93	21.76	0.07	0.49	0.85	0.1	0.05	0.04	<0.02	0.02	0.02	<0.01	0.03	<0.01	22.97	99.73
4.0	RC09	J690	36.03	0.38	6.19	9.47	0.24	0.58	23.20	0.71	1.18	2.83	<0.1	0.01	0.05	0.02	0.05	<0.01	<0.01	0.01	<0.01	18.64	99.59
		Mean	*17.88*	*0.33*	*6.95*	*23.22*	*0.29*	*0.81*	*23.78*	*0.25*	*0.65*	*1.20*	*<0.01*	*0.05*	*0.05*	*<0.02*	*0.03*	*0.02*	*<0.01*	*0.03*	*<0.01*	*23.92*	*99.48*
	Std error (2 s)		*9.35*	*0.06*	*1.25*	*8.41*	*0.08*	*0.17*	*2.34*	*0.23*	*0.29*	*0.83*		*0.02*	*0.01*		*0.01*	*0.00*		*0.01*		*3.33*	*0.30*
Pickwell village																							
?	PV02	J692	5.36	0.14	3.36	12.97	0.22	0.73	40.10	0.11	0.31	0.35	<0.1	0.03	0.04	<0.02	<0.02	<0.01	<0.01	0.02	<0.01	35.52	99.27
0.0	PV03	J693	7.83	0.23	5.45	21.51	0.33	0.78	31.51	0.12	0.30	0.44	0.1	0.05	0.04	0.02	<0.02	0.02	<0.01	0.03	<0.01	30.87	99.64
0.4	PV06	J696	7.23	0.20	4.60	16.88	0.29	0.85	35.18	0.13	0.48	1.21	0.2	0.03	0.12	<0.02	0.02	0.01	<0.01	0.04	<0.01	31.98	99.46
0.5	PV04	J694	8.18	0.21	5.11	35.93	0.37	0.74	22.51	0.05	0.63	1.62	0.1	0.04	0.04	<0.02	<0.02	0.02	<0.01	0.03	<0.01	24.05	99.65
1.0	PV01	J691	7.37	0.18	3.60	9.97	0.21	0.64	40.97	0.14	0.61	0.51	<0.1	0.02	0.05	<0.02	<0.02	0.01	<0.01	0.02	<0.01	35.23	99.55
1.5	PV05	J695	15.37	0.14	2.56	6.34	0.14	0.55	40.04	0.19	0.47	0.12	<0.1	0.02	0.04	<0.02	0.02	0.01	<0.01	0.01	<0.01	33.74	99.77
		Mean	*8.56*	*0.18*	*4.11*	*17.27*	*0.26*	*0.72*	*35.05*	*0.12*	*0.47*	*0.71*	*<0.12*	*0.03*	*0.06*	*<0.02*	*<0.02*	*<0.01*	*<0.01*	*0.03*	*<0.01*	*31.90*	*99.56*
	Std error (2 s)		*2.84*	*0.03*	*0.91*	*8.62*	*0.07*	*0.09*	*5.83*	*0.04*	*0.12*	*0.47*		*0.01*	*0.03*					*0.01*		*3.47*	*0.14*
Sauvey Castle																							
0.6	SC01	J697	9.57	0.28	6.78	29.91	0.28	1.06	23.45	0.11	0.23	0.96	0.1	0.05	0.16	<0.02	<0.02	0.01	<0.01	0.03	<0.01	26.35	99.35
1.1	SC02	J698	7.84	0.22	4.56	11.35	0.23	0.88	39.02	0.11	0.35	0.80	0.1	0.04	0.12	0.02	<0.02	0.01	<0.01	0.01	<0.01	33.97	99.64
1.8	SC03	J699	25.93	0.27	5.37	18.73	0.29	0.78	23.03	0.35	0.79	1.02	0.1	0.03	0.05	0.02	0.02	0.01	<0.01	0.01	<0.01	22.45	99.25
2.3	SC04	J700	16.48	0.13	2.54	6.09	0.20	0.63	39.26	0.24	0.42	0.17	0.2	0.01	0.03	<0.02	<0.02	0.01	<0.01	0.01	<0.01	33.05	99.49
3.0	SC05	J701	32.02	0.27	4.76	15.69	0.39	0.68	22.00	0.54	0.77	0.30	0.1	0.03	0.04	<0.02	0.02	0.01	<0.01	0.01	<0.01	21.57	99.21
3.35 (nr base)	SC06	J702	35.27	0.39	5.48	7.19	0.39	0.81	25.10	0.60	0.94	1.04	0.4	0.02	0.05	0.04	0.04	0.01	<0.01	0.02	<0.01	21.24	99.03
		Mean	*21.19*	*0.26*	*4.92*	*14.83*	*0.30*	*0.81*	*28.64*	*0.33*	*0.58*	*0.72*	*0.17*	*0.03*	*0.08*	*<0.02*	*<0.02*	*0.01*	*<0.01*	*0.02*	*<0.01*	*26.44*	*99.33*
	Std error (2 s)		*9.48*	*0.07*	*1.14*	*7.21*	*0.06*	*0.13*	*6.69*	*0.17*	*0.23*	*0.31*	*0.10*	*0.01*	*0.04*			*0.00*		*0.01*		*4.72*	*0.18*
Lias (3.5)	SC08	J704	54.06	0.98	19.43	8.14	0.03	1.91	0.58	0.86	2.80	0.16	0.3	0.02	0.01	0.02	0.05	0.02	<0.01	0.01	<0.01	9.71	99.09
Lias (4.0)	SC07	J703	61.06	0.94	17.33	5.55	0.04	1.69	1.09	1.07	2.72	0.11	0.2	0.02	0.01	0.03	0.05	0.01	<0.01	0.01	<0.01	7.08	99.01
AVERAGE MARLSTONE ROCK:																							
Mean			**15.75**	**0.25**	**5.23**	**18.16**	**0.28**	**0.78**	**29.47**	**0.23**	**0.56**	**0.86**	**<0.13**	**0.04**	**0.06**	**<0.02**	**<0.02**	**0.01**	**<0.01**	**0.02**	**<0.01**	**27.62**	**99.45**
Std error (2 s)			**4.97**	**0.04**	**0.83**	**4.70**	**0.04**	**0.07**	**3.78**	**0.10**	**0.12**	**0.31**		**0.01**	**0.02**			**0.00**		**0.01**		**2.71**	**0.12**
Maximum			**36.03**	**0.42**	**8.85**	**35.93**	**0.44**	**1.06**	**40.97**	**0.71**	**1.18**	**2.83**	**0.40**	**0.08**	**0.16**	**0.04**	**0.05**	**0.02**	**0.01**	**0.04**	**0.01**	**35.52**	**99.81**
Minimum			**5**	**0**	**3**	**6**	**0**	**1**	**22**	**0**	**0**	**0**	**0**	**0**	**0**	**0**	**0**	**0**	**0**	**0**	**0**	**19**	**99**

Table 7 Trace element bulk chemical data for Northampton Sand Formation, by XRFS.

Depth in	Field	Sample	Sc	V	Cr	Co	Ni	Cu	Zn	Ga	Ge	As	Se	Br	Rb	Sr	Y	Zr	Nb	Mo	Cs	Ba	La	Ce	Nd	Sm	Hf	Ta	W	Tl	Pb	Bi	Th	U
ironstone (m)	code	no.	ppm	ppm	ppm	ppm	ppm	ppm	ppm	ppm	ppm	ppm	ppm	ppm	ppm	ppm	ppm	ppm	ppm	ppm	ppm	ppm	ppm	ppm	ppm	ppm	ppm	ppm	ppm	ppm	ppm	ppm	ppm	ppm
NORTHAMPTON SAND:																																		
Twywell Gullet																																		
0.15	TW01	J649	26.0	626	278	82.2	177	<1	375	7.2	<1	54.8	<1	<1	11.5	584	89.4	113	5.9	2.4	<4	138	59.2	182	92.3	13.7	1.9	<1	N.D.	<1	52.1	7.4	14.5	4.5
1.2	TW04	J652	25.7	694	348	49.2	129	1.4	268	6.4	1.3	101	<1	<1	18.5	>1500	116	117	9.0	3.2	<4	252	121	308	174	25.4	7.8	<1	N.D.	<1	69.1	7.9	22.4	1.1
1.3	TW05	J653	25.9	847	488	58.8	143	2.8	309	11.2	2.3	64.1	<1	<1	24.0	>1500	75.7	144	10.3	2.5	<4	324	106	300	147	17.4	7.4	<1	N.D.	<1	58.2	7.5	29.3	2.3
1.4	TW06	J654	21.3	654	324	59.1	192	3.2	235	10.4	<1	120	<1	<1	15.0	>1500	69.6	109	6.2	2.5	<4	171	68.1	209	108	14.8	8.3	<1	N.D.	<1	56.4	6.9	20.3	<1
		Mean	*24.7*	*705*	*360*	*62.3*	*160*	*<2.1*	*296.9*	*8.8*	*<1.4*	*84.9*	*<1*	*<1*	*17.3*	*>1271*	*87.6*	*121*	*7.85*	*2.65*	*<4*	*221*	*88.7*	*249.7*	*130*	*17.8*	*6.35*	*<1*	*0*	*<1*	*59.0*	*7.43*	*21.6*	*<2.2*
	Std error (2 s)		*2.0*	*85*	*79*	*12.1*	*25*		*52.2*	*2.0*		*26.5*			*4.6*		*17.7*	*14*	*1.86*	*0.32*		*72*	*25.8*	*55*	*32*	*4.58*	*2.59*				*6.27*	*0.36*	*5.29*	
Pitsford Quarry																																		
0.20	PI02	J656	<1	247	117	23.3	45.5	<1	159	4.3	<1	95.8	<1	<1	13.2	213	54.7	70.3	3.2	<1	5.4	245	55.2	134	72.3	11.6	<1	<1	<1	<1	29.9	3.8	9.6	1.8
0.33	PI03	J657	N.D.	174	85.0	14.7	28.4	<1	258	2.6	1.2	52.1	<1	<1	9.1	206	47.3	43.2	1.3	<1	11.8	178	56.3	146	78.9	12.7	1.0	<1	<1	<1	18.2	4.2	6.7	2.7
0.65	PI04	J658	6.9	510	236	43.1	82.6	<1	378	4.9	2.2	37.7	<1	<1	12.4	210	67.9	104	5.8	1.3	<4	297	61.0	157	86.8	13.4	1.2	<1	<1	<1	60.5	4.5	16.2	2.6
1.18	PI06	J660	<1	251	118	20.0	42.2	<1	265	1.7	<1	23.0	<1	<1	8.5	201	49.1	58.7	2.5	<1	9.0	126	66.4	153	84.6	6.7	2.4	<1	<1	<1	25.3	4.9	8.8	3.2
1.43	PI07	J661	22.8	711	360	47.8	136	<1	150	9.9	2.3	103	<1	<1	19.8	179	81.9	150	9.2	1.0	<4	95.0	73.1	203	111	16.9	1.4	<1	N.D.	<1	60.5	6.0	24.9	3.5
1.84	PI08	J662	22.4	773	392	40.5	123	1.1	257	9.7	3.4	37.6	<1	<1	17.0	253	97.4	153	10.0	1.7	<4	150	86.8	243	130	19.9	2.2	<1	N.D.	<1	52.0	6.3	26.5	5.2
2.43	PI09	J663	18.0	691	324	35.3	83.9	<1	183	9.1	1.7	8.0	<1	<1	23.4	218	81.6	142	6.9	<1	<4	153	70.8	191	105	15.4	3.9	<1	<1	<1	58.0	5.0	25.2	3.7
4.00	PI11	J665	14.9	223	85.3	11.2	35.7	2.4	116	7.0	<1	38.3	<1	<1	25.4	111	40.5	160	2.7	1.1	4.5	160	39.9	130	70.3	3.5	5.2	<1	N.D.	<1	12.4	5.1	4.0	3.3
4.05 (base)	PI01	J655	11.4	264	158	13.0	35.6	4.4	106	7.4	2.6	932	<1	<1	30.8	229	30.5	129	5.5	1.3	8.9	160	29.5	86.8	38.4	2.9	2.9	<1	<1	<1	25.6	3.8	7.7	2.7
4.05 (base)	PI10	J664	7.2	115	66.1	12.1	25.8	2.0	196	5.9	<1	24.8	<1	<1	25.2	179	21.5	139	3.3	<1	6.0	164	31.0	61.1	30.1	4.1	3.1	<1	<1	<1	9.7	4.9	3.7	2.7
		Mean	*<10.6*	*396*	*194*	*26.1*	*63.9*	*<1.6*	*206.7*	*6.25*	*<1.7*	*135*	*<1*	*<1*	*18.5*	*200*	*57.2*	*114.88*	*5.04*	*<1.1*	*<6.2*	*173*	*57.0*	*150.4*	*80.7*	*10.7*	*<2.4*	*<1*	*<0.7*	*<1*	*35.2*	*4.85*	*13.3*	*3.14*
	Std error (2 s)			*158*	*79*	*9.0*	*25.4*		*53*	*1.83*		*178*			*4.8*	*24*	*15.5*	*27.2*	*1.87*			*37*	*11.9*	*34*	*19.5*	*3.83*					*12.9*	*0.53*	*5.76*	*0.57*
Lias (0.1)	PI12	J666	14.3	183	97	11.1	34.9	7.2	74.5	11.6	1.3	46.1	<1	<1	54.9	153	37.5	128	8.7	1.5	4.9	194	47.1	128	58.4	7.0	3.0	<1	N.D.	<1	16.4	4.6	6.5	5.5
Lias (2.0)	PI13	J667	16.9	111	116	13.2	48.0	20.4	79.4	23.4	<1	22.0	<1	<1	116.9	94.1	28.8	251	20.1	1.3	5.2	368	42.1	75.3	36.5	6.2	7.0	2.2	3.3	<1	21.7	2.5	14.5	3.4
Harlestone Quarry																																		
Grantham Fm	HQ01	J668	15.4	326	216	1.8	8.3	5.0	10.4	10.5	2.8	515	<1	<1	26.7	75.2	15.0	738	19.2	3.2	1.4	254	44.2	97.5	46.7	7.1	21.8	<1	1.0	<1	42.4	2.8	16.5	2.7
0.05	HQ03	J670	16.6	645	351	8.4	14.0	6.2	180	7.8	3.1	847	<1	<1	15.7	56.5	31.2	1090	17.8	6.3	<4	105	34.1	103	57.9	5.4	28.8	<1	N.D.	<1	25.6	5.0	21.1	6.1
0.51	HQ04	J671	7.1	162	129	6.7	14.3	7.3	266	3.8	1.2	76.2	<1	<1	18.7	78.3	17.0	224	5.2	1.4	<4	276	16.9	26.8	12.7	<2	6.7	<1	<1	<1	10.0	4.2	5.5	1.6
1.15	HQ05	J672	7.2	57.3	45.3	5.4	6.9	18.6	24.9	2.8	<1	43.7	<1	<1	29.3	124	5.9	59.7	1.8	1.1	<4	380	28.8	37.1	5.9	<2	1.4	<1	<1	<1	10.1	2.0	4.1	1.8
3.28	HQ08	J675	2.6	54.3	43.9	4.9	6.9	<1	10.3	2.7	<1	23.0	<1	<1	25.9	301	27.9	32.0	<1	<1	6.7	348	18.8	47.6	28.6	5.8	<1	<1	<1	<1	8.9	3.2	2.5	1.9
4.10	HQ12	J679	3.2	29.8	39.4	5.7	11.8	<1	12.0	2.2	<1	83.3	<1	<1	22.8	326	28.0	31.8	<1	<1	12.5	301	19.1	55.6	30.5	3.9	<1	<1	<1	<1	9.1	2.7	2.4	1.6
4.50	HQ09	J676	1.6	38.2	32.0	6.9	12.5	<1	26.1	<1	<1	113	<1	<1	20.4	324	26.4	52.7	<1	<1	6.6	263	27.3	52.5	30.8	6.6	1.0	<1	<1	<1	10.9	2.7	2.9	2.4
5.55	HQ10	J677	10.4	154	106	17.9	23.0	2.0	72.9	5.8	<1	27.8	<1	<1	27.2	182	42.1	184	4.3	<1	6.8	301	39.6	96.8	50.6	8.0	2.5	<1	<1	<1	16.4	3.3	6.2	1.7
6.30	HQ11	J678	7.0	149	113	13.2	20.3	<1	54.2	3.9	1.6	21.9	<1	<1	20.7	213	34.6	242	5.0	<1	5.5	246	30.3	86.1	41.8	3.0	6.5	<1	<1	<1	12.6	3.9	7.5	2.1
		Mean	*7.0*	*161.2*	*107.4*	*8.64*	*13.7*	*<4.8*	*80.79*	*<3.8*	*<1.4*	*154*	*<1*	*<1*	*22.6*	*200.8*	*26.6*	*240*	*<4.6*	*<1.7*	*6.26*	*278*	*26.9*	*63.14*	*32.4*	*<4.6*	*<6.1*	*<1*	*<0.9*	*<1*	*13.0*	*3.38*	*6.53*	*2.4*
	Std error (2 s)		*3.5*	*143.7*	*74.6*	*3.24*	*4.0*		*65.85*			*199*			*3.3*	*77.1*	*7.8*	*251*			*2.0*	*58*	*5.7*	*20.0*	*12.5*					*4.0*	*0.68*	*4.37*	*1.07*
AVERAGE NORTHAMPTON SAND:																																		
Mean			**11.8**	**370.4**	**196.4**	**25.4**	**62.4**	**<2.9**	**173.7**	**5.9**	**<1.6**	**134.4**	**<1.0**	**<1.0**	**20.0**	**426.2**	**51.6**	**161.6**	**5.5**	**<1.6**	**<5.8**	**223.4**	**53.1**	**139.8**	**73.9**	**10.0**	**4.7**	**<1.0**	**<0.6**	**<1.0**	**31.7**	**4.8**	**12.7**	**2.6**
Std error (2 s)			**3.8**	**122.4**	**61.1**	**8.5**	**24.8**		**46.5**	**1.3**		**105.3**			**2.6**	**211.9**	**12.4**	**91.8**	**1.7**			**34.9**	**12.6**	**36.1**	**19.7**	**2.9**	**2.5**				**9.5**	**0.7**	**4.0**	**0.5**
Maximum			**25.9**	**846.6**	**488.3**	**62.3**	**191.9**	**18.6**	**378.2**	**11.2**	**3.4**	**932.1**	**1.0**	**1.0**	**30.8**	**1500.0**	**115.7**	**1089.6**	**17.8**	**6.3**	**12.5**	**379.8**	**121.1**	**308.2**	**174.0**	**25.4**	**28.8**	**1.0**	**1.0**	**1.0**	**69.1**	**7.9**	**29.3**	**6.1**
Minimum			**0.0**	**29.8**	**32.0**	**4.9**	**6.9**	**<1.0**	**10.3**	**<1.0**	**<1.0**	**8.0**	**<1.0**	**<1.0**	**8.5**	**56.5**	**5.9**	**31.8**	**1.0**	**<1.0**	**<4.0**	**95.0**	**16.9**	**26.8**	**5.9**	**2.0**	**1.0**	**<1.0**	**0.0**	**<1.0**	**8.9**	**2.0**	**2.4**	**1.0**

Table 8 Trace element bulk chemical data for Marlstone Rock Formation, by XRFS.

Depth in	Field	Sample	Sc	V	Cr	Co	Ni	Cu	Zn	Ga	Ge	As	Se	Br	Rb	Sr	Y	Zr	Nb	Mo	Cs	Ba	La	Ce	Nd	Sm	Hf	Ta	W	Tl	Pb	Bi	Th	U
ironstone (m)	code	no.	ppm	ppm	ppm	ppm	ppm	ppm	ppm	ppm	ppm	ppm	ppm	ppm	ppm	ppm	ppm	ppm	ppm	ppm	ppm	ppm	ppm	ppm	ppm	ppm	ppm	ppm	ppm	ppm	ppm	ppm	ppm	ppm
MARLSTONE ROCK:																																		
Scalford railway cutting																																		
0.6	RC05	J686	12.3	360	352	26.3	89.6	1.8	155	6.6	<1	52.6	<1	<1	13.7	257	23.9	102	7.7	2.5	4.9	113	16.5	53.1	28.9	2.6	3.7	<1	<1	<1	11.6	4.2	18.1	2.9
1.6	RC06	J687	21.8	638	587	45.2	147	5.2	292	9.5	2.2	66.0	<1	<1	25.3	457	43.9	178	11.3	1.1	<4	113	36.9	113	55.5	10.1	6.2	<1	<1	<1	23.1	4.5	32.1	2.3
1.8	RC07	J688	28.7	771	466	55.6	186	6.7	279	9.1	3.1	129	<1	12.1	16.2	429	48.5	152	8.4	<1	<4	84.9	100	213	74.0	7.9	2.6	<1	1.1	<1	28.7	4.1	35.3	2.9
2.0	RC08	J689	18.9	522	377	42.2	137	6.5	263	8.5	2.5	54.9	<1	<1	18.1	360	41.1	131	7.4	1.5	<4	85.4	27.5	104	58.0	7.3	4.1	2.7	<1	<1	18.9	5.0	24.8	3.5
4	RC09	J690	13.5	101	94.1	14.3	32.9	6.4	62.9	6.6	1.3	23.7	<1	<1	32.0	423	44.2	167	5.0	<1	9.9	261	67.5	228	116	18.2	4.0	<1	<1	<1	11.7	3.0	7.3	5.2
		Mean	*19.0*	*478*	*375*	*36.7*	*119*	*5.3*	*211*	*8.1*	*<2.0*	*65*	*<1*	*<3.2*	*21.1*	*385*	*40.3*	*146*	*8.0*	*<1.4*	*<5.4*	*131*	*49.7*	*142*	*66.5*	*9.2*	*4.1*	*<1.3*	*<1*	*<1*	*18.8*	*4.2*	*23.5*	*3.4*
	Std error (2 s)		*6.0*	*232*	*163*	*14.6*	*53*	*1.8*	*88*	*1.2*		*35*			*6.7*	*71*	*8.5*	*27*	*2.0*			*66*	*30.5*	*67*	*28.7*	*5.1*	*1.2*				*6.6*	*0.7*	*10.1*	*1.0*
Pickwell village																																		
?	PV02	J692	<1	285	219	14.2	48.6	<1	130	3.4	2.0	22.7	<1	<1	6.8	347	31.0	65.6	3.4	<1	<4	57.9	19.4	60.7	32.6	4.0	1.3	<1	<1	<1	11.7	4.0	13.5	3.6
0.05	PV03	J693	13.8	487	384	31.0	97.5	5.2	232	7.7	1.3	78.1	<1	<1	9.2	336	39.1	117	6.1	1.8	<4	69.5	15.3	60.6	34.0	<2	4.7	<1	<1	<1	13.8	5.0	24.2	3.6
0.4	PV06	J696	7.6	338	243	19.0	78.5	3.4	304	5.5	1.1	28.3	<1	2.8	13.3	948	63.4	95.2	4.5	<1	5.4	85.0	59.9	148	69.5	12.8	2.6	<1	2.1	<1	15.0	3.7	16.3	7.1
0.5	PV04	J694	17.5	422	264	38.0	112	4.3	224	7.2	3.3	73.0	<1	<1	14.9	342	56.4	111	4.1	1.3	6.1	60.5	26.3	116	70.4	10.8	<1	<1	N.D.	<1	13.6	4.0	18.7	3.6
1.0	PV01	J691	<1	310	195	11.4	52.1	3.3	155	3.4	1.4	15.9	<1	<1	12.9	370	33.2	79.5	3.6	<1	13.1	98.8	37.4	102	56.3	10.6	1.9	<1	<1	<1	10.9	3.3	13.3	3.6
1.5	PV05	J695	N.D.	168	119	8.1	28.5	1.1	69.5	3.4	<1	9.9	<1	<1	12.0	293	14.9	68.7	2.0	<1	10.6	112	21.8	62.7	35.3	4.3	2.0	<1	<1	<1	8.0	2.8	7.7	2.2
		Mean	*<6.8*	*335*	*237*	*20.3*	*69.5*	*<3.1*	*185.7*	*5.1*	*<1.7*	*38.0*	*<1*	*<1.3*	*11.5*	*439*	*39.7*	*89.4*	*4.0*	*<1.2*	*<7.2*	*80.6*	*30.0*	*91.65*	*49.7*	*<7.4*	*<2.3*	*<1*	*<1.0*	*<1*	*12.2*	*3.8*	*15.6*	*4.0*
	Std error (2 s)			*91*	*71*	*9.6*	*26.0*		*68*	*1.63*		*24.3*			*2.4*	*204*	*14.5*	*17.598*	*1.11*			*17.8*	*13.5*	*29.73*	*14.7*						*2.1*	*0.6*	*4.6*	*1.3*
Sauvey Castle																																		
0.6	SC01	J697	23.0	535	419	27.7	104	3.4	237	8.5	2.0	66.1	<1	<1	9.9	1274	43.9	140	6.9	<1	4.9	103	29.8	96.1	45.5	3.0	3.1	<1	<1	<1	18.4	4.2	24.5	3.0
1.1	SC02	J698	<1	361	295	20.8	65.3	3.7	134	5.6	1.5	32.8	<1	<1	11.2	987	34.9	97.0	5.2	<1	<4	90.1	32.3	79.5	41.3	6.6	4.3	<1	<1	<1	10.3	4.1	17.9	4.4
1.8	SC03	J699	14.7	286	205	23.7	65.4	12.3	97.3	6.0	1.3	43.1	<1	<1	26.1	376	34.8	150	5.3	<1	<4	160	50.1	148	83.8	7.5	3.5	<1	<1	<1	11.2	4.1	14.7	2.4
2.3	SC04	J700	N.D.	121	105	13.2	30.1	2.2	52.7	2.3	1.4	25.8	<1	<1	12.0	294	17.8	65.1	2.1	<1	12.6	111	17.2	78.1	39.6	7.9	1.5	<1	<1	<1	9.0	3.2	6.5	5.3
3.0	SC05	J701	12.2	280	202	11.8	39.5	3.5	75.6	5.7	2.0	9.1	<1	1.9	23.5	372	21.9	148	5.1	<1	7.4	180	25.2	98.7	45.2	6.3	3.4	<1	<1	<1	9.1	3.5	13.6	2.4
3.35 (nr base)	SC06	J702	13.9	213	174	10.4	38.2	4.5	167	6.2	1.5	29.5	<1	<1	29.0	421	62.8	240	6.4	<1	<4	238	56.1	158	92.2	21.6	7.6	<1	3.0	<1	15.4	3.1	12.1	3.3
		Mean	*<10.8*	*299*	*233*	*17.9*	*57.1*	*4.9*	*127.2*	*5.72*	*1.62*	*34.4*	*<1*	*<1.2*	*18.6*	*621*	*36.0*	*140.0*	*5.17*	*<1*	*<6.2*	*147*	*35.1*	*109.6*	*57.9*	*8.82*	*3.9*	*<1*	*<1.3*	*<1*	*12.2*	*3.7*	*14.9*	*3.47*
	Std error (2 s)			*115*	*90*	*5.82*	*22.3*	*3.0*	*55.0*	*1.62*	*0.25*	*15.6*			*7.0*	*333*	*13.2*	*48.459*	*1.36*			*46*	*12.2*	*28.18*	*19.2*	*5.3*	*1.66*				*3.12*	*0.4*	*4.92*	*0.95*
Lias (3.5)	SC08	J704	18.1	171	129	37.0	121	28.5	113.0	21.8	2.4	345	<1	<1	104	82.0	25.9	183	13.5	1.8	<4	340	33.0	79.7	34.0	6.8	4.9	1.2	3.4	<1	27.5	2.7	12.4	3.4
Lias (4.0)	SC07	J703	19.3	149	125	20.9	56.6	23.1	97.7	19.4	1.2	20.2	<1	<1	92.2	101	24.5	255	14.1	<1	5.4	354	38.1	87.7	35.2	4.9	6.0	<1	3.2	<1	18.1	2.3	12.3	3.2
AVERAGE MARLSTONE ROCK:																																		
Mean			**11.8**	**364.5**	**276.4**	**24.3**	**79.5**	**4.4**	**172.3**	**6.2**	**1.8**	**44.8**	**<1.0**	**<1.8**	**16.8**	**487.4**	**38.6**	**123.9**	**5.6**	**<1.2**	**<6/3**	**119.0**	**37.6**	**112.8**	**57.5**	**8.4**	**3.4**	**<1.1**	**<1.1**	**<1.0**	**14.1**	**3.9**	**17.7**	**3.6**
Std error (2 s)			**4.3**	**87.9**	**66.4**	**6.8**	**22.4**	**1.3**	**41.5**	**1.0**	**0.3**	**15.1**			**3.7**	**140.4**	**7.0**	**22.6**	**1.1**			**28.3**	**11.0**	**24.9**	**11.7**	**2.6**	**0.8**				**2.7**	**0.3**	**4.0**	**0.6**
Maximum			**28.7**	**770.6**	**587.2**	**55.6**	**186.2**	**12.3**	**303.5**	**9.5**	**3.3**	**129.4**	**1.0**	**12.1**	**32.0**	**1274.0**	**63.4**	**239.9**	**11.3**	**2.5**	**13.1**	**261.3**	**100.3**	**227.8**	**116.1**	**21.6**	**7.6**	**2.7**	**3.0**	**1.0**	**28.7**	**5.0**	**35.3**	**7.1**
Minimum			**0.0**	**100.8**	**94.1**	**8.1**	**28.5**	**1.0**	**52.7**	**2.3**	**1.0**	**9.1**	**<1.0**	**<1.0**	**6.8**	**257.3**	**14.9**	**65.1**	**2.0**	**<1.0**	**<4.0**	**57.9**	**15.3**	**53.1**	**28.9**	**2.0**	**1.0**	**<1.0**	**<1.0**	**<1.0**	**8.0**	**2.8**	**6.5**	**2.2**

Table 9 Bulk chemical data for ironstones: uranium (by ICP-MS), 226-Ra (by LSC) and reduced Fe (by titration).

Depth in ironstone (m)	*Field code*	*Sample no.*	*U by ICP mg/kg*	*226-Ra Bq/kg*	*FeO %*
NORTHAMPTON SAND:					
Twywell Gullet					
0.2	TW01	J649	3.56	57.5	0.06
1.2	TW04	J652	2.75	25	0.17
1.3	TW05	J653	4.69	52.5	
1.4	TW06	J654	0.96	13	
		Mean	2.99	37	
	Std error (2 s)		1.57	21	
Pitsford Quarry					
0.2	PI02	J656	1.91	32.5	
0.3	PI03	J657	1.44	21	
0.7	PI04	J658	2.34	24	
1.18	PI06	J660	2.61	22	
1.4	PI07	J661	3.32	37.5	
1.8	PI08	J662	5.01	73	0.2
2.4	PI09	J663	2.57	38.5	
4.0	PI11	J665	2.76	33	
4.05 (base)	PI10	J664	1.51	22	15.26
		Mean	2.61	34	
	Std error (2 s)		0.73	11	
Lias (0.1)	PI12	J666	2.50	21	
Harlestone Quarry					
Grantham Fm	HQ01	J668	0.97	19.5	
0.05	HQ03	J670	4.47	67.5	
0.51	HQ04	J671	0.90	17.5	
1.15	HQ05	J672	0.60	21	
3.28	HQ08	J675	0.62	7.5	
4.10	HQ12	J679	0.76		0.69
4.50	HQ09	J676	1.00	8.5	
5.55	HQ10	J677	1.36	15.5	0.3
6.30	HQ11	J678	1.09	12.75	
		Mean	1.35	21	
	Std error (2 s)		0.91	15	
Mean Northampton Sand			2.20	30	
	Std error (2 s)		0.60	7	
	Maximum		5.01	73	15.26
	Minimum		0.60	8	0.06

Depth in ironstone (m)	*Field code*	*Sample no.*	*U by ICP mg/kg*	*226-Ra Bq/kg*	*FeO %*
MARLSTONE ROCK:					
Scalford railway cutting					
0.6	RC05	J686	1.52	11.5	
1.6	RC06	J687	1.99	17.5	
1.8	RC07	J688	2.13	29.5	Not detected
2.0	RC08	J689	3.69	50.5	0.07
4.0	RC09	J690	2.58	27	
		Mean	2.38	27	
		Std error (2 s)	0.73	13	
Pickwell village					
?	PV02	J692	2.84	29.5	
0.05	PV03	J693	2.04	39	0.78
0.4	PV06	J696	5.40	83	
0.5	PV04	J694	3.27	33	0.13
1.0	PV01	J691	2.22	25	
1.5	PV05	J695	1.62	22.5	
		Mean	2.90	39	
		Std error (2 s)	1.11	18	
Sauvey Castle					
0.6	SC01	J697	2.33	17.5	1.45
1.1	SC02	J698	3.19	62.5	
1.8	SC03	J699	1.59	16	
2.3	SC04	J700	3.61	33.5	2.1
3.0	SC05	J701	1.17	14	
3.35 (nr base)	SC06	J702	2.41	51	
		Mean	2.38	32	
		Std error (2 s)	0.75	17	
Mean Marlstone Rock			2.56	33	
	Std error (2 s)		0.50	9	
		Maximum	5.40	83	1.45
		Minimum	1.17	12	0.07

Table 10 Gamma spectrometry results obtained from milled laboratory samples of Northampton Sand.

Sample no		Weight	K-40	Error	Tl-208	Error	Bi-212	Error	Pb-212	Error	Bi-214	Error	equiv. U	Pb-214	Error	Ac-228	Error	Th-231	Error	Pa-234M	Error	U-235	Error
		g	mBq/g	(to 2 σ)	mBq/g	(to 2 σ)	mBq/g	(to 2 σ)	mBq/g	(to 2 σ)	mBq/g	(to 2 σ)	ppm	mBq/g	(to 2 σ)	mBq/g	(to 2 σ)	mBq/g	(to 2 σ)	mBq/g	(to 2 σ)	mBq/g	(to 2 σ)
Northampton Sand:																							
Twywell																							
	J649	272	92.3	3.5	46.0	5.4	76.7	1.3	29.8	2.0	33.8	2.0	2.7	72.5	9.6	27.7	37.2	29.4	1.2	2.5	N/a	3.7	N/a
	J652	255	72.4	6.8	54.4	4.6	48.5	3.6	80.7	5.6	10.7	0.8	0.9	12.4	1.0	79.8	2.2	16.1	6.1	0.8	24.7	2.9	0.5
	J653	196	105.0	9.5	74.1	6.3	68.6	5.0	113.2	7.9	22.7	1.3	1.8	24.0	1.7	109.2	3.0	33.9	12.0	40.6	38.7	4.9	0.7
	J654	217	62.2	6.6	49.3	4.3	50.3	3.7	77.0	5.6	5.0	0.7	0.4	5.9	0.7	75.8	2.1	18.9	7.0	9.7	29.7	0.7	0.3
	Mean		*83.0*	*19.3*	*55.9*	*12.6*	*61.0*	*13.8*	*75.2*	*34.3*	*18.1*	*12.8*	*1.5*	*28.7*	*30.2*	*73.1*	*33.7*	*24.6*	*8.5*	*13.4*	*18.5*	*3.1*	*1.8*
Pitsford																							
	J656	192	156.8	12.1	ND	0.0	38.7	3.6	60.3	4.5	16.3	1.1	1.3	17.3	1.9	53.2	1.7	22.9	7.9	5.8	43.5	2.5	1.2
	J657	189	112.6	9.0	26.3	2.3	22.1	2.5	35.6	2.9	16.9	1.0	1.4	19.7	1.3	33.2	1.2	17.6	6.1	97.9	45.3	1.0	1.0
	J658	196	81.5	8.0	40.4	3.6	39.8	3.4	65.6	4.9	18.3	1.1	1.5	22.2	1.4	59.1	1.8	20.3	7.3	15.6	34.6	2.2	1.3
	J660	213	57.7	6.2	22.2	2.0	20.8	2.3	34.5	2.9	16.5	1.0	1.3	19.3	1.2	33.5	1.2	10.4	4.1	1.2	27.0	1.3	1.1
	J661	174	86.0	8.9	61.8	5.4	58.6	4.7	92.1	6.8	26.2	1.5	2.1	31.7	2.0	94.7	2.7	27.9	10.0	77.1	43.0	6.3	0.9
	J662	185	98.2	8.6	76.4	6.4	60.3	4.8	106.2	7.5	52.1	2.1	4.2	58.3	3.3	99.2	2.8	41.8	14.3	163.3	45.4	1.2	1.4
	J663	114	124.2	9.6	45.3	3.9	41.3	2.9	69.3	4.8	14.0	0.8	1.1	13.7	1.6	74.9	1.9	21.9	7.6	32.1	30.5	1.4	1.0
	J664	216	161.6	12.5	9.0	1.0	9.5	1.8	16.2	1.6	9.2	0.8	0.7	10.8	0.8	17.5	0.8	7.5	3.2	ND	0.0	1.6	0.3
	J665	190	205.1	15.8	16.4	1.6	15.4	2.4	27.0	2.4	15.8	1.1	1.3	18.1	1.2	27.3	1.2	8.4	3.9	33.4	34.0	3.6	0.5
	Mean		*120.4*	*31.1*	*37.2*	*15.5*	*34.1*	*12.2*	*56.3*	*20.3*	*20.6*	*8.4*	*1.7*	*23.5*	*9.5*	*54.7*	*19.8*	*19.9*	*7.2*	*53.3*	*37.3*	*2.3*	*1.1*
Lias	J666	161	413.3	28.8	22.2	2.9	37.2	3.2	51.1	2.1	57.7	3.3	4.7	41.1	31.0	34.3	1.6	13.6	5.2	150.2	48.5	5.4	1.6
Harlstone																							
Grantha	J668	205	277.5	19.8	47.0	4.1	43.2	3.5	68.6	5.1	21.8	1.2	1.8	22.8	1.6	68.9	2.0	25.7	9.0	ND	0.0	1.8	1.2
	J670	230	141.5	11.2	45.3	3.9	42.6	3.5	71.1	5.4	35.1	1.5	2.8	41.0	2.4	70.5	2.0	26.6	9.4	73.6	35.2	3.3	1.4
	J671	229	187.6	14.0	16.3	1.6	16.9	2.0	25.2	2.2	8.6	0.7	0.7	9.7	0.8	26.0	1.0	ND	0.0	ND	0.0	0.9	1.0
	J672	211	389.8	28.0	14.4	1.4	15.1	2.5	19.2	1.8	8.2	0.8	0.7	9.9	0.8	18.6	1.0	7.8	3.2	25.1	46.8	1.1	0.4
	J675	210	284.4	19.4	7.2	0.8	8.5	1.3	13.0	1.2	1.8	0.4	0.1	1.9	0.4	13.4	0.6	3.8	1.9	13.1	23.5	0.7	0.2
	J676	187	264.2	19.6	10.5	1.1	15.3	2.3	17.7	1.7	11.6	0.9	0.9	14.5	1.0	17.4	0.9	10.7	4.0	ND	0.0	0.9	1.1
	J677	134	311.9	21.8	18.4	1.6	14.2	1.9	24.3	2.0	10.7	0.8	0.9	12.3	0.9	23.8	0.9	11.7	4.2	28.2	42.6	1.3	0.9
	J678	187	229.6	17.3	17.8	1.8	19.2	2.6	29.4	2.5	7.0	0.8	0.6	8.1	0.8	29.9	1.2	ND	0.0	ND	0.0	ND	0.0
	J679	212	260.5	18.9	6.2	0.8	8.1	1.7	11.1	1.2	3.4	0.6	0.3	3.1	0.5	11.7	0.7	ND	0.0	ND	0.0	ND	0.0
	Mean		*258.7*	*53.7*	*17.0*	*8.7*	*17.5*	*7.7*	*26.4*	*13.5*	*10.8*	*7.3*	*0.9*	*12.6*	*8.7*	*26.4*	*13.3*	*12.1*	*6.1*	*35.0*	*18.8*	*1.4*	*0.7*
Average Northampton Sand:																							
			166.0	*2.7*	*32.9*	*0.9*	*32.9*	*0.5*	*48.5*	*0.9*	*16.4*	*0.2*	*1.3*	*20.3*	*0.8*	*47.4*	*3.4*	*18.8*	*1.7*	*38.8*	*7.6*	*2.2*	*0.2*

Table 11 Gamma spectrometry results obtained from milled laboratory samples of Marlstone Rock.

Sample no		Weight	K-40	Error	Tl-208	Error	Bi-212	Error	Pb-212	Error	Bi-214	Error	equiv. U	Pb-214	Error	Ac-228	Error	Th-231	Error	Pa-234M	Error	U-235	Error
		g	mBq/g	(to 2 σ)	mBq/g	(to 2 σ)	mBq/g	(to 2 σ)	mBq/g	(to 2 σ)	mBq/g	(to 2 σ)	ppm	mBq/g	(to 2 σ)	mBq/g	(to 2 σ)	mBq/g	(to 2 σ)	mBq/g	(to 2 σ)	mBq/g	(to 2 σ)
Marlstone Rock:																							
Scalfor	J686	169	152.2	13.1	57.3	5.0	45.4	4.7	80.0	6.1	15.4	1.2	1.2	15.8	2.0	80.3	2.6	27.7	9.6	ND	0.0	3.0	0.6
	J687	174	164.8	11.9	81.2	6.8	73.8	4.2	118.4	7.7	11.9	0.8	1.0	12.5	1.0	121.5	2.9	35.2	12.0	46.8	28.9	2.0	1.0
	J688	171	121.2	9.3	104.5	8.6	84.5	5.5	141.1	9.2	19.2	1.1	1.6	17.6	1.9	144.6	3.6	45.3	15.2	38.9	48.9	1.4	1.3
	J689	188	100.4	9.3	59.1	5.1	52.5	4.2	87.1	6.4	29.7	1.5	2.4	36.1	2.2	86.7	2.5	24.7	8.9	66.5	37.8	2.2	1.4
	J690	170	295.9	21.5	19.1	1.9	19.6	2.6	31.5	2.9	21.3	1.4	1.7	23.2	1.5	31.1	1.3	12.7	5.0	ND	0.0	2.8	1.4
	Mean		*166.9*	*68.4*	*64.2*	*28.4*	*55.2*	*22.7*	*91.6*	*37.2*	*19.5*	*6.0*	*1.6*	*21.0*	*8.3*	*92.8*	*38.8*	*29.1*	*10.9*	*50.7*	*12.7*	*2.3*	*0.6*
Pickwell																							
	J691	197	150.3	11.5	37.4	3.2	34.3	3.0	56.9	4.1	21.6	1.1	1.8	28.4	1.7	50.6	1.5	23.1	7.9	40.0	41.1	0.9	1.0
	J692	173	57.9	7.3	36.0	3.3	32.6	3.4	57.8	4.7	22.2	1.3	1.8	26.3	1.7	55.3	1.8	16.0	6.1	ND	0.0	4.3	0.6
	J693	185	78.7	8.0	72.0	6.1	71.6	4.9	111.4	7.8	12.7	1.0	1.0	14.1	1.2	104.9	2.9	30.5	10.7	ND	0.0	3.1	0.5
	J694	202	177.8	12.8	60.4	5.0	50.4	3.7	84.8	5.8	23.7	1.1	1.9	25.6	2.6	82.6	2.2	29.3	10.1	22.9	41.2	2.5	1.1
	J695	201	106.6	8.0	21.2	1.9	20.3	1.7	32.3	2.6	11.5	0.7	0.9	13.7	0.9	33.2	1.0	6.9	2.5	20.6	22.6	1.7	0.8
	J696	188	112.7	10.0	34.8	3.1	35.6	3.3	58.0	4.6	53.8	2.0	4.4	59.8	3.4	55.4	1.8	27.3	9.7	51.3	40.2	5.7	1.7
	Mean		*114.0*	*36.2*	*43.6*	*15.3*	*40.8*	*14.6*	*66.9*	*22.4*	*24.3*	*12.5*	*2.0*	*28.0*	*13.8*	*63.7*	*20.9*	*22.2*	*7.5*	*33.7*	*11.9*	*3.0*	*1.4*
Sauvey Cas																							
	J697	187	87.9	7.5	71.9	6.0	60.3	4.5	101.1	6.9	22.2	1.2	1.8	25.1	2.6	98.9	2.7	35.9	12.2	ND	0.0	2.0	1.3
	J698	166	73.3	8.3	47.7	4.2	46.2	4.1	74.7	5.8	33.5	1.7	2.7	41.2	2.5	35.4	30.3	74.6	2.3	26.5	9.5	3.6	1.7
	J699	174	181.5	14.5	32.3	3.0	35.3	3.3	54.6	4.3	6.5	0.8	0.5	8.4	0.9	53.4	1.8	14.1	5.5	9.7	37.0	2.1	0.4
	J700	193	132.1	9.9	24.2	2.1	21.2	2.3	32.4	2.6	47.6	1.6	3.9	53.3	2.9	29.8	1.1	13.5	4.9	80.7	30.9	3.4	1.2
	J701	185	187.3	14.5	33.2	3.0	31.6	3.0	52.9	4.2	3.7	0.7	0.3	4.5	0.7	53.2	1.7	12.3	4.9	12.3	32.2	1.3	0.4
	J702	176	246.0	18.4	41.9	3.6	34.8	3.6	60.2	4.5	30.1	1.5	2.4	34.0	2.0	55.0	1.8	26.5	9.1	44.2	51.8	1.0	1.3
	Mean		*151.3*	*53.7*	*41.9*	*13.7*	*38.2*	*11.0*	*62.6*	*19.0*	*23.9*	*13.7*	*1.9*	*27.8*	*15.5*	*54.3*	*19.8*	*29.5*	*19.6*	*34.7*	*23.8*	*2.2*	*0.9*
Average Marlstone Rock:																							
			142.7	*1.9*	*49.1*	*0.9*	*44.1*	*0.5*	*72.7*	*0.9*	*22.7*	*0.2*	*1.8*	*25.9*	*0.4*	*68.9*	*3.3*	*26.8*	*1.7*	*38.4*	*9.3*	*2.5*	*0.2*

Table 12 Results of radon emanation (LSC) tests on hand specimens of ironstone.

Sample no.	Surface Area (cm^2)	Dry Volume, V_d (cm^3)	Internal porosity volume, V_i (cm^3)	Rock volume V_r (V_d-V_i) (cm^3)	Volume of water (cm^3)	Radon activity / area (Bq/m^2)	Std error (to 2σ) (Bq/m^2)	% Std error	Radon activity / volume V_r (Bq/l)	Std error (to 2σ) (Bq/l)	% Std error
J649	140	165	25	140	915	**130.4**	23.6	18	**13.0**	2.4	18
J651	110	43	25	18	517	**111.0**	9.7	9	**71.8**	7.5	11
J652	125	33	10	23	527	**33.0**	4.9	15	**18.8**	2.9	16
J653	140	73	30	43	487	**124.7**	11.0	9	**40.6**	3.7	9
J654	95	38	10	28	522	**15.4**	2.2	14	**4.9**	0.7	15
J655	115	56	20	36	504	**50.1**	22.3	44	**15.2**	6.8	45
J656	290	144	35	109	936	**36.6**	11.5	32	**9.6**	3.0	32
J657	150	75	25	50	485	**75.4**	5.4	7	**22.2**	1.7	7
J658	100	66	20	46	494	**97.4**	8.0	8	**22.1**	1.9	8
J660	215	160	35	125	400	**112.6**	43.3	38	**19.2**	7.4	38
J661	180	111	40	71	449	**85.9**	154.9	180	**22.4**	40.4	180
J662	45	22	5	17	538	**282.6**	7.6	3	**84.8**	6.1	7
J663	150	80	45	35	480	**104.0**	14.5	14	**47.3**	6.8	14
J664	161	124	15	109	436	**9.9**	7.3	74	**1.5**	1.1	74
J665	80	26	10	16	534	**88.7**	6.9	8	**44.4**	4.4	10
J668	70	40	20	20	520	**160.2**	78.8	49	**59.0**	29.2	49
J669	135	58	25	33	502	**169.7**	7.1	4	**73.9**	3.9	5
J670	290	200	55	145	880	**150.2**	5.6	4	**29.6**	1.1	4
J671	570	297	100	197	1828	**<0**			**<0**		
J672	140	85	20	65	475	**<0**			**<0**		
J673	260	152	55	97	928	**9.9**	0.0	0	**2.7**	0.0	1
J674	170	120	40	80	440	**7.0**	27.2	376	**1.9**	5.9	376
J675	130	71	20	51	489	**<0**			**<0**		
J676	260	95	45	50	465	**11.9**	11.2	94	**6.1**	5.7	94
J678	220	125	30	95	435	**10.0**	20.5	208	**2.2**	4.7	208
J679	210	115	20	95	445	**<0**			**<0**		
J682	200	90	20	70	470	**35.8**	35.8	100	**10.4**	10.4	100
J684	280	161	55	106	919	**15.7**	4.8	31	**4.1**	1.3	31
J685	215	117	15	102	963	**<0**			**<0**		
J686	330	180	50	130	900	**9.5**	11.9	124	**2.5**	3.1	124
J687	150	80	30	50	480	**18.0**	41.9	236	**5.3**	12.6	236
J688	160	82	25	57	478	**95.0**	1.5	2	**27.1**	0.7	2
J689	160	70	30	40	490	**101.3**	37.4	37	**42.7**	15.8	37
J690	270	95	30	65	465	**<0**			**<0**		
J691	390	330	65	265	750	**22.9**	7.4	32	**3.4**	1.1	32
J692	430	197	35	162	1928	**<0**			**<0**		
J693	180	76	45	31	1004	**9.4**	15.6	165	**5.3**	8.8	165
J694	250	103	35	68	977	**22.5**	29.1	129	**8.4**	10.9	129
J695	120	60	15	45	500	**<0**			**<0**		
J696	355	230	40	190	850	**<0**			**<0**		
J697	300	127.5	45	82.5	1997.5	**7.0**	6.8	98	**2.6**	2.5	98
J698	285	155	50	105	405	**76.4**	9.0	12	**21.2**	2.5	12
J699	90	38	15	23	522	**<0**			**<0**		
J700	345	200	35	165	880	**12.2**	3.5	29	**2.6**	0.7	29
J701	170	95	30	65	465	**<0**			**<0**		
J702	240	145	40	105	1980	**<0**			**<0**		

NB Errors for radon activity are obtained by conducting a duplicate measurement for each sample and finding the mean. Errors from surface area and volume (V_i) measurements are estimate to be ± 5 cm^2 and 5 cm^3 respectively. Overall standard errors are given to 2 sigma and are produced by combining the above errors according to theory as described by Squires (1985). However, the errors due to surface area and volume calculations were found to be negligible compared to those arising from the LSC measurements.

Appendix 5 SEM images

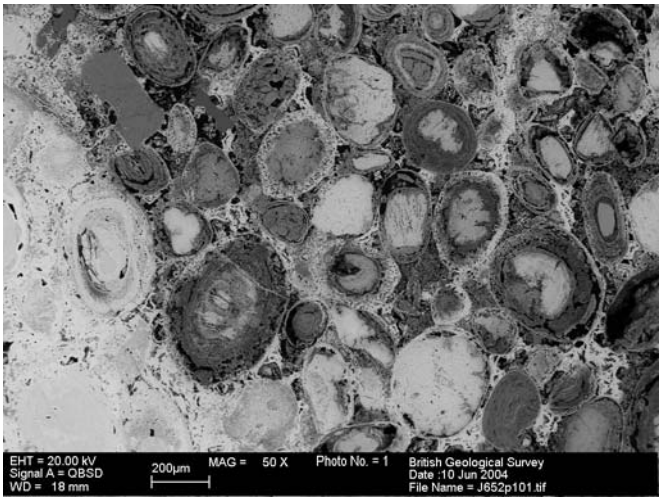

Plate 8 J652-01. Northampton Sand at Twywell, sample TW04 (depth 1.2 m). Ooliths and matrix have been largely replaced by Fe oxides.

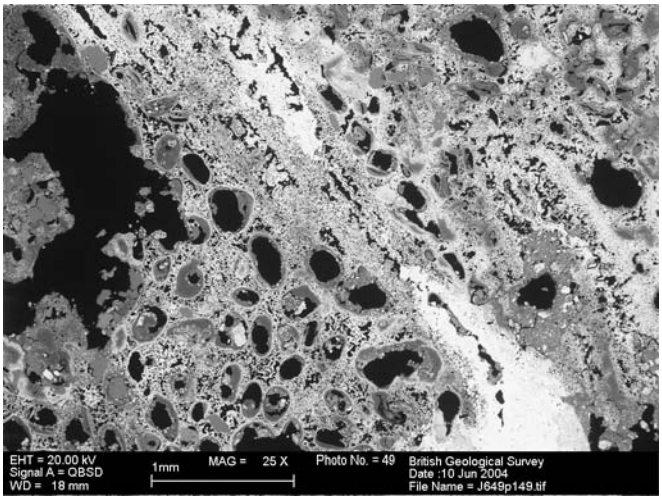

Plate 9 J649-49. Northampton Sand at Twywell, sample TW01 (depth 0.1 m). Replacement of ooliths and matrix by Fe oxides, and Fe oxide fracture mineralisation, very pronounced towards the top of the Formation.

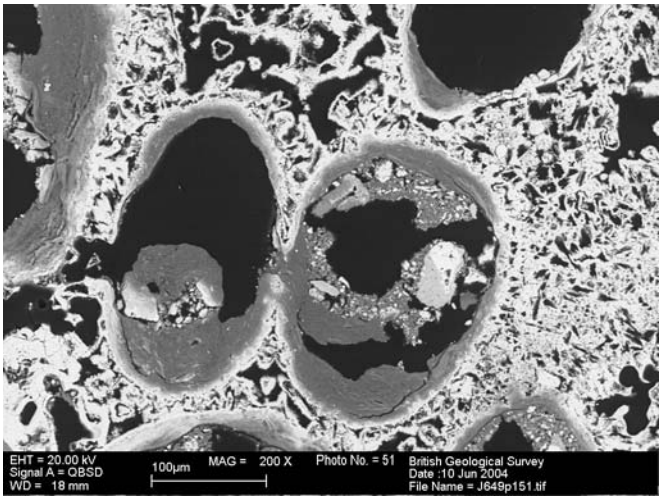

Plate 10 J649-51. NSF at Twywell, sample TW01 (depth 0.1 m). Enlargement of Plate 9 showing typical ooids with empty centres surrounded by surviving Fe-rich clay, while matrix is almost entirely replaced by Fe oxide.

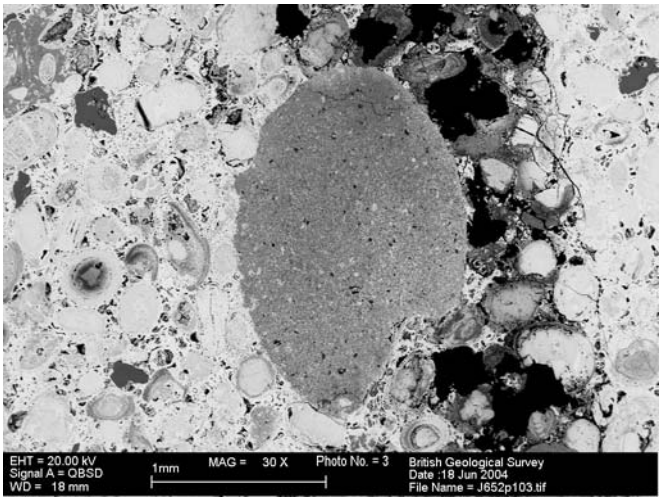

Plate 11 J652-03.NSF at Twywell, sample TW04 (depth 1.2 m). Unusually large Ca-Al phosphate pellet.

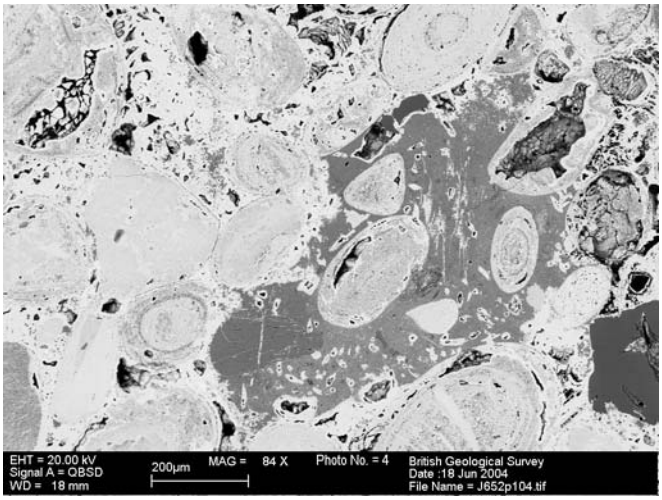

Plate 12 J652-04. NSF at Twywell, sample TW04 (depth 1.2 m). Phosphate pellet with a matrix-filling phosphate cement overgrowth.

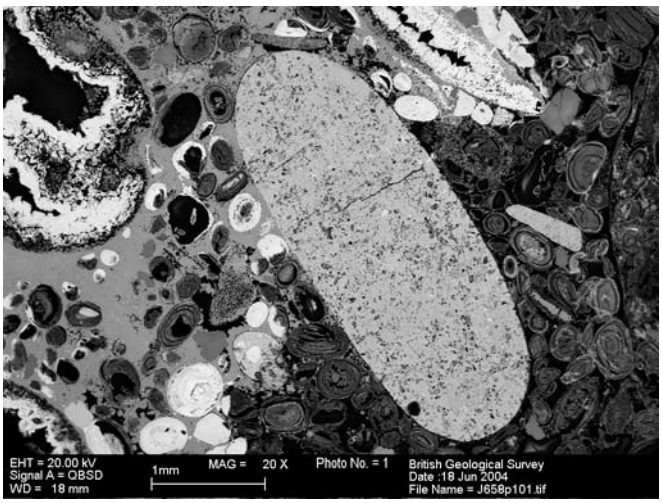

Plate 13 J658-01. NSF at Pitsford, sample PI04 (depth 0.6 m). Ca phosphate pellet.

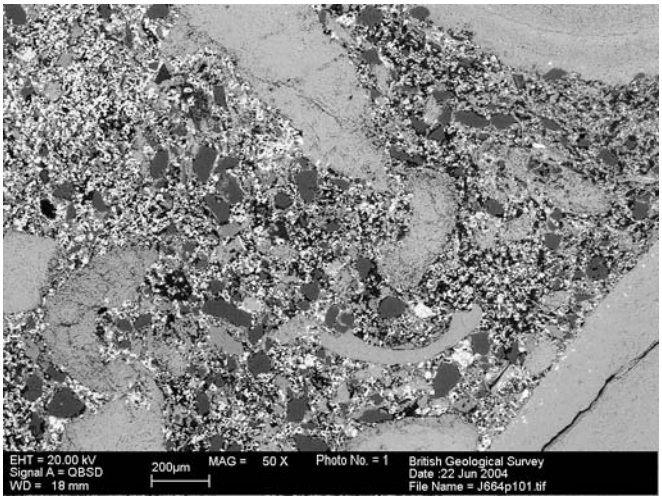

Plate 14 J664-01. NSF at Pitsford, sample PI10. Basal bed (depth 4m). Siliciclastic sand with calcareous bioclasts.

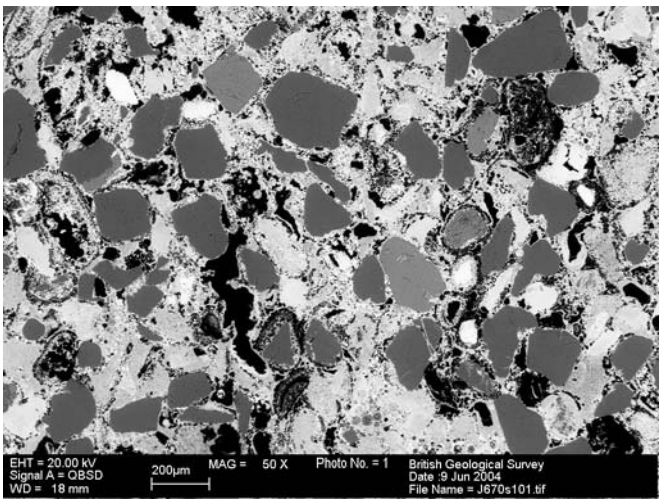

Plate 15 J670-01. NSF at Harlestone, sample HQ03 (top of Formation). Siliciclastic sandstone with minor ooliths. Ooids and matrix consist of Fe-rich clay and grains surfaces are coated with meniscus-style Fe oxide cement, resulting in poorly interconnected porosity.

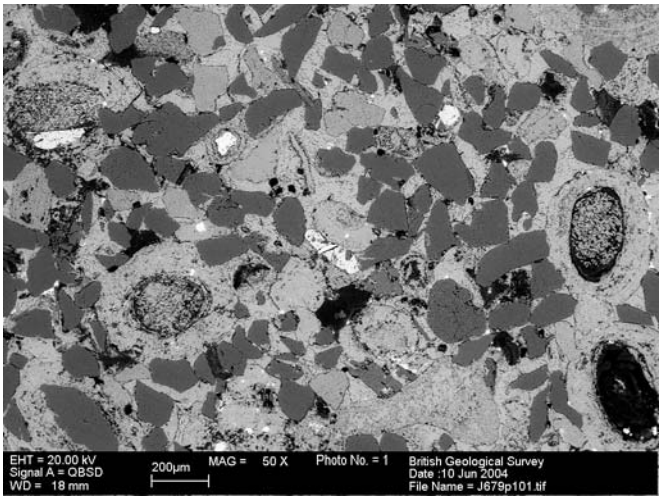

Plate 16 J679-01. NSF at Harlestone, sample HQ12 (depth 4 m). Siliciclastic sandstone with minor ooliths, tightly cemented by sparry calcite.

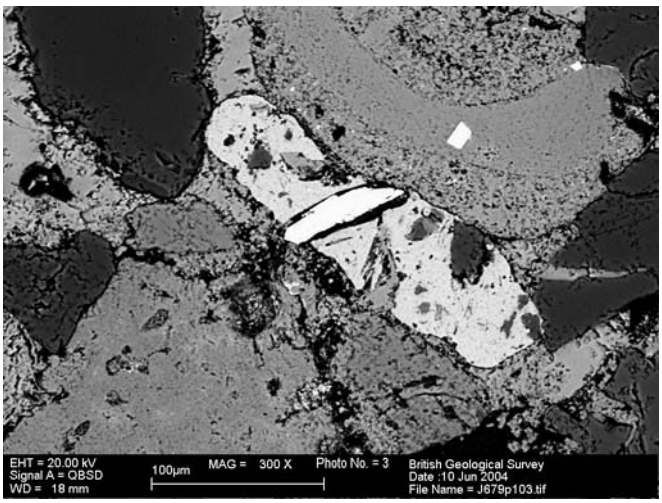

Plate 17 J679-03. NSF at Harlestone, sample HQ12 (depth 4 m). Rare phosphate pellet.

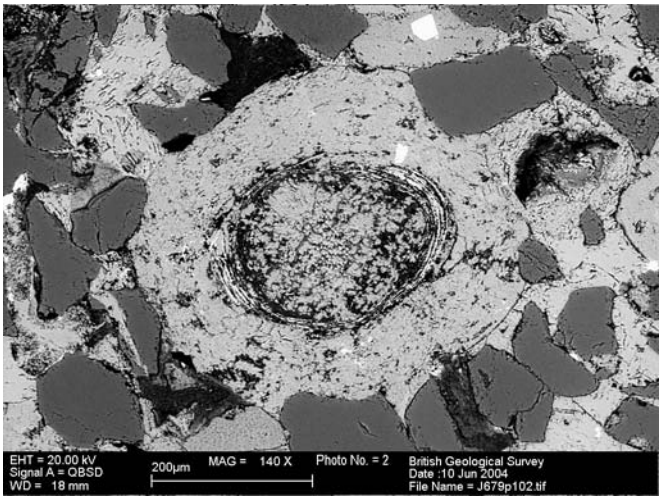

Plate 18 J679-02. NSF at Harlestone, sample HQ12 (depth 4 m). Rare oolith with central phosphate cement.

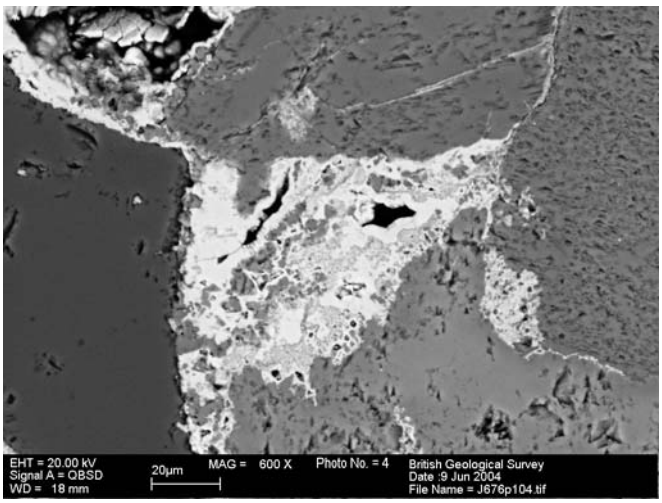

Plate 19 J676-04. NSF at Harlestone, sample HQ09 (depth 4 m). Rare phosphate/Fe oxide late cement.

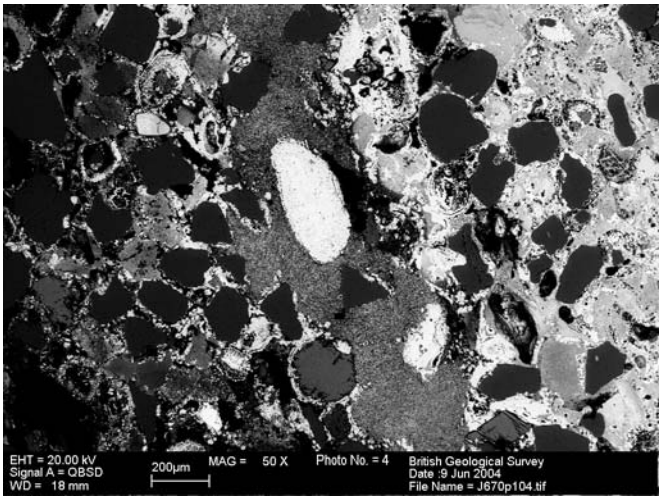

Plate 20 J670-04. NSF at Harlestone, sample HQ03 (top of Formation). Central vertical band is a fine grained, Fe-Si-K phase, possibly jarosite.

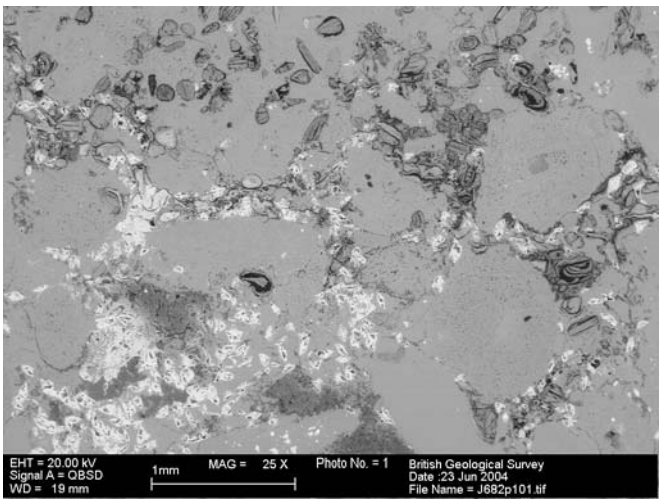

Plate 21 J682-01. MRF at Scalford, sample RC01 (depth 1.8 m). Bed rich in calcareous bioclasts, with minor ooliths and siliciclastic sand.

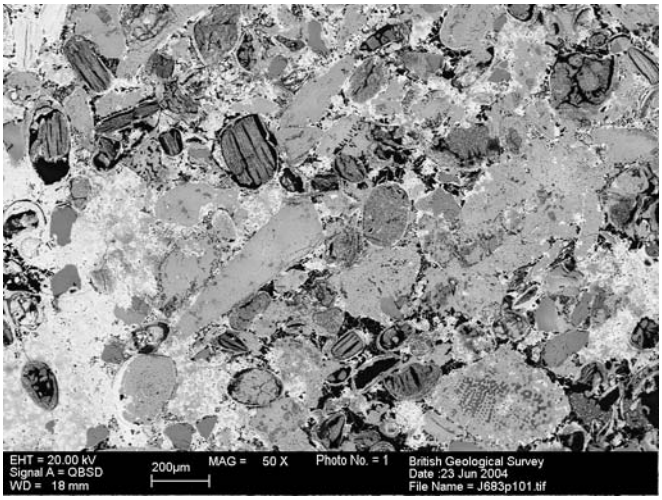

Plate 22 J683-01. Marlstone Rock at Scalford, sample RC02. Rock here contains similar proportions of bioclasts, ooliths and siliciclastic sand.

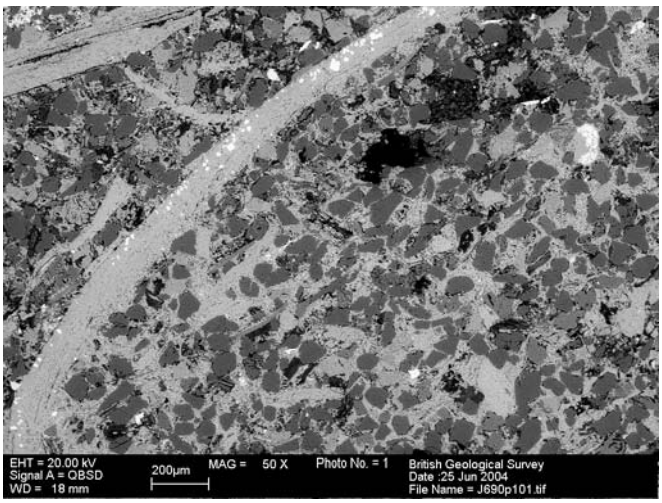

Plate 23 J690-01. MRF at Scalford, sample RC09 (depth 4 m). Rock here consists mostly of siliciclastic sand with bioclasts but few ooliths.

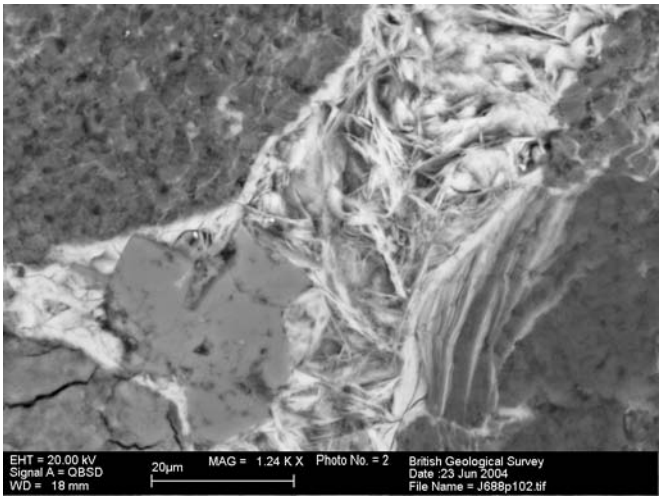

Plate 24 J688-02. MRF at Scalford, sample RC07 (depth 1.8 m). Late fracture filled with platy Mn oxide, a source of alpha tracks.

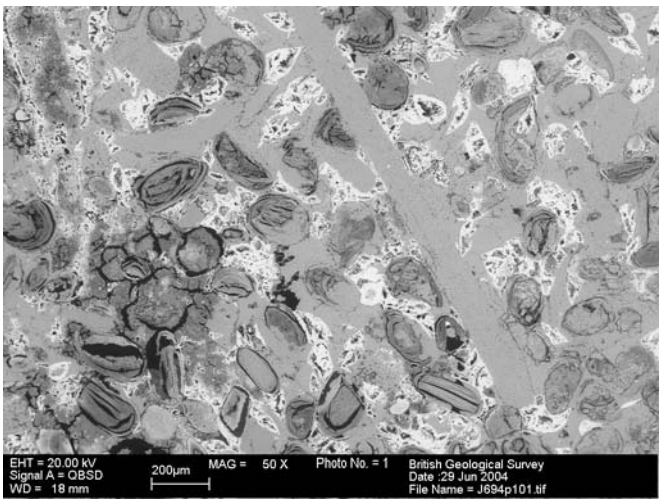

Plate 25 J694-01. MRF at Pickwell, sample PV04 (depth 0.5 m). Oolite with coarse grained calcareous bioclasts. Ooliths consist of clay and calcite. An early rhombic matrix cement is now replaced by Fe oxide.

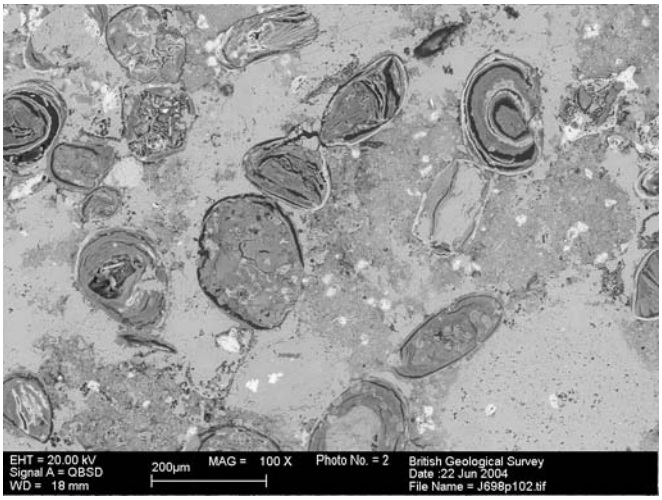

Plate 26 J698-02. MRF at Sauvey Castle, sample SC02 (depth 1.1 m). Calcite-cement oolite of upper part of the Formation.

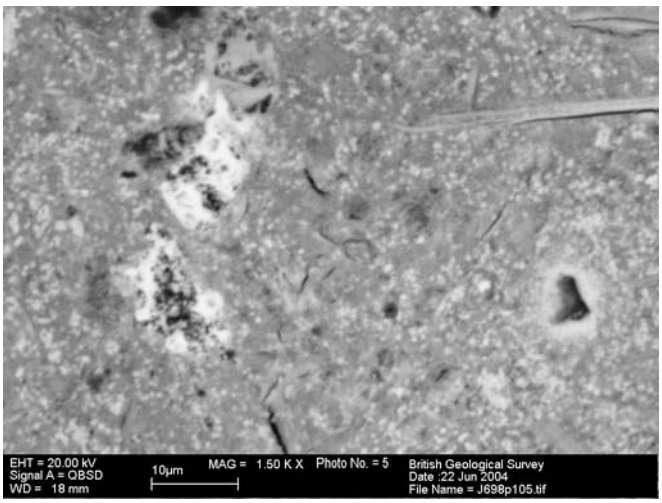

Plate 27 J698-05. MRF at Sauvey Castle, sample SC02 (depth 1.1 m). Ca phosphate-cemented matrix seen in many places.

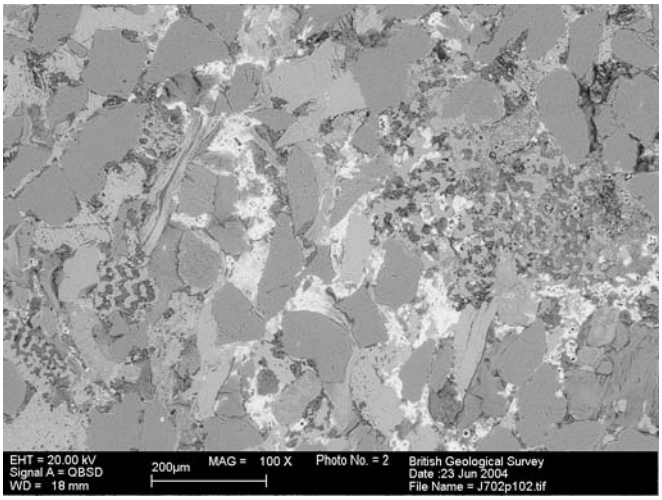

Plate 28 J702-02. MRF at Sauvey Castle, sample SC06 (depth 3.3 m). Basal beds: siliciclastic sand with calcareous bioclasts and a calcite and Fe oxide-cemented matrix.

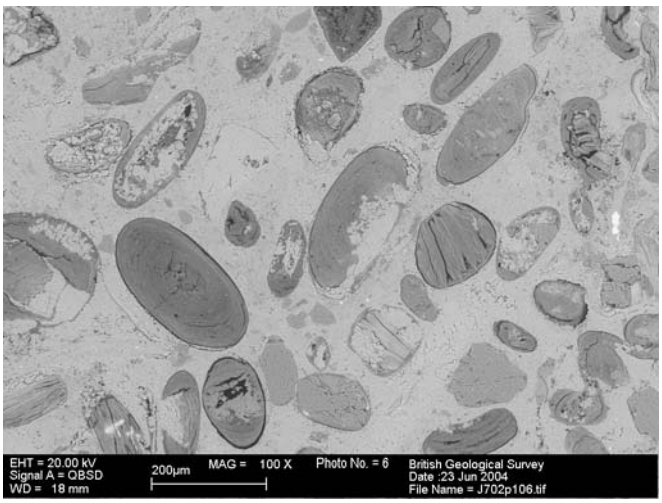

Plate 29 J702-06. MRF at Sauvey Castle, sample SC06 (depth 3.3 m). Oolitic interior of one of the common, large calcite nodules.

Appendix 6 XRD spectra

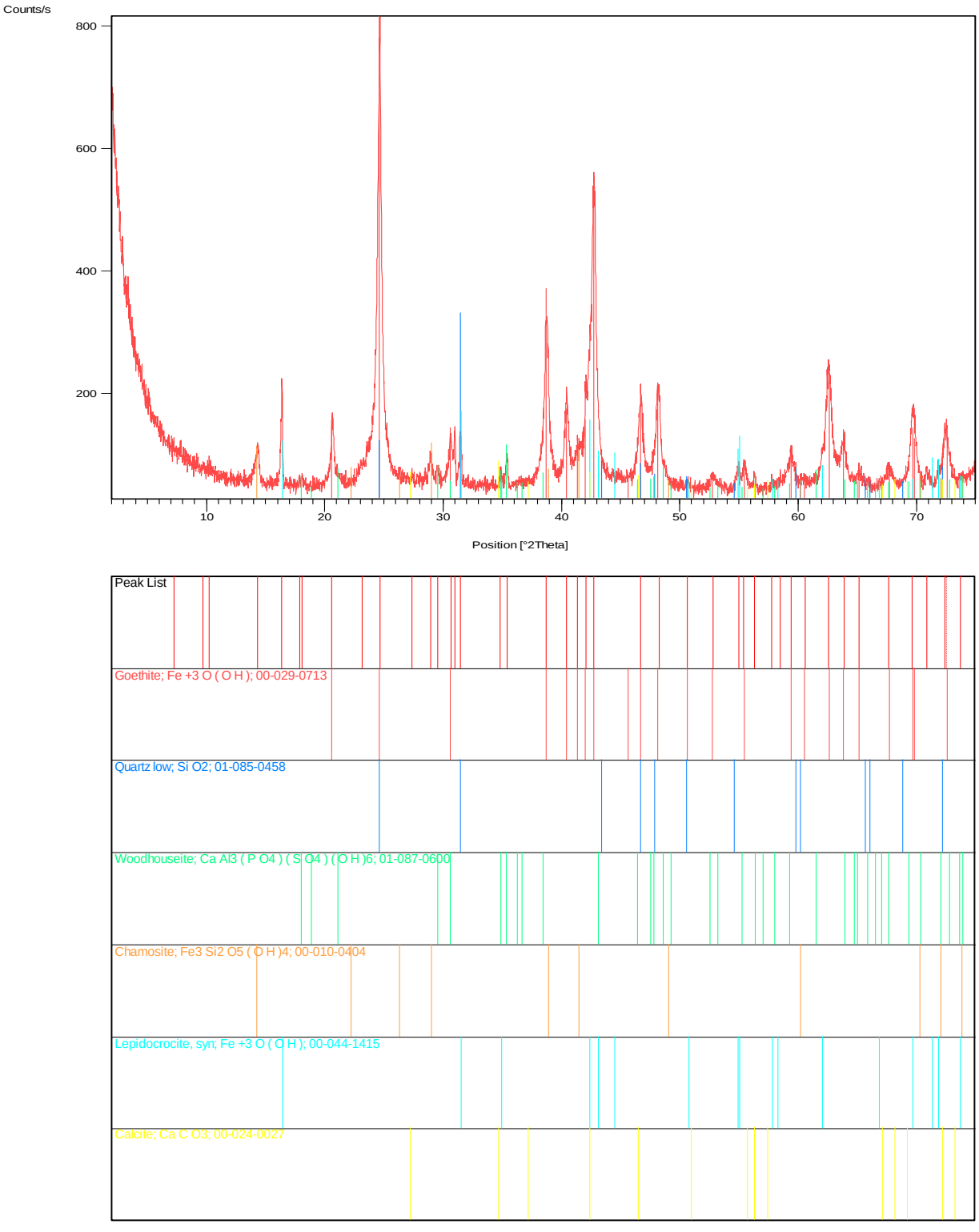

Figure 31 XRD trace for J649. The upper image shows the XRD trace (in red) with lines marking the peak positions of reference minerals. The lower image shows the fingerprints of peak positions for the same reference minerals which match the sample.

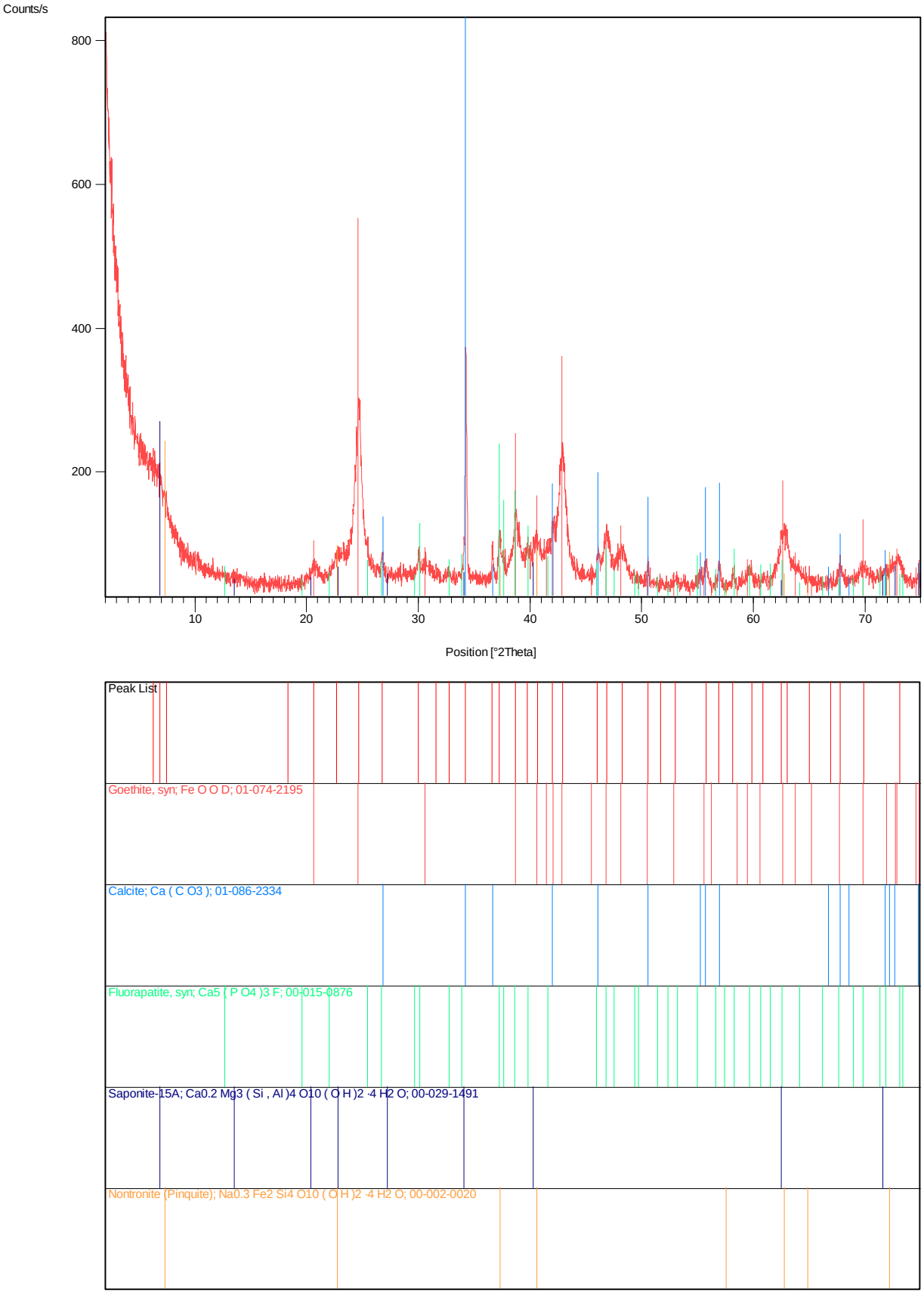

Figure 32 XRD trace for sample J662. Saponite and nontronite references are used to indicate the probable presence of a generic swelling clay, probably iron-rich.

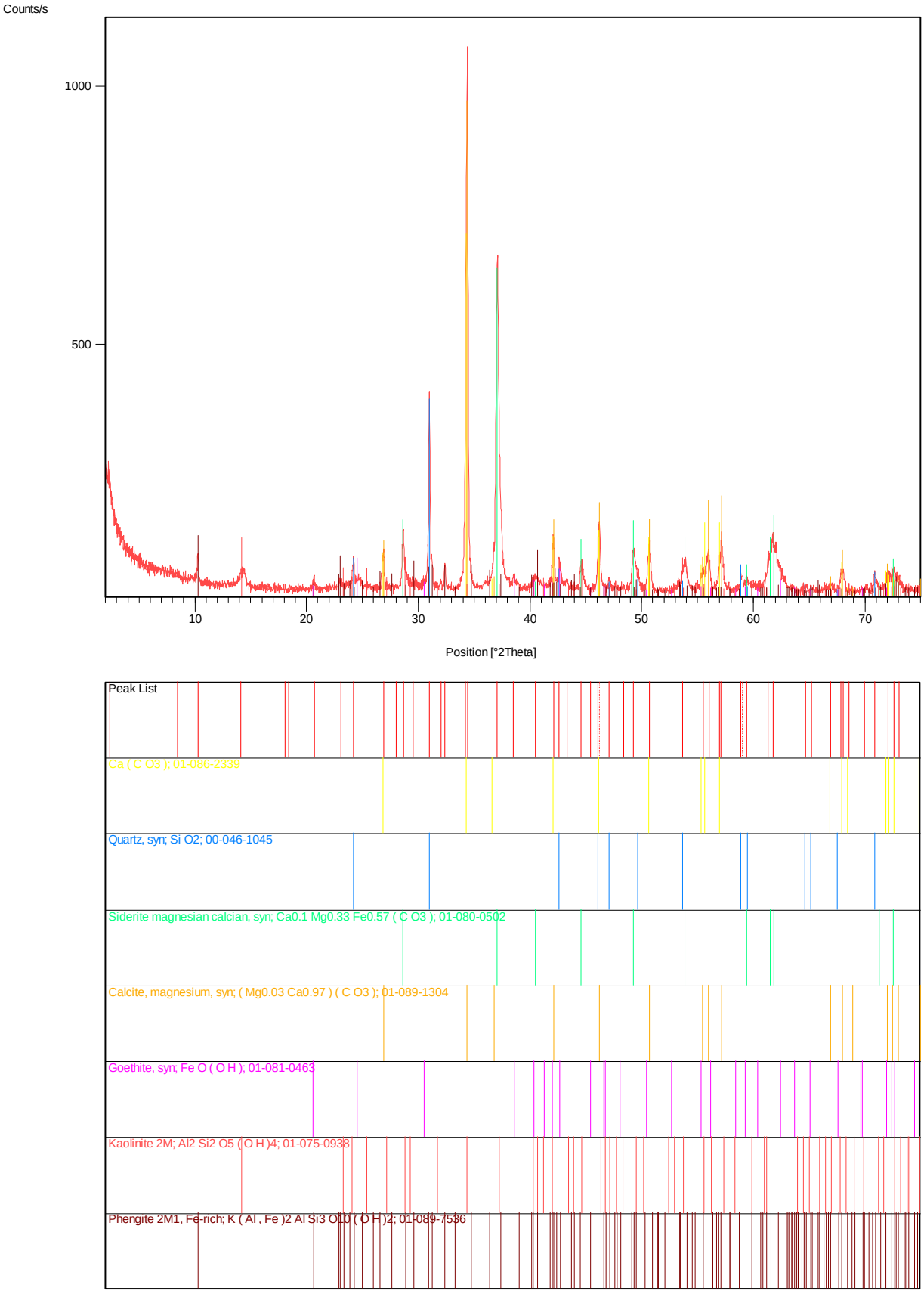

Figure 33 XRD trace for sample J664. Phengite is used to represent a generic mica phase.

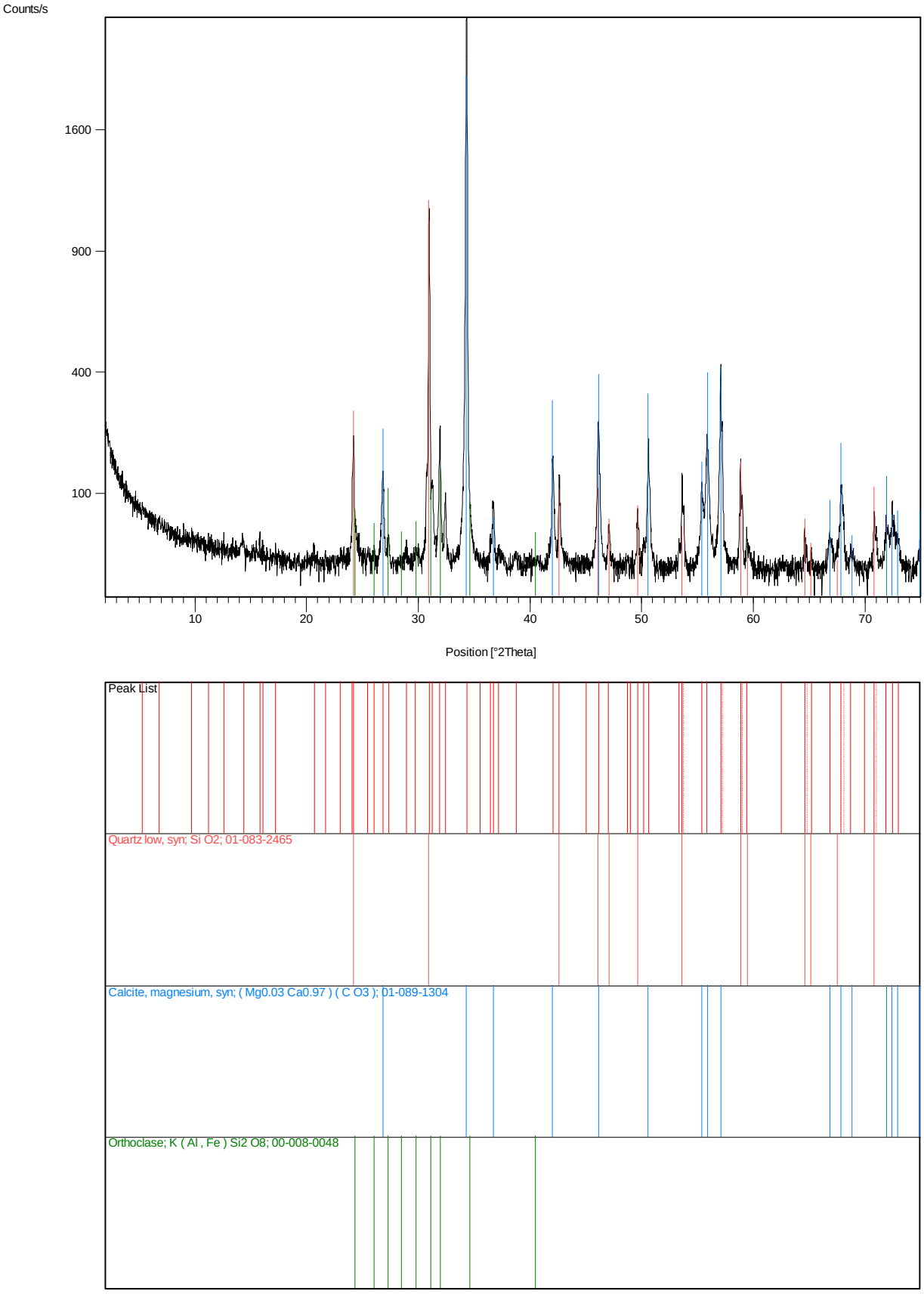

Figure 34 XRD trace for sample J679.

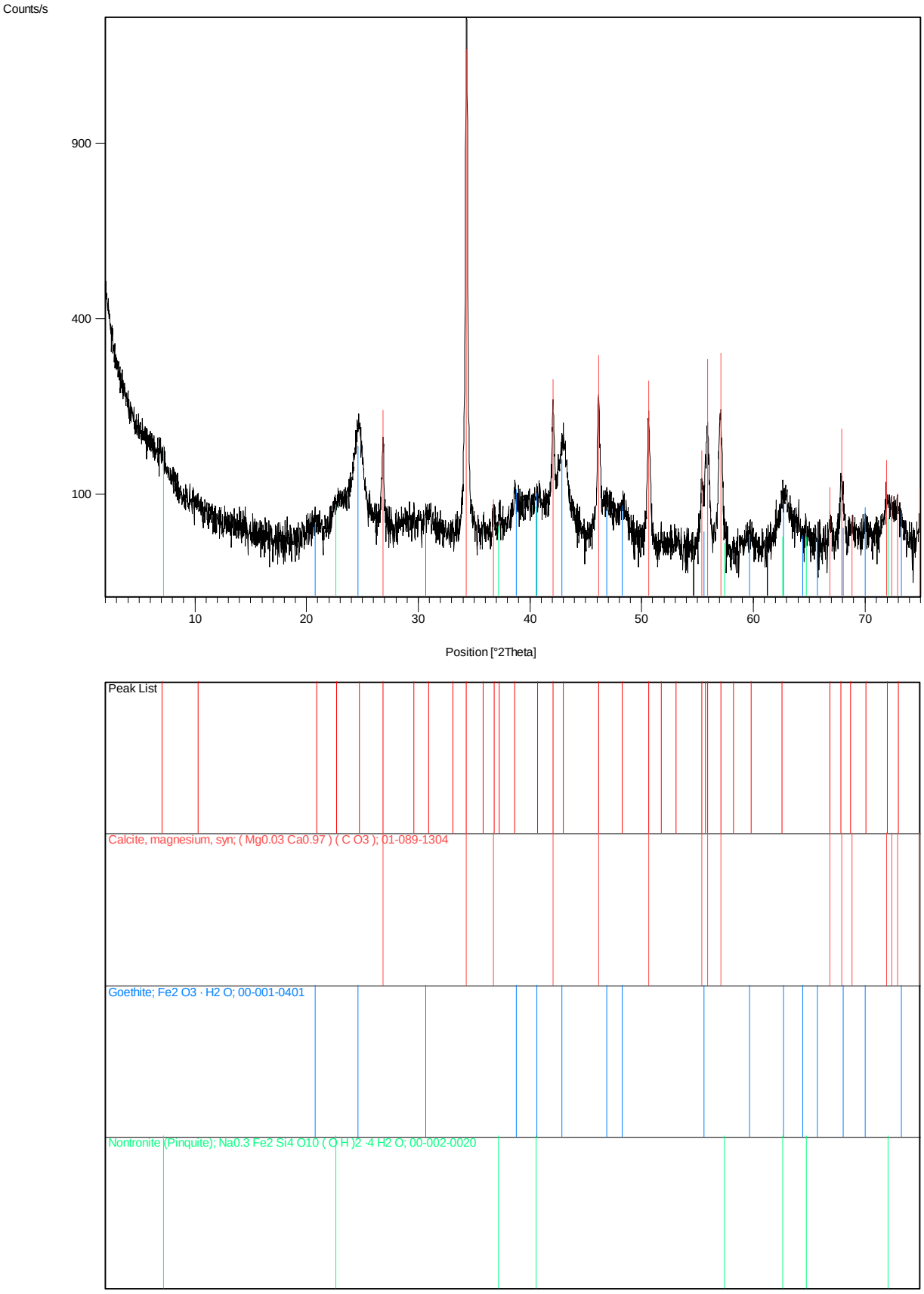

Figure 35 XRD trace for sample J693. Nontronite is shown to represent a generic swelling clay, possibly iron-rich.

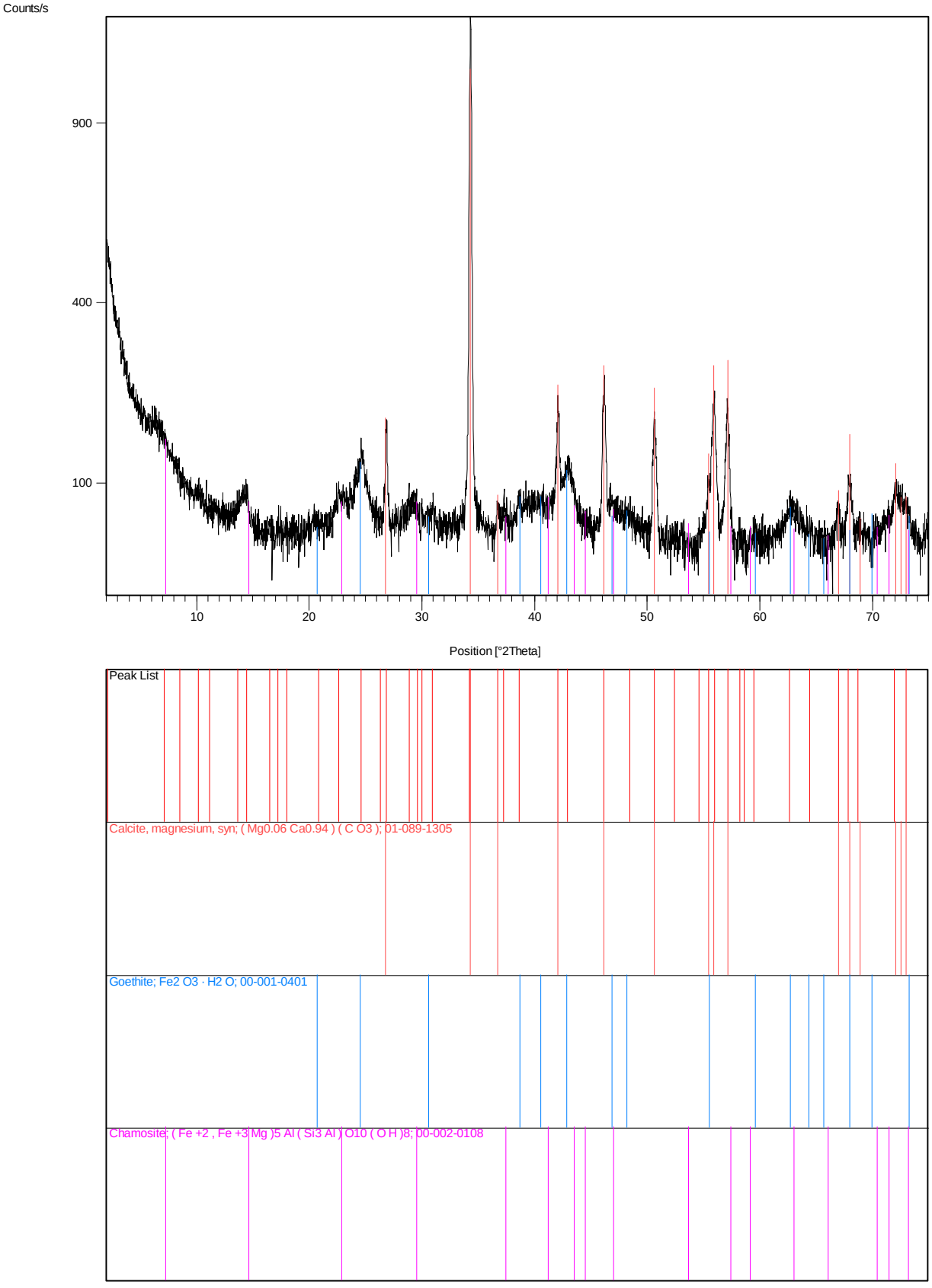

Figure 36 XRD trace for sample J697.

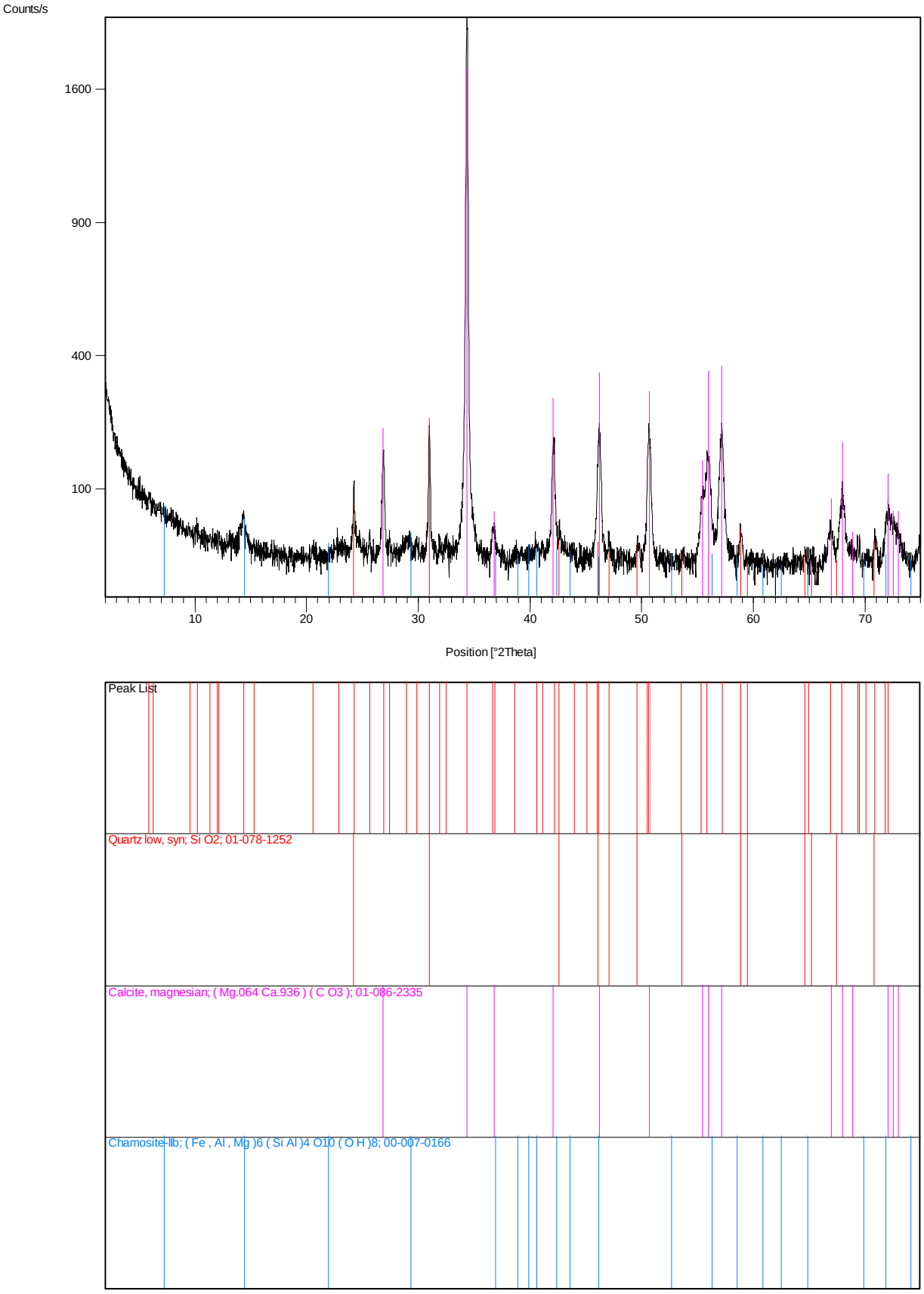

Figure 37 XRD trace for sample J700.

References

APPLETON, J.D. and BALL, T.K. 1995. Radon and background radioactivity from natural sources: characteristics, extent and the relevance to planning and development in Great Britain. *British Geological Survey, Technical Report* WP/95/2. Nottinghamshire.

APPLETON, J.D. and MILES, J. C. H., and TALBOT, D. K. 2000. Dealing with radon emissions in respect of new development. Evaluation of mapping and site investigation methods for targeting areas where new development may require radon protective measures.. *British Geological Survey Research Report* RR/00/12. Nottinghamshire.

BASHAM, I R. 1981. Some applications of autoradiographs in textural analysis of uranium-bearing samples -a discussion. *Economic Geology*, **76**, 974-982.

BRITISH GEOLOGICAL SURVEY 2006. The British Geological Survey Lexicon of Named Rock Units. http://www.bgs.ac.uk/Lexicon/home.html

BRONSON, F, L, YOUNG, B, VENKATARAMAN, R, 1998. Mathematical efficiency calibration of Ge detectors for laboratory sample gamma spectroscopy. Presented at the 44th Annual Conference on Bioassay, Analytical, and Environmental Radiochemistry, November 15-19, 1998; Albuqerque NM.

BRONSON, F, L, VENKATARAMAN, R, 2000. Validation of the accuracy of the labsocs mathematical efficiency calibration for typical laboratory samples. Presented at the 46th Annual Conference on Bioassay, Analytical, and Environmental Radiochemistry, November 12-17, 2000; Seattle, Washington.

FORD, J, KESSLER, H, COOPER, A H, PRICE, S J, and HUMPAGE A J. 2010. An enhanced classification for artificial ground. British Geological Survey Open Report, OR/10/36 http://nora.nerc.ac.uk/10931/

GRASTY, R L, HOLMAN, P B and BLANCHARD, Y B. 1991. *Transportable calibration pads for ground and airborne gamma-ray spectrometers*. Geological Survey of Canada, 1991.

HODGKINSON, E. S. 2002. Northampton Ironstones: mineralogy, petrography and paragensis of radiogenic phases. *British Geological Survey Internal Report* IR/02/058.

HOLLINGWORTH, S. E., and TAYLOR, J. H. 1951. The Northampton Sand Ironstone, Stratigraphy, Structure and Reserves. Memoir of the Geological Survey of Great Britain.

HYSLOP, E. 2000. Natural element distribution in fracture wallrocks of selected flowing features from Sellafield boreholes 2, 5, 7A & 12A : *British Geological Survey, Mineralogy & Petrology Series, Technical Report* WG/95/33.

LAHTI, M and JONES, D. G. 2003. Environmental applications of airborne radiometric surveys. *First Break*, **21**, 35-41.

LØVBORG, L. and KIRKEGAARD, P. 1974. Response of 3"x 3" NaI(TI) Detectors to terrestrial gamma radiation. Nuclear Instruments and methods. Vol 121, 239-251.

MILES, J. C. H., and APPLETON, J. D. 2000. Identification of localised areas of England where radon concentrations are most likely to have greater than 5% probability of being above the Action Level. London, Department of the Environment, Transport and the Regions, Report No. DETR/RAS/00.01.

MILES, J.C.H, and APPLETON J.D. 2005. Mapping variation in radon potential both between and within geological units. Journal of Radiological Protection 25, 257-276.

MILES, J. C. H., APPLETON, J. D, REES, D. M., GREEN, B. M. R., ADLAM, K. A., MYERS, A. H. 2007. Indicative Atlas of Radon in England and Wales. ISBN:978-0-85951-608-2. 29pp.

PEART, R. J., CUSS, R. J., BEAMISH, D., JONES, D.G. 2003. The High Resolution Airborne Resource and Environmental Survey- (Phase 1) (HiRES-1): background, data processing and dissemination and future prospects. *British Geological Survey Internal Report* IR/03/112.

SEMKOW, T. M. 1990. Recoil-emanation theory applied to radon release from mineral grains. *Geochimica et Cosmochimica Acta*, 54:2, 425-440.

SHARMAN, G. 1991. Radiometric investigation of radon in soil gas over Jurassic rocks of Northamptonshire, England. *Environmental Geochemistry & Health* **13**(3): 146-147.

SHARMAN, G. 1992. Seasonal and spatial variations in Rn-222 and Rn-220 in soil gas and implications for indoor radon levels. *Environmental Geochemistry & Health* **14**(4): 113-120.

SHARMAN, G. 1995. *Radon, an environmental hazard: a geological case study of Northamptonshire*. Unpublished PhD, University of Leicester.

SQUIRES, G L. 1985. Practical Physics. 3rd edition, Cambridge: Cambridge University Press.

SUTHERLAND, D S. 1991. Radon in Northamptonshire, England: geochemical investigation of some Jurassic sedimentary rocks. *Environmental Geochemistry and Health*, **13** (3), 143-145.

SUTHERLAND, D S and SHARMAN, G. 1996. Radon – *in Northamptonshire*? *Geology Today*, **12**: 63-67.

TAYLOR, J. H. 1949. Petrology of the Northampton sand ironstone formation. London, H.M. Stationery Office.

TONKS, E. S. 1989. The Ironstone Quarries of the Midlands: Rutland Pt.&: History, Operation and Railways. Runpast Publishing. ISBN: 978187075471.

TONKS, E. S. 1991. The Ironstone Quarries of the Midlands: Kettering Area Pt. 5: History, Operation and Railways. Runpast Publishing. ISBN: 9781870754057.

TONKS, E. S. 1992. The Ironstone Quarries of the Midlands: Leicestershire Pt. 9: History, Operation and Railways. Runpast Publishing. ISBN: 9781870754088.

WHITEHEAD *et al*., 1952. The Mesozoic ironstones of England; the Liassic ironstones. *Memoirs of The Geological Survey of Great Britain*. London.

WRIXON, A. D., GREEN B. M. R., LOMAS, P. R., MILES, J. C. H. CLIFF, K. D., FRANCIS, E. A., DRISCOLL, C. M. H., JAMES, M. C., and O'RIORDAN, M. C. 1998. Natural Radiation exposure in UK dwellings. Chilton, NRPB-R 190.